Ingvild Kvien

# Characterization of biopolymer based nanocomposites

Thesis for the degree of philosophiae doctor

Trondheim, January 2007

Norwegian University of
Science and Technology
Faculty of Engineering Science and Technology
Department of Engineering Design and Materials

NTNU
Innovation and Creativity

NTNU
Norwegian University of Science and Technology

Thesis for the degree of philosophiae doctor

Faculty of Engineering Science and Technology
Department of Engineering Design and Materials



ISBN 978-82-471-0248-0 (printed ver.)
ISBN 978-82-471-0251-0 (electronic ver.)
ISSN 1503-8181

Doctoral Theses at NTNU, 2007:12

Printed by Tapir Uttrykk

## Abstract

The field of nanocomposites is gaining considerable attention due to its potential for providing new materials with extraordinary physical properties compared to traditional composite materials. In this thesis cellulose nanowhiskers (CNW) were separated from microcrystalline cellulose (MCC) and dispersed in different biopolymer matrices to obtain polymer nanocomposites based on renewable resources. Moving from microstructure to nanostructure creates new challenges for structure characterization of materials. The overall aim of this work was to characterize the structure of CNW and their nanocomposites with different matrices. The sample preparation and microscopic examination of the bio-nanocomposites showed to be challenging because they are non-conductive, soft and water sensitive materials and consist of low atomic number elements. In the studies field emission scanning electron microscope was found to be a convenient and important first step in the analysis of the nanocomposite structure. More detailed information about the distribution of CNW was however obtained using transmission electron microscope (TEM) and atomic force microscope. X-ray diffraction analysis showed that the MCC consisted of both amorphous and crystalline regions. The sulfuric acid isolation treatment removed the amorphous regions and separated the cellulose nanowhiskers. From TEM analysis the size of the whiskers was measured to be 210 ± 75 nm in length and 5 ± 2 nm in width. It was also possible to separate the CNW from MCC using dimethyl acetamide containing a small amount of LiCl. It was however difficult to remove the organic solvent after treatment. CNW were well distributed in a hydrophobic matrix by the aid of a surfactant. Untreated CNW or untreated layered silicates in a thermoplastic starch matrix resulted in well dispersed nanocomposites. It was further found that it was possible to obtain oriented CNW in a matrix after exposure to a magnetic field. The dynamic mechanical thermal analysis of the different nanocomposites in this thesis showed that well dispersed cellulose whiskers have a large potential for improving the thermal mechanical properties of biopolymers.

## Preface

This thesis has been financially supported by the Norwegian Research Council under the 'NANOMAT' program. The work has been carried out at the Department of Engineering Design and Materials at NTNU from November 2003 to December 2006.

There are a number of people who have contributed to realize this work. First of all, I would like to express my sincere gratitude to my supervisor Kristiina Oksman for giving me the opportunity to start my research and for her guidance and enthusiasm in my work. A special thanks to Bjørn Steinar Tanem at SINTEF Materials and Chemistry for all his help with the microscopy work and for all the good advices. I would like to thank all my former and present colleagues at the Department of Engineering Design and Materials for technical and administrative assistance and social activities. A special thanks to the members of the bio-composite group; Linnea Petersson, Marie Le Baillif, Daniel Bondeson, Magnus Bengtsson and Aji Mathew for all their help, support and for their friendship. This thesis is the result of a close collaboration with Linnea and Daniel to whom I owe many thanks. I would like to thank people at other departments at NTNU for providing equipment and for their assistance and advice in the experimental work. A special thanks to the members of The Laboratory of Biomass Morphogenesis and Information at the Research Institute for Sustainable Humanosphere (RISH), Kyoto University, Japan, and in particular Professor Junji Sugiyama for giving me the opportunity to do part of my research there and together with Chiori Itoh and Dr. Thi Thi Nge for all the help with the experimental work and the interesting discussions. I would like to thank the Norwegian Research Council for the financial support and for the scholarship for the 3 months research stay in Japan.

Finally, I would like to thank my friends and family for all your support and patience. A very special thanks to Magnus.

Trondheim, January 2006
Ingvild Kvien

## List of appended papers

This thesis contains an introduction and the following appended papers, which are referred to by roman numerals in the text.

I Kvien, I.; Oksman, K. Microscopic Examination of Cellulose Whiskers and Their Nanocomposites. In: Characterization of Lignocellulosic Materials; T. Q. Hu (ed); Blackwell Publishing

II Bondeson, D.; Kvien, I.; Oksman, K. Strategies for Preparation of Cellulose Whiskers from Microcrystalline Cellulose as Reinforcement in Nanocomposites. In: Cellulose Nanocomposites Processing, Characterization and Properties; Oksman, K.; Sain, M. (ed); ACS Symposium series 938; Oxford press, 2006; pp 10-25

III Kvien, I.; Tanem, B.S.; Oksman, K. Investigation of the Structure of Cellulose Whiskers and Its Nanocomposites using TEM, SEM, AFM and X-ray Diffraction. 8th International Conference on Woodfiber-Plastic Composites, Madison, WI, USA, May 23-25, 2005

IV Petersson, L.; Kvien, I.; Oksman, K. Structure and Thermal Properties of Poly(lactic acid)/Cellulose Whiskers Nanocomposite Materials. Accepted for publication in Composite Science and Technology

V Kvien, I.; Tanem, B.S.; Oksman, K. Characterization of Cellulose Whiskers and Their Nanocomposites by Atomic Force and Electron Microscopy. Biomacromolecules 2005, 6, 3160-3165

VI Kvien, I.; Sugiyama, J.; Vortrubec, M.; Oksman, K. Characterization of Starch Based Nanocomposites. Submitted to Journal of Material Science

VII Kvien, I.; Oksman, K. Orientation of Cellulose Nanowhiskers in Polyvinyl Alcohol (PVA). Accepted for publication in Applied Physics A

The PhD research also resulted in the following article and conference contributions:

Tanem, B.S.; Kvien, I.; van Helvoort, A.T.J.; Oksman, K. Morphology of Cellulose and Its Nanocomposites. In Oksman, K.; Sain, M. (ed); Cellulose Nanocomposites Processing, Characterization and Properties; ACS Symposium series 938; Oxford press, 2006; pp 48-62

Oksman, K.; Mathew, A. P.; Bondeson, D.; Kvien, I. Manufacturing Process of Polylactic Acid (PLA) - Cellulose Whiskers Nanocomposites. Composite Science and Technology 2006, 66, 2776-2784

Kvien, I.; Oksman, K. Orientation of Cellulose Whiskers in Nanocomposites. Progress in wood and bio fibre plastic composites 2006 International Conference, Toronto, Ontario, Canada, 1-2 May 2006

Kvien, I.; Vortrubec, M.; Oksman, K. Starch Based Nanocomposites. Student Conference, Toronto University, May 2006

Bondeson, D.; Kvien, I.; Oksman, K. Bio-Nanocomposites Based on Cellulose Whiskers, 6th Global Wood and Natural Fibre Composites Symposium, Kongress Palais Kassel – Stadthalle, Kassel, Germany, April 5-6, 2006

Oksman, K.; Kvien, I.; Petersson, L.; Bondeson, D.; Mathew, A.P.: Bio-Nanocomposites, International Conference on Science and Technology of Composite Materials, Buenos Aires, Argentina, 11-14 December 2005

Kvien, I.; Tanem, B.S.; Oksman, K. Structure Determination of Cellulose Whiskers and Its Nanocomposites, 2nd Kyoto International Forum for Environment and Energy, Kyoto, Japan, October, 2005

Oksman, K.; Kvien, I.; Petersson, L.; Bondeson, D. Cellulose Nanocomposites; Challenges to Overcome, NSF Workshop, Georgia Tech. Atlanta, USA. 22-23 Sept. 2005

Tanem, B.S.; Kvien, I.; Oksman, K. Structural Characterization of Cellulose and Its Nanocomposites, 229th ACS National Meeting San Diego, CA, USA, March 13-17, 2005

Oksman, K.; Mathew, A. P.; Petersson, L.; Bondeson, D.; Kvien, I.; Tanem, B.S. Activities on Cellulose Based Bio-Nanocomposites in Norway, Symposium on Green Composites, RISH, Kyoto University, Kyoto, Japan, November 18, 2004

Oksman, K.; Mathew, A. P.; Petersson, L.; Kvien, I., Bondeson, D.; Tanem, B.S. Processing of Cellulose Nanocomposites, Functional Fillers for Plastics, Hamburg, Germany, 15-17 September, 2004

# Table of contents

# 1. Introduction

## *1.1 Background*

Nanocomposites are a relatively new generation of composite materials where at least one of the constituent phases has one dimension of less than 100 nm.[1] This new family of composites is reported to exhibit remarkable improvements in material properties when compared to conventional composite materials.[2,3] The small size of the reinforcement leads to an enormous surface area and thereby to increased interaction with the matrix polymer on molecular level, leading to materials with new properties. Well dispersed nano particles can improve tensile properties and even improve the ductility because their small size does not create large stress concentrations in the matrix.[1] The small size also increases the probability of structural perfection and will in this way be a more efficient reinforcement compared to microsized reinforcements. One of the fields in which nanotechnology has great potential, is in the development of high quality biopolymer based products.[4] Biopolymers are attracting considerable attention as a potential replacement for petroleum based plastics due to an increased consciousness for sustainable development and high price of crude oil. Biopolymers maintain ideally the carbon dioxide balance after their degradation or incineration. By using biodegradable grades they will also save energy on waste disposal. The limited performance and high cost of these materials are today restricting the competitiveness to traditional thermoplastics. There is now ongoing research to enhance the properties of biopolymers by preparing nanocomposites using either layered silicates (LS)[4] or cellulose nano whiskers (CNW)[5-7] as nanoreinforcement. The performance of the materials is strongly dependent on the distribution of the reinforcement in the matrix. Layered silicates and cellulose nano whiskers are in principle hydrophilic and may be difficult to distribute in a typically hydrophobic matrix. Organically modified layered silicates are however commercially available and their nanocomposites have been used in the plastic industry for decades. Cellulose nanowhiskers are on the other hand today only produced in lab-scale from different sources. The interest to utilize cellulose nanowhiskers as reinforcement is due to their renewable nature, abundance and good mechanical properties.[8]

### *1.2 Nanoreinforcements*

The nanoreinforcements are divided into three types depending on their size and shape: [9]

1) *Spherical particles*. These are particles with all three dimensions in the nanometer range. Examples of this type are spherical silica and spherical gold particles [10].

2) *Nanotubes and whiskers*. These particles have two dimensions in the nanometer range and thus forming an elongated structure. Examples of this type are carbon nanotubes [11] and cellulose whiskers [5].

3) *Sheets*. These particles have only one dimension in the nanometer range, i.e. the thickness, and are thus formed as a sheet. Layered silicates are examples of this type.[4]

Layered silicates (Paper VI) and cellulose whiskers (Paper I-VII) are both used as reinforcements in this thesis and will therefore be shortly described in the following.

#### 1.2.1 Layered silicates

The layered silicates used for preparation of nanocomposites belong to the structural family called 2:1 phyllosilicates.[12] The crystal lattice of 2:1 phyllosilicates consists of two silicon tetrahedral layers and one aluminium octahedral layer, forming a layer thickness of around 1 nm.[9,12] The structure of a 2:1 phyllosilicate is shown in Figure 1.

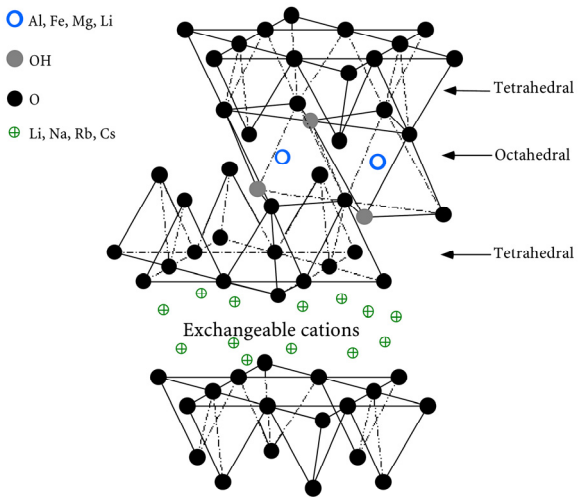


**Figure 1** *Structure of 2:1 phyllosilicates (with permission from ref 12)*

The layers are forming stacks with van der Waals gap in between called the interlayer or the gallery. Negative charges are generated when isomorphic substitution occurs within the layer ($Al^{3+}$ is for example replaced by $Mg^{2+}$).[9,12] These charges are balanced by alkali or alkaline earth cations, $Na^+$, $Ca^+$ or $K^+$, situated in the interlayer.[13]

The presence of positive ions on the surface of the silicate sheets makes them hydrophilic and thus incompatible with many polymers.[13] To make a nanocomposite, it is therefore often necessary to modify the layered silicates (LS) in order to make them more compatible with the organic polymer matrix. To do this, the interlayer cations can be replaced by cations bearing long alkyl chains, such as alkylammonium or alkylphosphonium.[9] The role of the alkyl ammonium cations is to lower the surface energy and improve the wetting characteristics with the polymer.[12] Modified layered silicates are commercially available with different surface treatments to fit a wide variety of polymer systems. By insertion of polymers (or monomers) into the interlayer, a nanocomposite may be formed. The description of the different structures obtained for polymer/layered silicate nanocomposites differs slightly in literature, but two extreme morphologies are throughout described:

A) *Intercalated nanocomposites* where the polymer chains penetrate in between silicate layers and thereby increase the gallery height.

B) *Exfoliated nanocomposites* where the silicate layers are totally and homogeneously delaminated and dispersed in the polymers matrix. Maximum benefits for most applications are achieved for exfoliated nanocomposites.[14]

Most commonly, a morphology is observed where both intercalation and exfoliation co-exist.[15] The amount of intercalation and exfoliation depends on the nature of the matrix, the type and treatment of the layered silicates and the processing method. Montmorillonite, hectorite and saponite are the most commonly used layered silicates.[9] They belong to the smectite-group, which is a subgroup of clay. Clay is a subgroup of the 2:1 phyllosilicates. Mica is another subgroup of 2:1 phyllosilicates also often used for the preparation of layered silicate nanocomposites.

### 1.2.2 Cellulose nanowhiskers

The interest to utilize cellulose nanowhiskers (CNW) as reinforcement is due to their renewable nature, biodegradability, abundance and good mechanical properties.[16] They can be obtained from different sources, such as different plants,[17,18] tunicin,[6] and bacteria[5]. The term whisker refers to the needle-like structure of cellulose monocrystals. These crystals, linked by amorphous regions build up cellulose microfibrils in for example the wood cell wall. The hierarchic structure of wood is shown in Figure 2. From left, the figure shows a pine tree which is build up of wood cells (fibres). From the walls of the wood cells, cellulose microfibrils can be isolated. These microfibrils consist of elementary fibrils which contain monocrystalline cellulose domains [19], or cellulose whiskers.

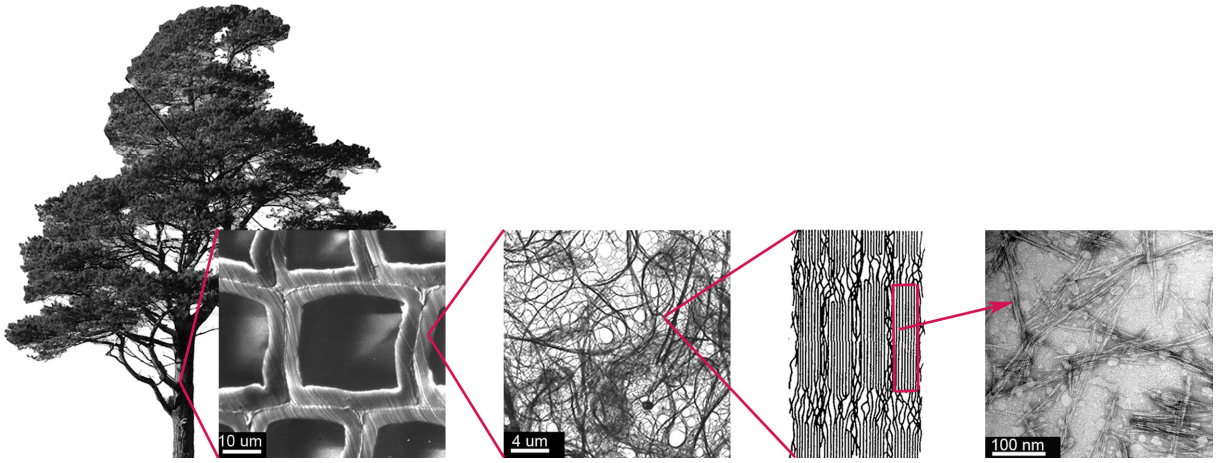


**Figure 2** *Hierarchic structure of wood showing from left: a tree, cross-section of wood cells, microfibrils, elementary fibrils with crystalline domains and cellulose whiskers.*

Both microfibrils and whiskers are utilized as cellulose nanoreinforcements. Microfibrils contain both amorphous and crystalline regions, while whiskers consist of monocrystals. The size of the CNW depends on the source of cellulose and can be around 5 nm in width and 200 nm in length for whiskers from wood.[17]

A challenge when using CNW as reinforcement is the tendency of the whiskers to agglomerate when dispersed in a typically more hydrophobic matrix due to hydrogen bonding between hydroxyl groups at the whiskers surface. Strategies to prevent re-aggregation in a polymer are described in Paper IV. As opposed to layered silicates the CNW are not yet commercially available, nor untreated or treated with different surface modifications. CNW based nanocomposites are still subject to basic research.

#### 1.2.2.1 Micro crystalline cellulose

CNW are not commercially available, they can however be isolated from microcrystalline cellulose (MCC), which is used as a starting material in this work and is commercially available. MCC is widely used in food industry and as a binder in tablets and capsules.[20] MCC is prepared by hot-treating cellulose from wood with strong mineral acids, vigorous agitation of the slurry and spray drying.[21] Strong hydrogen bonding between the individual cellulose whiskers produced promotes re-aggregation during drying procedures.[20] Thus, the MCC produced consists of aggregated bundles of whiskers. To utilize cellulose whiskers as reinforcement, the hydrogen bonds between the whiskers must be broken. Strategies for isolation of cellulose whiskers from MCC are described in Paper II. By using MCC as a starting material for the production of CNW the tedious processing steps by means of purification, bleaching, fibrillation and hydrolysis[6] are reduced.

## *1.3 Matrices: Biopolymers and biodegradable polymers*

Biopolymers can be divided into three main groups depending on their source:[22]

- Polymers that are directly extracted from biomass, in other words natural polymers. Polysaccharides such as starch and cellulose and proteins like casein and gluten belong to this group.

- Polymers that are produced through classical chemical synthesis using renewable biobased monomers, such as polylactic acid (PLA).

- Polymers produced by microorganisms or bacteria, like polyhydroxyalkanoates and bacterial cellulose.

Biodegradation is a process where organic materials are converted to simpler compounds, mineralized and redistributed through elemental cycles such as the carbon, nitrogen and sulphur cycles.[23] It is important to note that depending on their structure and modifications, biopolymers can both be biodegradable and inert to biodegradation. Synthetic polymers can be biodegradable, such as for example poly vinyl alcohol (PVA). Rate of biodegradation has not been subject in this thesis. In the following, the different biopolymers and synthetic biodegradable polymer used in this thesis are described.

### 1.3.1 Poly-lactic acid, PLA

PLA is a linear aliphatic thermoplastic polyester mostly produced from corn, but other starch/sugar rich plants such as rice, wheat and sweet potatoes can be used.[24] In addition, there is ongoing research to develop new conversion technologies to facilitate the use of lignocellulosic biomass feedstock, which enables the use of for instance residues left in the field.[24] Today, PLA is produced from the corn kernel by separation of starch which is converted via enzymatic hydrolysis into dextrose, which again is fermented into lactic acid.[24,25] There are two main routes to produce PLA from the lactic acid monomer, either by direct condensation polymerization or by ring-opening polymerization through the lactide intermediate.[24,25] The polymer is modified to enhance temperature stability and reduce residual monomer content,[25,26] and the resulting polylactic acid can then be processed as for polyolefins and other thermoplastics. PLA has found its way to a wide range of packaging, film and fiber applications.[24]

### 1.3.2 Cellulose esters

Cellulose is the most common biopolymer on earth. It is insoluble in all but the most aggressive hydrogen bond-breaking solvents.[27] Because of this, cellulose is usually converted into derivatives such as cellulose esters to make it more processable. Cellulose plastics such as cellulose acetate (CA), cellulose acetate propriate (CAP) and cellulose acetate butyrate (CAB) are thermoplastic materials produced through esterification of cellulose.[4] Raw materials such as cotton, recycled paper, wood cellulose and sugarcane are used for making the cellulose ester biopolymer in powder form. These cellulose ester powders are extruded to produce various grades of commercial cellulose plastics in pelletized form in the presence of different plasticizers and additives.[4]

### 1.3.3 Starch

Starch is the major form of stored energy in plants.[4] It is usually obtained from potato, maize or wheat. Starch is composed of a mixture of amylose, a linear polysaccharide, and amylopectin, a highly branched molecule. Natural starches contain 10-20% amylose and 80-90% amylopectin.[4] Thermoplastic starch (TPS) or destructurised starch is made from native starch by swelling in a plasticizer and subsequently treatment of a combined kneading and heating process.[28] Water and glycerol are mainly used as plasticizers. Other plasticizers as sorbitol, urea and dextran are also employed.[29] TPS can be processed as a traditional plastic. It

shows a very low permeability for oxygen, but is very sensitive to humidity, thus making starch as such unsuitable for most applications.[28,30]

### 1.3.4 Polyvinylalcohol, PVA

Poly(vinyl alcohol) (PVA) is a water soluble, synthetic and biodegradable polymer.[4] It is prepared by hydrolysis (or alcoholysis) of a poly(vinyl ester). The extent of hydrolysis will determine the amount of residual acetyl groups which affects the viscosity properties.[4] Commercial PVA is available in a number of grades with different molecular weight and residual acetate content. Vinyl polymers are being used in a number of industrial applications[4], but also for packaging applications.[28] Their biodegradation requires an oxidation process, and most of the biodegradable vinyl polymers contain an easily oxidisable functional group. Polyvinylalcohol (PVA) is the most readily biodegradable of vinyl polymers.

## *1.4 Aim of study*

This thesis is mainly focused on CNW based biopolymer nanocomposites in order to prepare new materials which are fully based on renewable resources. This is a new field and considerable basic research in processing, analysis of material properties and structure characterization is crucial to obtain true biopolymer nanocomposites by processes which can be implemented in the industry. This study focused first on the preparation of CNW and then on how to distribute them in various biopolymers. One major challenge for the CNW based nanocomposites is to enable compatibility between the CNW and matrix and thereby obtain well distributed CNW to ensure true nanocomposites. However, only limited work has been reported on structure characterization of CNW based nanocomposites. The overall aim of my research has therefore been to utilize different microscopy techniques in order to obtain more information of the structure of these new materials. Figure 3 summarizes the contents of this thesis.

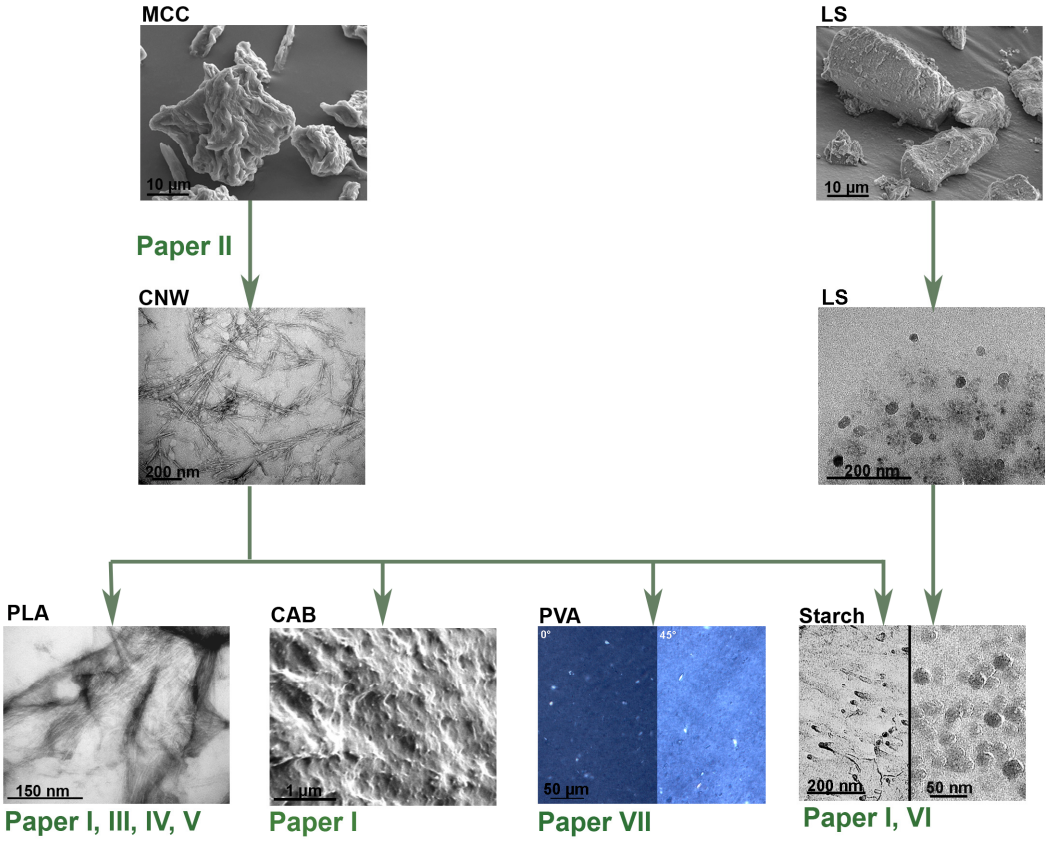


**Figure 3** *A schematic overview of the contents of this thesis*

# 2. Structure characterization

## *2.1 Flow birefringence*

The presence of individual cellulose nanowhiskers in a suspension is not visible to the eye due to their small size. When the suspension is stirred, the CNW will align in the direction of the flow, creating macroscopic domains where the whiskers are parallel.[31] Because cellulose is birefringent the macroscopic alignment will give rise to a macroscopic birefringence which is visible when the suspension is placed between two polarizing filters (one 90° to the other).[31] Examination of flow birefringence properties of a suspension can therefore be a way to verify the presence of well dispersed CNW in a suspension.

## *2.2 Microscopy techniques*

In this study the aim was to utilize different microscope techniques and X-ray diffraction for structure characterization of CNW and their nanocomposites, such as field emission scanning electron microscope (FESEM), transmission electron microscope (TEM), atomic force microscope (AFM) and Wide angle X-ray diffraction (WAXD). Sample preparation and instrumentation of bio-nanocomposites are challenging because they are non-conductive, soft and water sensitive materials and consist of low atomic number elements. The principles of the microscopes are described in Paper I together with examples of sample preparation for the different materials and microscopes. Challenges for structure characterization of biopolymer based nanocomposites are discussed in Paper I, III, V. The principles of WAXD are given in the following.

## *2.3 Wide angle X-ray diffraction*

X-rays are electromagnetic radiation with wavelength between 0,1-100 Å.[32] For diffraction, X-rays with wavelength of the same magnitude as interatomic distances are used, i.e.: 2,5 Å < $\lambda$ < 3 Å. For diffraction of polymers it is standard to use a copper $K\alpha_{1,2}$-beam.[33] The x-ray beam approaching a crystalline specimen is viewed in Figure 4. The wavefront is specularly reflected from the parallel crystal planes spaced *d* units apart. If the distance ABC equals an integer number of wavelengths, then the reflected beam will combine in phase and an intensity maximum will occur.[34] This is seen as a peak in the diffractogram. For a particular

spacing $d$ and wavelength $\lambda$ there exists an angle $\theta$ at which this occurs. The angle and layer spacing are related through the Braggs' equation:[34]

$$n\lambda = 2d\sin\theta \qquad \text{(eq. 1)}$$

where $n$ is an integer, 1,2,3,…; $d$ is the spacing between lattice planes; $\lambda$ is the wavelength of the x-ray radiation used and $\theta$ is the diffraction angle.

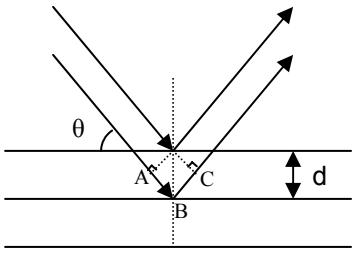


**Figure 4** *Principle of x-ray diffraction (after ref 34)*

The Bragg's equation will be fulfilled for any whole number of the integer n, thus giving rise to different reflection orders.

WAXD is used as a tool to determine the structure of layered silicate based nanocomposites.[2] When an intercalated structure is obtained after nanocomposite processing, the peak which was due to reflection from the pure layered silicates is shifted to lower angles. This is due to the increased distance between the silicate sheets in the nanocomposite (increased $d$ in Bragg's equation) compared to pure layered silicates with no polymer intercalated. This is illustrated in Figure 5. A smaller angle in the diffractogram corresponds to a larger gallery height (001-diffraction). For exfoliated nanocomposites there will be no coherent x-ray diffraction from the distributed silicate layers because the gallery height is too large to detect and because there may be a no-ordered layer separation. When both intercalation and exfoliation co-exist, a broadening of the diffraction peak is often observed.[9]

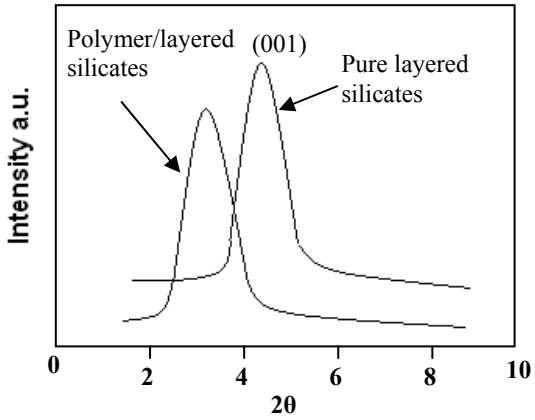


**Figure 5** *Illustration of the formation of intercalated polymer/layered silicate nanocomposite analyzed by WAXD showing that the gallery height of the layered silicates is larger in the nanocomposite compared to pure layered silicates*

When polymer-layered silicate nanocomposites are investigated in WAXD, three factors need to be considered.[35] First, when only a small amount of layered silicate is present in the composite, WAXD analysis must be sensitive enough to detect the crystalline structure of the layered silicates in the polymer. If not, false conclusions about no peak appearing in the diffraction pattern because of exfoliation can be drawn. Then, the analysis is performed at low angle in order to evaluate the d-spacing between the silicate layers. As a consequence, the irradiated surface may include not only the sample but also the sample holder. This might create a large amount of noise and complicate the interpretation of the XRD patterns. And, the depth of penetration of X-rays is inversely proportional to the diffraction angle. It means that the x-ray analysis at low angle will only reflect the structure present in a thin layer close to the surface. Therefore, a thin sample with a large surface area is recommended. Finally, if the layered silicates have a large distribution of interlamellar spacing, this will result in a smooth shoulder rather than a distinct peak in the WAXD-spectrum so that the nanocomposites might appear exfoliated.

For a cellulose crystal, as shown in Figure 6, there will be reflections from three different planes, as well as reflections from higher orders. The structure of cellulose I (native cellulose) will typically have reflection peaks at $2\theta = 14.6^{\circ}$, $16.4^{\circ}$ and $22.7^{\circ}$.[36] There will however be no peaks corresponding to the stacking of the crystallites as for layered silicates and therefore, the WAXD method can not be utilized to determine the structure of CNW based

nanocomposites. Utilization of WAXD on CNW, layered silicates and their nanocomposites will be described in Paper III and VI.

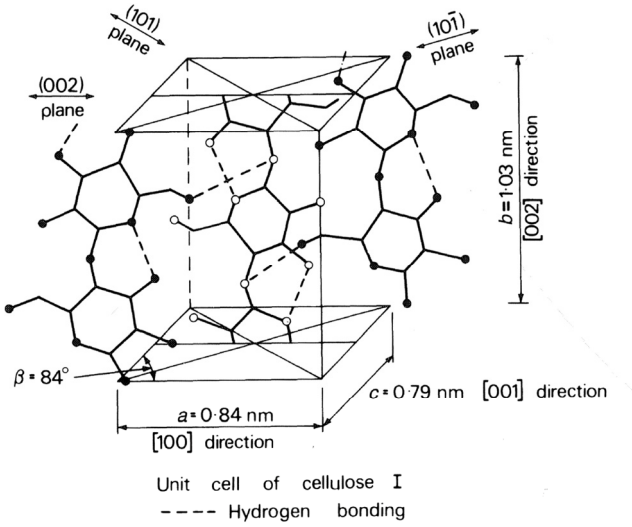


**Figure 6** *The unit cell of cellulose I* [19]

# 3. Summary of appended papers

**Paper I**

**Microscopic Examination of Cellulose Whiskers and Their Nanocomposites**

This chapter describes the principle of different microscopes which can be utilized for structure characterization of cellulose nanowhiskers (CNW) and their nanocomposites. The microscopes explored were field emission scanning electron microscope (FESEM), transmission electron microscope (TEM) and atomic force microscope (AFM). Examples of different sample preparation techniques are presented and results from structure characterization of CNW and their nanocomposites with various matrices are summarized. Sample preparation of CNW was easy and it was possible to study the CNW in all microscopes, however more detailed information was obtained from TEM. It was possible to study the structure of both coated and uncoated surfaces of the nanocomposites in FESEM. Sample preparation and instrumentation of the nanocomposites for TEM examination was challenging and depended on the matrix used. It was possible to study the distribution of CNW in poly lactic acid (PLA), thermoplastic starch and cellulose acetate butyrate (CAB), however, lack of contrast was challenging in particular for the CNW in the CAB matrix. AFM is a surface technique and has therefore limited access to the bulk structure, it was however possible to obtain detailed information of the distribution of CNW in a PLA matrix.

**Paper II**

**Strategies for Preparation of Cellulose Whiskers from Microcrystalline Cellulose (MCC) as Reinforcement in Nanocomposites**

In this chapter two possible ways to isolate cellulose nanowhiskers from microcrystalline cellulose were explored. In the first procedure the CNW were isolated from MCC and dispersed in water by sulfuric acid treatment. In the second procedure the cellulose nanowhiskers were isolated from MCC using dimethylacetamide/lithium chloride (DMAc/LiCl) and then dispersed in the same organic medium. The separation with DMAc was carried out with and without LiCl. The suspensions were characterized by evaluation of flow birefringence, yield calculations, optical light microscope and atomic force microscope. It was found that the treatment with sulfuric acid was a more efficient way to separate the CNW from MCC compared to the treatment with DMAc(/LiCl). DMAc containing LiCl seemed to be more efficient than pure DMAc. Yield calculation and atomic force microscopy

examination of the CNW from the DMAc/LiCl suspension were however restricted because it was found to be difficult to completely remove the solvent from CNW.

**Paper III**

**Investigation of the Structure of Cellulose Whiskers and Its Nanocomposites Using TEM, SEM, AFM and X-ray Diffraction**

In this study the structure of cellulose whiskers and their novel nanocomposites with a biopolymer matrix was investigated combining FESEM, TEM, AFM and wide angle x-ray diffraction (WAXD). The cellulose whiskers used in this study were isolated from MCC by acid hydrolysis. X-ray diffraction patterns indicated that the MCC contained both amorphous and crystalline regions. It was concluded that the isolation treatment with sulfuric acid removed the residual amorphous regions. The x-ray diffraction analysis of the nanocomposites showed that the diffraction peaks from cellulose were not detectable due to overlap by the biopolymer itself. However, information regarding change of matrix crystallinity before and after processing was obtained. The microscopic examination gave both nano- and microstructural information of CNW and the nanocomposites. In FESEM the metal coating influenced the size of the whiskers in the biopolymer matrix. Effort was made to obtain images without metal coating by lowering the accelerating voltage. However, the resolution appeared then to be insufficient. AFM was the most convenient method because the analysis could be performed under ambient conditions without any need for pretreatment of the samples, in contrast to electron microscopy. TEM analysis seemed to give the most genuine information of the cellulose whiskers in the matrix, however lack of contrast was challenging.

**Paper IV**

**Structure and Thermal Properties of Poly(lactic acid)/Cellulose Whiskers Nanocomposite Materials.**

The goal of this article was to produce nanocomposites based on poly(lactic acid) (PLA) and CNW. PLA is a hydrophobic matrix and it is therefore difficult to disperse the hydrophilic CNW in the polymer. The nanocomposites were prepared by solution casting using chloroform as solvent. The sulfuric acid treated CNW were transferred from water to chloroform by first freeze-drying the CNW. Two strategies to obtain well dispersed CNW in the chloroform and hence in the PLA matrix after freeze-drying were studied in this paper. The CNW water suspension was treated with either a surfactant or the CNW were transferred

to tert-butanol prior to freeze-drying. FESEM showed that untreated whiskers formed flakes, while tert-butanol treated whiskers formed loose networks during freeze drying. The surfactant treated whiskers showed flow birefringence in chloroform. Transmission electron microscope showed that the surfactant treated whiskers produced a well dispersed nanocomposite. The dynamic mechanical thermal analysis showed that both the untreated and the tert-butanol treated whiskers were able to improve the storage modulus of PLA at higher temperatures and a 20 °C shift in the tan δ peak was recorded for the tert-butanol treated whiskers.

**Paper V**

**Characterization of Cellulose Whiskers and Their Nanocomposites by Atomic Force and Electron Microscopy**

The aim of this paper was to compare and explore electron microscopy and atomic force microscopy for structure determination of CNW and their nanocomposites with poly(lactic acid). From conventional bright-field transmission electron microscopy it was possible to identify individual whiskers which were determined to be 210 ± 75 nm in length and 5 ± 2 nm in width. AFM overestimated the width of the whiskers due to the tip broadening effect. Field emission scanning electron microscopy allowed for a quick examination giving an overview of the sample, however, the resolution was considered insufficient for detailed information. Ultramicrotomy of nanocomposite films at cryogenic temperatures enabled detailed inspection of the cellulose whiskers in the poly(lactic acid) matrix by AFM. FESEM applied on fractured surfaces allowed insight into the morphology of the nanocomposite, but rather restricted due to the metal coating and limited resolution. Detailed information was obtained from TEM, however this technique required staining and suffered in general from limited contrast and beam sensitivity of the material.

**Paper VI**

**Characterization of Starch Based Nanocomposites**

In this article the aim was to study the structure of biopolymer nanocomposites with well dispersed nanoreinforcements. Plasticized starch is a water soluble biopolymer and was therefore chosen as the matrix for the hydrophilic CNW and untreated layered silicate reinforcements. Sorbitol and water were used as plasticizers. From FESEM examination of the nanocomposites no agglomerates of the reinforcements in the matrix were found which indicated a uniform distribution. Sample preparation for TEM examination of the

nanocomposites showed to be difficult due to the water affinity of starch and therefore, conventional sample preparation for polymers was not applicable for these nanocomposites. Two methods were therefore explored to prepare samples for TEM examination; chemical fixation and freeze etching. It was found that it was possible to characterize the nanostructure both parallel and perpendicular to the nanocomposite surface by the freeze etching technique. Both nanocomposites showed well distributed reinforcements in the starch matrix. Dynamic mechanical thermal analysis showed that the storage modulus was significantly improved at elevated temperatures, especially for the layered silicate nanocomposite. Both nanocomposites showed a significant improvement in tensile properties compared to the pure matrix.

**Paper VII**

**Orientation of Cellulose Nanowhiskers in Polyvinyl Alcohol (PVA)**

The goal of this paper was to characterize the structure of aligned cellulose nanowhiskers in a polymer after exposure to a strong magnetic field. The matrix used was water soluble polyvinyl alcohol (PVA) in order to obtain well distributed CNW in the matrix. To avoid water in the sample preparation step, light microscope, FESEM and AFM were used for the structure characterization of the nanocomposite. To get access to the bulk structure when using FESEM and AFM, a method for etching the PVA with ionized argon gas was explored. The different microscopy investigations of prepared nanocomposites indicated that the cellulose whiskers were oriented perpendicular to the direction of the magnetic field. The dynamic mechanical thermal analysis further strengthened the idea of alignment because the results showed that the dynamic modulus of the nanocomposite was around 2 GPa higher at room temperature in the aligned direction compared to the transverse direction.

# 4. Conclusions

In this thesis cellulose nanowhiskers (CNW) were separated from microcrystalline cellulose (MCC) and incorporated in different biopolymers to obtain nanocomposites based on renewable resources. The overall aim of this work was to characterize the structure of both CNW and their nanocomposites with different matrices. X-ray diffraction analysis showed that the MCC consisted of both amorphous and crystalline regions. It was found that the sulfuric acid isolation treatment removed the amorphous regions. From TEM analysis the size of the whiskers were measured to be 210 ± 75 nm in length and 5 ± 2 nm in width. The sample preparation and instrumentation of biopolymer based nanocomposites showed to be challenging because they are non-conductive, soft, often water sensitive and consist of low atomic number elements. In the studies it was found that field emission scanning electron microscope (FESEM) was a very convenient method to get an overview of the material on microlevel and can therefore be an important first-step in the analysis of the nanocomposite structure. Lack of aggregates in a sample indicates well distributed CNW in the matrix. For nanostructured information about the distribution of CNW in a polymer matrix transmission electron microscope (TEM) and atomic force microscope (AFM) can be used. In TEM it is possible to access the bulk structure of the material, but the whiskers might be cut in the sample preparation step and therefore TEM examination of the nanocomposites may underestimate the length of the whiskers. TEM analysis of the CNW nanocomposites can be challenging due to sample preparation of a water sensitive or soft matrix, beam sensitivity and lack of contrast between the whiskers and the matrix. AFM could therefore be a powerful alternative to TEM because it has sufficient resolution capabilities without the need of staining, and beam sensitivity is no issue. The AFM technique described here is however a surface technique and therefore has only limited access to the bulk structure.

# 5. Future work

Different microscopes have mainly been utilized to examine the structure of CNW and their nanocomposites in this thesis. There are other techniques found in literature which would be interesting to explore, such as small angle x-ray scattering, small angle neutron scattering and light scattering. For well dispersed nanocomposites it would be interesting to explore in more detail how the CNW are oriented in the matrix by preparing samples both parallel and perpendicular to the surface. For AFM examination it would be interesting to utilize its ability to measure forces in materials to get more knowledge of the interface between the CNW and the matrix. For TEM examination of nanocomposites there are a vast number of parameters which can be explored, such as using other staining agents, increase contrast by labeling the whiskers with high atomic number elements, chemical fixation of water soluble polymers, varying operating parameters and modes etc. There are new FESEMs on the marked which have resolution approaching that of an AFM which would be interesting to explore further for structure characterization of CNW and their nanocomposites.

There are two important issues concerning these new materials which are not dealt with in this thesis which should be mentioned. First of all, the aim of replacing fossil fuel based plastics with plastics from renewable resources is to limit emission of fossil fuel based carbon dioxide. It is therefore important to carry out a life cycle analysis of the bioplastics in question to evaluate how much fossil fuel based energy is put into the production of the materials. Other sources as starting materials for both CNW and matrix should also be explored, such as the utilization of food wastes. Another concern is what impact the nanoparticles will have on the environment. There is a need for a thorough evaluation of the health aspect of these materials and of which processing precautions are needed.

# References


1. Ajayan, P.M.; Schadler, L.S.; Braun, P.V. Nanocomposite Science and Technology 1th Edition; Wiley VCH Verlag GmbH & CO, Weinheim; 2003
2. Ray, S.S.; Okamoto, M. Polymer/layered silicate nanocomposites: a review from preparation to processing; Prog. Polym. Sci. 2003, 28, 1539-1641
3. Garces, J.M.; Moll, D.J.; Bicerano, J.; Fibiger, R.; McLeod, D.G. Polymeric nanocomposites for automotive applications; Adv. Matr. 2000, 12, 1835-1839
4. Ray, S.S; Bousmina, M. Biodegradable polymers and their layered silicate nanocomposites: In greening the 21st century materials world; Prog. Mater Sci. 2005, 50, 962-1079
5. Grunert, M; Winter, W.T. Nanocomposites of Cellulose Acetate Butyrate Reinforced with Cellulose Nanocrystals; J. Polym. Environ. 2002, 10, 27-30
6. Anglés, M.N.; Dufresne, A. Plastisized starch/tunicin whiskers nanocomposites. 1. Structural analysis; Macromolecules 2000, 33, 8344-8353
7. Petersson, L.; Oksman, K. Preparation and Properties of Biopolymer-Based Nanocomposite Films Using Microcrystalline Cellulose. In: Cellulose Nanocomposites Processing, Characterization and Properties; Oksman, K.; Sain M. (ed); ACS Symposium series 938; Oxford Press, 2006; 132-150
8. Hamad, W. Cellulosic Materials Fibers, Networks and Composites, Kluwer Academic Publishers, Boston/Dordrecht/London, 2002
9. Alexandre, M.; Dubois, P. Polymer-layered silicate nanocomposites: preparation, properties and uses of a new class of materials; Mater. Sci. Eng., R. 2000, 28, 1-63
10. Liu, F.K.; Hsieh, S.Y.; Ko, F.H.; Chu, T.C. Synthesis of gold/poly(methyl methacrylate) hybrid nanocomposites; Colloids Surf., A: Physicochem. Eng. Aspects 2003, 231, 31-38
11. Thostenson, E.; Ren, Z.; Chou, T.W. Advances in the science and technology of carbon nanotubes and their composites: a review; Compos. Sci. Technol. 2001, 61, 1899-1912
12. Giannelis, E.P.; Krishnamoorti, R.; Manias, E. Polymer-silicate nanocomposites: model systems for confined polymers and polymer brushes; Adv. Polym. Sci. 1999, 138, 107-147
13. Bafna, A.; Beaucage, G.; Mirabella, F.; Mehta, S. 3D Hierarchical orientation in polymer-clay nanocomposite films; Polymer 2003, 44, 1103-1115

14. Dennis, H.R.; Hunter, D.L.; Chang, D.; Kim, S.; White, J.L.; Cho, J.W.; Paul, D.R.; Dennis H.R. Effect of melt processing conditions on the extent of exfoliation in organoclay-based nanocomposites; Polymer 2001, 42, 9513-9522
15. Paul, M.A.; Alexandre, M.; Degee, P.; Henrist, C.; Rulmont, A.; Dubois, P. New nanocomposite materials based on plasticized poly($_L$-lactide) and organomodified montmorillonites: thermal and morphological study; Polymer 2003, 44, 443-450
16. Tashiro, K.; Kobayashi, M. Theoretical evaluation of three-dimensional elastic constants of native and regenerated celluloses: role of hydrogen bonds; Polymer 1991, 32, 1516-1526
17. Bondeson, D.; Mathew, A.; Oksman, K. Optimization of the isolation of nanocrystals from microcrystalline cellulose by acid hydrolysis; Cellulose 2006, 13, 171-180
18. Helbert, W.; Cavaillé, J.Y.; Dufresne, A. Thermoplastic nanocomposites filled with wheat straw cellulose whiskers. Part I: Processing and mechanical behavior; Polym. Compos. 1996, 17, 604-61
19. Krässig, H.A. Cellulose Structure, Accessibility and Reactivity; Polymer Monographs, Volume 11, Gordon and Breach Science Publishers, 1993
20. Levis, S.R.; Deasy, P.B. Production and evaluation of size reduced grades of microcrystalline cellulose; Int. J. Pharm. 2001, 213, 13-24
21. Battista, O.A.; Smith, P.A., Microcrystalline cellulose; J. Ind. Eng. Chem. 1962, 54, 20-29
22. Petersen, K.; Væggemose Nielsen, P.; Bertelsen, G.; Lawther, M.; Olsen, M.B.; Nilsson, N.H.; Mortensen, G. Potential of biobased materials for food packaging; Trends Food Sci. Tech. 1999, 10, 52-68
23. Chandra, R.; Rustgi, R. Biodegradable Polymers, Prog. Polym. Sci. 1998, 23, 1273-1335
24. Vink, E.T.H.; Rabago, K.R.; Glassner, D.A.; Gruber, P.R. Applications of life cycle assessment to NatureWorks polylactide (PLA) production; Polym. Degrad. Stab. 2003, 80, 403-419
25. Lunt, J. Large-scale production, properties and commercial applications of polylactic acid; Polym. Degrad. Stab. 1998, 59, 145-152
26. Oksman, K., Selin, J-F. Plastics and composites from polylactic acid**.** In: Natural Fibers, Plastics and Composites; Wallenberger, F.T.; Weston, N.E. (ed); Kluwer Academic Publishers, 2004, 149-165

27. Striegel, A.M. Theory and applications of DMAc/LiCl in the analysis of polysaccharides; Carbohydr. Polym. 1997, 34, 267-274
28. de Vlieger, J.J. Green plastics for food packaging. In: Novel food packaging techniques; Ahvenainen, R. (ed); Woodhead Publishing Limited, 2003, 519-534
29. Fischer, S. Nanoparticle Reinforced Natural Plastics. In: Natural Fibers, Plastics and Composites; Wallenberger, F.T.; Weston, N. (ed); Kluwer Academic Publishers; New York, 2004
30. Mohanty, A.K.; Drzal, L.T.; Misra, M. Nano Reinforcements of Bio-based Polymers -- The Hope and the Reality; Polym. Mater. Sci. Eng. 2003, 88, 60-61
31. Heux, L.; Chauve, G.; Bonini, C. Nonflocculating and chiral nematic self-ordering of cellulose microcrystals suspensions in nonpolar solvents; Langmuir 2000, 16, 8210-8212
32. Røst, E.; Furuseth, S. Røntgendiffraksjon, Anvendelse til analyse av faste, krystallinske stoffer, KJ-MV 213, Kjemisk institutt, 1996
33. Gedde, U.W. Polymer Physics, Kluwer Academic Publishers; Dortrecht/Boston/London, 1993
34. Goldstein, J.; Newbury, D.; Joy, D.; Lyman, C.; Echlin, P.; Lifshin, E.; Sawyer, L.; Michael, J. Scanning Electron Microscopy and X-Ray Microanalysis, 3rd Edition, Kluwer Academic/Plenum Publishers; New York, 2003
35. Kornmann, X. Synthesis and Characterisation of Thermoset-Layered Silicate Nanocomposites, Doctoral Thesis, Luleå University of Technology, 2001
36. Mathew, A.; Dufresne, A. Morphological Investigation of Nanocomposites from Sorbitol Plasticized Starch and Tunicin Whiskers; Biomacromolecules 2002, 3, 609-617

# Papers

| | |
|---|---|
| Paper I | Microscopic Examination of Cellulose Whiskers and Their Nanocomposites |
| Paper II | Strategies for Preparation of Cellulose Whiskers from Microcrystalline Cellulose as Reinforcement in Nanocomposites |
| Paper III | Investigation of the Structure of Cellulose Whiskers and Its Nanocomposites using TEM, SEM, AFM and X-ray Diffraction |
| Paper IV | Structure and Thermal Properties of Poly(lactic acid)/Cellulose Whiskers Nanocomposite Materials |
| Paper V | Characterization of Cellulose Whiskers and Their Nanocomposites by Atomic Force and Electron Microscopy |
| Paper VI | Characterization of Starch Based Nanocomposites |
| Paper VII | Orientation of Cellulose Nanowhiskers in Polyvinyl Alcohol (PVA) |

Paper I

Paper I: Kvien, I ; Oksman, K: Microscopic Examination of Cellulose Whiskers and Their Nanocomposites. Characterization of Lignocellulosic Materials / Hu, TQ: Blackwell Publishing is not included in the pdf due to copyright.

Paper II

## Chapter 2

# Strategies for Preparation of Cellulose Whiskers from Microcrystalline Cellulose as Reinforcement in Nanocomposites

**Daniel Bondeson, Ingvild Kvien, and Kristiina Oksman**

**Department of Engineering Design and Materials, Norwegian University of Science and Technology, Rich Birkelands vei 2b, N7491 Trondheim, Norway**

In this chapter we present two possible ways to prepare nanosized cellulose whiskers from microcrystalline cellulose (MCC) derived from Norwegian spruce (Picea abies). The first procedure was to prepare a stable water suspension of cellulose whiskers after treatment with sulfuric acid ($H_2SO_4$). In the second procedure, the whiskers were dispersed in an organic medium; dimethylacetamide/lithium chloride (DMAc/LiCl). It was possible to produce a stable colloidal suspension of cellulose whiskers with $H_2SO_4$. The whisker size was measured to be between 200-400 nm in length and less than 10 nm in width. The dispersion with DMAc was carried out with and without LiCl. Atomic force microscopy analysis of the sample without LiCl confirmed the presence of both whiskers and MCC particles. Characterization of the suspension containing LiCl was restricted due to difficulties in solvent removal.

## Introduction

The interest in producing composite materials with nanosized reinforcement, i.e. nanocomposites, has grown tremendously in recent years. The enthusiasm is due to the extraordinary properties this kind of materials exhibit because of the nanometric size effect of the reinforcement. The challenge has been, especially for a continuous and large scale production, to get the reinforcement well dispersed and without agglomerates in a continuous matrix. Most efforts have been to produce nanocomposites with inorganic reinforcements, but organic material has also been used, including cellulose. Among the advantages of using cellulose as a renewable reinforcement is its abundance, together with easier recycling by combustion in comparison with inorganic filled systems. There are also limitations on the use of unmodified cellulose crystals due to their incompatibility with a typically more hydrophobic thermoplastic matrix and difficulties in achieving acceptable dispersion levels (*1*). Preparation of nanocomposites from a stable aqueous suspension is limited to either hydrosoluble polymers or an aqueous suspension of polymer, i.e. a latex to achieve a good level of dispersion (2). Several methods have been explored to achieve a dispersion of cellulose crystals, or cellulose whiskers referring to its needle like structure, in low-polar solvents to widen the possible matrixes for nanocomposite processing. The use of a surfactant (*3*), grafting of poly(ethylene glycol) onto whiskers (*4*), partially silylation of whiskers (*5, 6*) all led to stable suspensions in various low-polarity solvents. Azizi Samir et al (*2*) redispersed cellulose whiskers in an organic solvent without addition of a surfactant or any chemical modification.

Another challenge is the tedious processing steps by means of purification, bleaching, fibrillation, hydrolysis and the low yield of the final dispersion of cellulose whiskers. There are different techniques to accomplish this isolation of cellulose whiskers. Acid hydrolysis of cellulose is a well know process to remove amorphous regions and several studies have been reported where cellulose crystallites/whiskers were identified and separated from various sources. Nickerson and Habrle (*7*) talked about cellulose crystallites from cellulosic materials by hydrochloric and sulfuric acid hydrolysis in 1947, and in 1952 Ranby (*8*) reported the preparation of cellulose whiskers from microfibrils by acid hydrolysis. Marchessault with co workers studied the hydrolysis of chitin, native, mercerized, and bacterial cellulose using acid hydrolysis and reported birefringence (9*,10*). At CERMAV-CNRS in France, cellulose whiskers have been separated from various sources like wheat straws, tunicin etc, and have been used as reinforcements in polymer matrices (*1*, *11-14*). Incorporation of these nanosized elements into a polymeric matrix usually resulted in outstanding properties, with respect to their conventional microcomposite counterpart. Recently, microcrystalline cellulose (MCC) has

attracted attention as a possible starting material for the preparation of cellulose based nanocomposites (*15*). MCC is a commercially available material which is mainly used as a binder in tablets and capsules. It is prepared from native cellulose by acid hydrolysis, back-neutralisation with alkali and spray-drying (*16*). Strong hydrogen bonding between the individual cellulose crystals produced promotes re-aggregation during drying procedures (*16*). Thus, the MCC produced consists of aggregated bundles of crystallites with different particle sizes. To utilize cellulose crystals as reinforcement, the hydrogen bonds between the crystals must be broken and the cellulose crystals must be well dispersed in the matrix.

In this study we present two possible ways to prepare nanozised cellulose whiskers from microcrystalline cellulose (MCC) derived from Norway spruce (Picea abies). The aim of the first preparation technique was to prepare a stable colloidal water suspension of cellulose whiskers after treatment with sulphuric acid. In the second route the aim was to disperse the whiskers in an organic medium, DMAc/LiCl, to make the suspension compatible with low polarity polymers. This method is expected to be a new route to isolate whiskers from commercially available wood sources and obtain a stable dispersion in an organic medium, in a single step.

## Sulphuric acid

Treating the cellulose with acid, the cellulose undergoes acidic hydrolysis. It is preferably the amorphous parts of the cellulose that undergoes acidic hydrolysis rather than the crystalline (*17*). Hydrolysis of cellulose is greatly influenced by the acid concentration and concentrated sulfuric acid can smoothly hydrolyze the crystalline cellulose (*17*). Treating cellulose with sulfuric acid involves an esterification of hydroxyl groups by sulfate ions, see Figure 1 (*18*).

Introduction of sulfate groups along the surface of the crystallites will result in a negative charge of the surface as the pH increase. This anionic stabilization via the attraction/repulsion forces of electrical double layers at the crystallites is probably the reason for the stability of the colloidal suspensions of crystallites (*10*). Above critical concentrations, the suspension form a chiral nematic phase (*19*). It is possible to disrupt this chiral nematic phase by shear and the rods will align parallel to flow direction, exhibiting nematic ordering (*20*).

The cellulosic material is either directly immersed in sulfuric acid with known concentration (*10,21*) or immersed in water, which is kept in ice, where at sulfuric acid is added slowly to reach final concentration (*12*). The ice bath and slow addition of sulfuric acid is utilized to prevent elevated temperatures and to hinder hydrolysis of cellulose in the suspension during addition of acid. After this step, the suspension is heated while stirring, and it is in principal here the hydrolysis of cellulose take place. As mentioned earlier, the sulfuric acid concentration greatly influences the cellulose hydrolysis (*17*). Mukherjee *et al.*

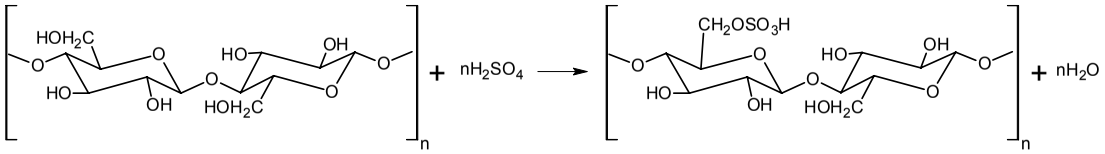


*Figure 1. Esterification of hydroxyl groups by sulfate ions from sulfuric acid treatment of cellulose.*

(*21*) observed that ramie and cotton hydrolysis was effective in a sulfuric acid concentration between 9.69 and 9.94 mol/L at 20 °C in leading to a colloidal suspension. The effect of a lower concentration of acid, 9.18 mol/L, was negligible in 24 h, and relatively slight after 72 h. A concentration of 10.04 mol/L or more lead ultimately to complete solution in the acid, and if the treatment was stopped before this stage was reached, the cellulose was found to be partially transformed to Cellulose II. Along with acid concentration, time and temperature of hydrolysis are also important parameters (*22*). It has been reported that an increased hydrolysis time increased the surface charge and amount of sulfate groups (*22*).

After the hydrolysis step, the excess sulfuric acid in the suspension has to be removed and this is done by either centrifugation (*10,12,19,21,23*), filtration (7), or by solely dialysis (*12*). In centrifugation, the sediment is kept and the supernatant is removed and replaced by distilled/deionized water. The sediment is then mixed with the new distilled/deionized water and centrifuged. This procedure is continued until the supernatant is becoming turbid, often at pH between 1 and 3, and as mentioned before, this is most likely due to repulsive forces between the crystallites which come into play as the pH increases (*10*). The suspension is then dialyzed against distilled/deionized water to remove the last residue of the sulfuric acid, and this usually takes a couple of days. To further disperse the preparations, some minutes of ultrasonic treatment can be used (*12,19,22,23*). The ultrasonic treatment can be carried out in an ice bath in order to avoid overheating which might cause desulfation of the sulfate groups on the surface of the crystallites (*22*). Helbert *et al.* (12) concentrated the cellulose suspension by dialysis against high molecular weight polyethylene glycol (PEG 35 000).

## Dimethyl Acetamide/Lithium Chloride

N,N-dimethyl acetamide (DMAc) containing lithium chloride (LiCl) is a well-known and favorable solvent system for cellulose (*24*). It was originally developed in 1976 to dissolve chitin (*25*). The optimum concentration of LiCl in the solvent mixture is reported to be between 5 and 9 wt% (26). Different mechanisms for the interaction between cellulose and DMAc/LiCl are suggested (*27*). Turbak (*28*) suggested that LiCl is forming a complex with dimethylacetamide, releasing $Cl^-$, which acts as a base toward the hydrogen on the cellulose hydroxyl group, thus $Cl^-$ plays a major role in the dissolution by breaking up the inter- and intrahydrogen bonds. It is found that the use of other salts such as LiBr, $LiNO_3$ etc does not work (*28*). Water has to be excluded from the solvent system since both LiCl and DMAc are very hygroscopic (*27*). Water hinders complexation with cellulose and promotes the formation of polymer aggregates (*29*). Several authors report the risk of degradation of the cellulose upon treatment with DMAc/LiCl, thus the processing conditions have to be

carefully considered. According to Potthast et al (*30*) the treatment of cellulose with DMAc/LiCl might cause severe degradation of cellulose dependent of the heating time and temperature. They found that the degradation occurred via endwise peeling reactions due to N,N-dimethylacetoacetamide, which is a condensation product of DMAc formed during heating. N,N-dimethylketenium ions are formed at temperatures above 80ºC and causes random cleavage of cellulose molecules. Further, they found that the degradation of pulp is strongly accelerated in the presence of LiCl. Additionally they reported a yellowing of the mixture caused by chromophores formed in LiCl-catalyzed condensation reactions from DMAc. The discoloration of the pulp also originated from furan-type structures which are formed upon heating in DMAc or DMAc/LiCl.

Apart from being an effective solvent for cellulose, DMAc/LiCl is an interesting swelling agent for cellulose. Berthold et al (*31*) reported that pure DMAc or DMAc containing only small amounts of LiCl (0,5% w/v) was sufficient for swelling of unbleached sulphate fibres which facilitated fibrillation of the fibres. It is expected that similar conditions is able to penetrate in between the cellulose whiskers in microcrystalline cellulose, which will lead to isolation of the cellulose whiskers by breaking the hydrogen bonds between the crystals.

## Experimental

### *Materials*

Microcrystalline cellulose from Norway spruce (Picea abies) supplied by Borregaard ChemCell, Sarpsborg, Norway, with a particle size between 10 to 15 μm, was used as starting material for preparation of cellulose whiskers.

Sulphuric acid of analytical purity was purchased from Merck (Darmstadt, Germany). DMAc of analytical purity was purchased from LAB Scan (Dublin, Ireland). Extra pure LiCl, was purchased from Merck (Darmstadt, Germany).

### *Methods*

Microcrystalline cellulose, 10 g/100 mL, was hydrolyzed in 9mol/L sulfuric acid at 44°C in 130 min. The excess of sulfuric acid was removed by repeated cycles of centrifugation (10 min at 12 000 rpm, Sorvall RC-5B), i.e. the supernatant was removed from the sediment and replaced by new deionized water and mixed. The centrifugation step was continued until the supernatant became turbid. The last washing step was carried out by dialysis against deionized water until the washing water was constant in pH, i.e. about neutrality.

The swelling and separation of MCC with DMAc was carried out with and without LiCl. Two suspensions of 1 wt% MCC in DMAc containing 0 and 1 wt% LiCl were prepared. The suspensions were heated and mechanically stirred for 5 days. The heating temperature was set to 60°C and 80°C for the suspensions containing 1 and 0 wt% LiCl, respectively. The suspensions were subsequently treated in an ultrasonic bath for 60 minutes. After the treatment unseparated particles were removed by centrifugation at 1000 rpm for 5 minutes. The final suspensions were stored in a refrigerator.

*Characterization*

Yield was calculated as % (of initial weight) of MCC after hydrolysis. For calculation of the yield after DMAc(/LiCl) treatment, a small amount of the suspensions was vacuum-dried for ~15 hours and oven-dried at 100°C for ~15 hours to remove residual DMAc(/LiCl). The dried cellulose whiskers were then kept in a desiccator before weighing.

Flow birefringence in the suspensions was investigated by using two crossed polarization filters. The samples were diluted before examination.

Optical light microscope (OM) observations were performed using a Leica DMLB. OM was used in order to detect bigger particles and to get an overview in the microscopic level. The magnifications used were × 100, ×500 and × 1000. The sulphuric acid treated sample was diluted to a concentration of 0.1 g/100 mL before examination.

Atomic force microscopy (AFM) observation was performed using a NanoScope IIIa, Multimode™ SPM from Veeco. Calibration was performed by scanning a calibration grid with precisely known dimensions. All scans were performed in air with commercial Si Nanoprobes™ SPM Tips. Height- and phase images were obtained simultaneously in Tapping mode at the fundamental resonance frequency of the cantilever with a scan rate of 0.5 line/s using j-type scanner. The free oscillating amplitude was 3.0V, while the set point amplitude was chosen individually for each sample. A droplet of the suspension was placed on a freshly cleaved mica surface and allowed to dry at 80°C over-night before analysis.

Transmission electron microscope (TEM) observations were performed using a Philips CM30 operated at 100kV. A droplet of suspension was placed on a copper grid covered by a thin carbon film and allowed to dry at 80°C overnight.

## Results and Discussion

The yield after acid hydrolysis of the MCC was 30 % (of initial weigth). In an earlier study it was found from wide angle X-ray (WAXD) analysis that the MCC used in this study consisted not only of crystalline cellulose but also

included amorphous regions (*32*). One of the reasons why such a low yield was obtained might thus be that the residue amorphous regions in the starting material disintegrated during the hydrolysis. Further, the highest priority was to obtain a suspension of nanosized whiskers and it is possible that some of the cellulose crystals degraded during the treatment. It is also likely that cellulose whiskers were removed during the washing steps. For the DMAc(/LiCl) treated samples, the yield was only 1,5wt% for the suspension without LiCl. However, the suspension containing LiCl had a yield above 300wt%. An explanation for this unrealistic high yield is that the complex formed between the cellulose and the DMAc/LiCl system was still present in the dried sample, i.e. the DMAc/LiCl was not thoroughly removed.

Clear flow birefringence was seen for the acid hydrolyzed sample (0.1 g cellulose/100 mL) in cross polarized light, see Figure 2a. This indicates a nematic liquid crystalline alignment and reveals the existence of whiskers (*20*). The DMAc(/LiCl) suspensions appeared ivory and showed no signs of sedimentation when observed after two hours. Both suspensions showed flow birefringence, as seen in Figure 2b and c, but not as pronounced as for the hydrolyzed suspension.

A comparison of the sample prepared by acid hydrolysis with untreated MCC in OM at ×1000 magnification is shown in Figure 3. No particles could be seen for the treated sample due to restricted resolution of the light microscope. This indicates that there were possibly only nanosized cellulose whiskers in the suspension.

After treatment of MCC in DMAc(/LiCl) there were still a large number of micro-sized particles in the suspensions, but a swelling and partly separation of the MCC agglomerates had clearly occurred. The suspension without LiCl appeared to contain more scarcely separated particles than the suspension containing LiCl. It thus seemed that the solvent containing LiCl was more effective in releasing cellulose whiskers from the MCC particles. In Figure 4 OM pictures of the samples after removal of the largest particles by centrifugation are shown. The suspensions still contained a few micro-sized particles. It was however expected that in addition the suspensions contained nanosized whiskers which were not detectable in the light-microscope.

From AFM investigation of the acid hydrolyzed sample (0.1 g cellulose/100 mL), it was seen that a mat of whiskers were covering the surface after water had been permitted to evaporate, see Figure 5a. The AFM image reveals needle like structure of the cellulose, i.e. whiskers. One has to be aware of that the whiskers look thicker in AFM than in reality due to the well-known broadening effect due to tip convolution (33) in AFM. This will lead to a general broadening of the whiskers. Therefore, to determine the length and width of the whiskers, highly diluted samples of the hydrolyzed suspension were analysed in TEM. Figure 5b shows a TEM image of the hydrolyzed sample. Measurements from TEM images gave whiskers with a length between 200 – 400 nm and a width less than 10 nm. A tendency of agglomeration could be observed from TEM. It is not clear whether this was due to drying of the suspension or if it reflected the state of the suspension.

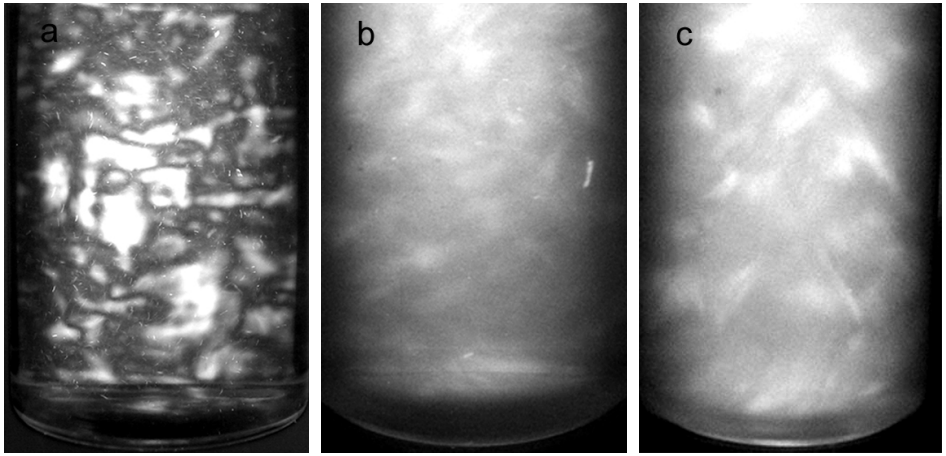


*Figure 2. Flow birefringence seen between two crossed polarizing films of the a) hydrolyzed suspension b) DMAc suspension c) DMAc/LiCl suspension (Container with 24 mm in diameter)*

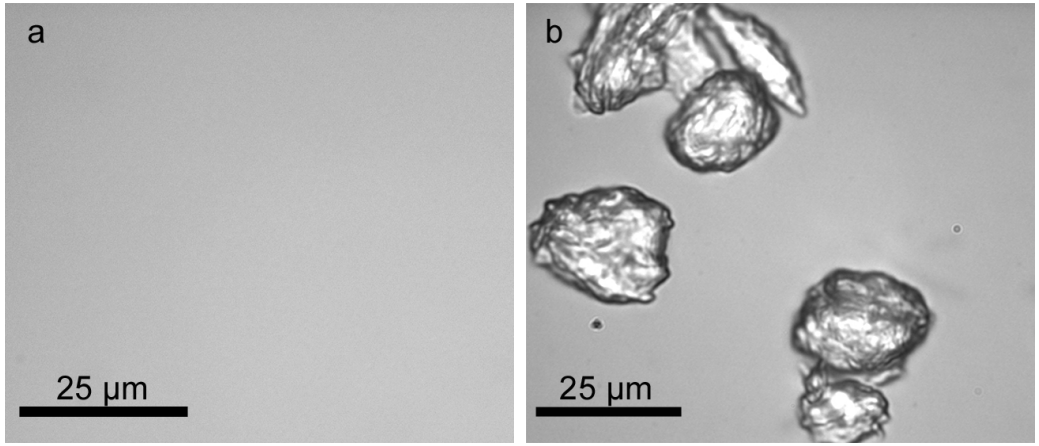


*Figure 3. (a) Sample produced with sulfuric acid hydrolysis and (b) untreated sample seen at ×1000 in light microscope. Agglomerates of cellulose are seen for untreated MCC but are abundant in the hydrolyzed sample.*

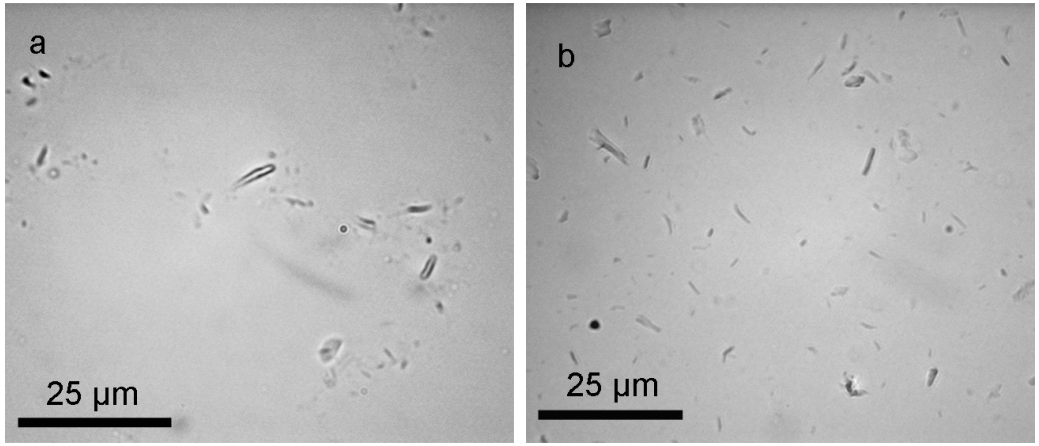


*Figure 4. a) MCC treated with DMAc and b) MCC treated with DMAc/LiCl seen at x1000 in the light microscope*

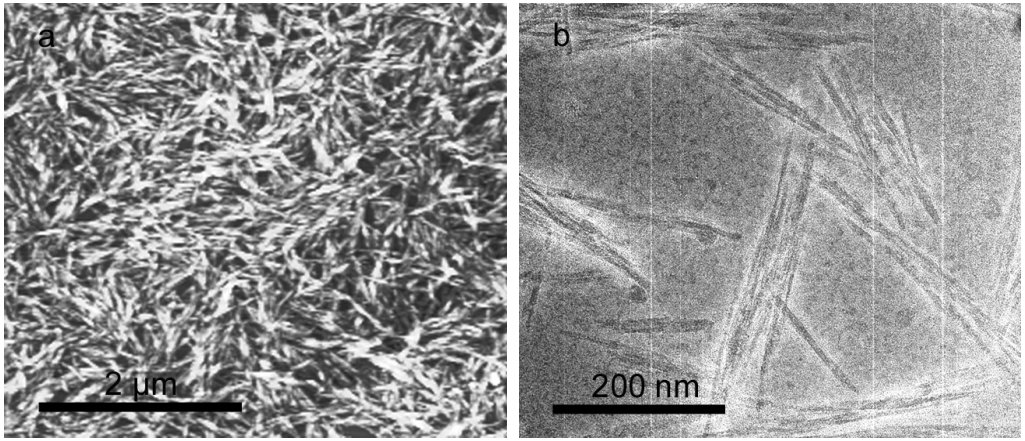


*Figure 5. a) Topography AFM image of whisker suspension b) TEM image of the whisker suspension after acid hydrolysis.*

Droplets of the DMAc(/LiCl) suspensions were dried onto a mica surface for observation by AFM. However, the dried sample of the suspension containing LiCl seemed to attrack moisture, even after prolonged treatment in vacuum oven at 100°C. A large number of droplets appeared on the sample which made it impossible for AFM analysis. Both LiCl and DMAc are known to be very hygroscopic (*27*). This indicates that the DMAc/LiCl solvent was still present in the dried sample, as found for the yield calculation. The sample without LiCl, however, showed no development of water droplets and was successfully analysed by AFM. From AFM it was evident that the suspension without LiCl was not homogenous but consisted of particles at different stages of separation. This is clearly demonstrated in Figure 6a showing a tightly packed particle separating into a large number of cellulose whiskers. Due to the broadening effect it was difficult to judge whether the structures observed were individual whiskers or several whiskers, agglomerated side-by-side. Determination of the whiskers length and width was therefore uncertain. In Figure 6b it is evident that even in the sample without LiCl there was still a remainder of solvent. The underlying mica surface can be observed from a hole in the solvent film.

In addition to cellulose whiskers the picture reveals spherical particles, which are believed to be fragments of cellulose. However, these fragments were already present in the MCC before DMAc was added. These fragments are presumably resulting from the sulphuric acid treatment of cellulose in the production of MCC. It is expected that the sample with LiCl contained more cellulose whiskers compared to the sample without LiCl due to the higher yield and visible water uptake from the dried sample. This was however not possible to confirm by AFM analysis.

## Conclusions

Two possible ways to prepare cellulose whiskers from commercially available microcrystalline cellulose (MCC) based on wood were explored. The aim of the first method was to prepare a stable water suspension of cellulose whiskers after treatment with sulfuric acid. In the second method the aim was to disperse the whiskers in an organic medium, DMAc/LiCl, to make it compatible with low polarity polymers.

With sulfuric acid concentration of 9 mol/L, it was possible to produce cellulose whiskers with length between 200 – 400 nm and a width less than 10 nm in approximately 2 h and with a yield of 30 % (of initial weigth). Disintegration of amorphous regions and degradation of crystalline parts during hydrolysis, and lost via the washing steps is probably the explanation for the low yield.

The swelling and separation with DMAc was carried out with and without LiCl to study the effect of LiCl in the separation process. Both suspensions appeared ivory and showed birefringence between cross polarizers, which is an

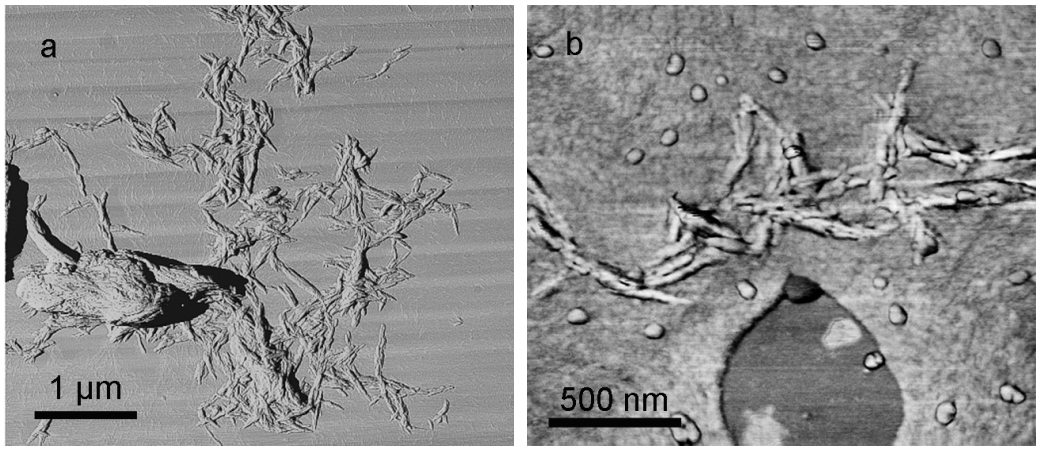


*Figure 6. a) AFM phase image of the dried suspension without LiCl showing both cellulose particles and cellulose whiskers b) AFM phase image of the dried suspension without LiCl showing remainder of solvent*

indication of the presence of whiskers. The solvent containing LiCl appeared to be more effective in releasing the cellulose whiskers from the MCC agglomerates. However, characterization of the suspension containing LiCl was challenging due to difficulties in removing the solvent. This was reflected in the unrealistic high yield of the sample containing LiCl. Atomic force microscopy analysis of the sample without LiCl confirmed the presence of cellulose whiskers, but also revealed unseparated MCC particles.

## Acknowledgements

We thank the Research Council of Norway for financial support and Borregaard ChemCell in Sarpsborg, Norway, for providing us with MCC. We also thank Kristin Brevik Antonsen and Dr. Simon Ballance at Department of Biotechnology at Norwegian University of Science and Technology for providing us with necessary equipment used in this research.

## References

1. Dufresne, A.; Cavaillé, J.Y. ACS Symp. Ser. **1999**, *723*, 39-54
2. Azizi Samir, M.A.S.; Alloin, F.; Sanchez, J-Y.; Kissi, N.E.; Dufresne, A. Macromolecules **2004**, *37*, 1386-1393
3. Heux, L.; Chauve, G.; Bonini, C. Langmuir **2000**, *16*, 8210-8212
4. Araki, J.; Wada, M.; Kuga, S. Langmuir **2001**, *17*, 21-27
5. Goussé, C.; Chanzy, H.; Excoffier, G.; Soubeyrand, L.; Fleury, E. Polymer **2002**, *43*, 2645-2651
6. Goussé, C.; Chanzy, H.; Cerrada, M.L.; Fleury, E.; Polymer **2004**, *45*, 1569-1575
7. Nickerson, R.F.; Habrle, J.A. Ind. Eng. Chem. **1947**, *39*, 1507-1512
8. Ranby, B.G. Tappi **1952**, *35*, 53-58
9. Marchessault, R.H.; Morehead, F.F.; Walter, N.M. Nature **1959**, *184*, 632-633
10. Marchessault, R.H.; Morehead, F.F.; Koch, M.J. J. Colloid Sci. **1961**, *16*, 327-344
11. Favier, V.; Chanzy, H.; Cavaillé J.Y. Macromolecules **1995**, *28*, 6365-6367
12. Helbert, W.; Cavaillé, J.Y.; Dufresne, A. Polym. Comp. **1996**, *17*, 604-610
13. Angles, M.N.; Dufresne, A. Macromolecules **2000**, *33*, 8344-8353
14. Morin, A.; Dufresne, A. Macromolecules **2002**, *35*, 2190-2199
15. Mathew, A.P.; Oksman, K.; Sain, M. *J. Appl. Polym. Sci.* **2005**, *97*, 2014-2025
16. Levis S. R.; Deasy P.B. Int. J. Pharm. **2001**, *213*, 13-24
17. Hon, D. N.-S.; Nobuo, S. Wood and Cellulosic Chemistry, Marcel Dekker, Inc., New York **1991**, pp 997-1013

18. Yao, S. Chin. J. Chem. Ing. **1999**, *7*, 47-55
19. Revol, J.-F.; Bradford, H.; Giasson, J.; Marchessault, R.H.; Gray, D.G. Int. J. Biol. Macromol. **1992**, *14*, 170-172
20. Orts, W.J.; Godbout, L.; Marchessault, R.H.; Revol, J.-F. Macromolecules **1998**, *31*, 5717-5725
21. Mukherjee, S.M.; Woods, H.J. Biochim. Biophys. Acta **1953**, *10*, 499-511
22. Dong, X.M.; Revol, J.-F.; Gray, D.G. Cellulose **1998**, *5*, 19-32
23. Araki, J.; Wada, M.; Kuga, S.; Okano, T. Colloids Surf. A: Physiochem. Eng. Aspects **1998**, *142*, 75-82
24. Striegel, A.M. Carbohydr. Polym. **1997**, *34*, 267-274
25. Austin, P.R. Ger. Offen. U.S. Patent 4,059,457, 1977
26. Dawsey, T. R.; McCormick, C.L. J. Macromol. Sci, Rev. Macromol. Chem. Phys. **1990**, *C30*, 405-40.
27. Dupont A.L. Polymer **2003**, *44*, 7-17
28. Turbak, A.F. Tappi J. **1984**, *67*, 94-96
29. Potthast, A.; Rosenau, T.; Buchner, R.; Roeder, T.; Ebner, G.; Bruglachner, H.; Sixta, H.; Kosma, P. Cellulose **2002**, *9*, 41-53
30. Potthast A.; Rosenau T.; Sartori J.; Sixta H.; Kosma P. Polymer **2003**, *44*, 7-17
31. Berthold, F.; Sjöholm, E.; Gustafsson, K.; Gamstedt, E.K.; Salmén, L. In Sustainable Natural and Polymeric Composites – Science and Technology; Lilholt, H.; Madsen, B.; Toftegaard, H.L., Cendre, E.; Megnis, M.; Mikkelsen, L.P.; Sørensen, B.F., Ed.; Risø National Laboratory; Roskilde, DK, 2002
32. Kvien, I.; Tanem, B.S.; Oksman, K. Proceeding, 8th Int. Conference on Woodfiber-Plastic Composites, Wisconsin, USA, 2005
33. Markiewiez P.; Goh M.C. J. Vac. Sci. Technol. **1995**, *B13*, 1115

Paper III

*The Eighth International Conference on Woodfiber-Plastic Composites*
~

# Investigation of the Structure of Cellulose Whiskers and Its Nanocomposites Using TEM, SEM, AFM, and X-ray Diffraction

*I. Kvien, B.S. Tanem, and K. Oksman*

**Abstract**

In this study the structure of cellulose whiskers and their novel nanocomposite with a biopolymer matrix was investigated combining transmission electron microscopy (TEM), scanning electron microscopy (SEM), atomic force microscopy (AFM), and wide angle x-ray diffraction (WAXD). The aim was to compare and explore these techniques. The cellulose whiskers used in this study were isolated from microcrystalline cellulose (MCC) by acid hydrolysis. X-ray diffraction patterns indicated that the isolation treatment did not degrade the cellulose whiskers, but removed the residue amorphous regions. From TEM images it was possible to detect the individual whiskers which enabled determination of their sizes and shape. Size determination from SEM was limited due to insufficient resolution. The x-ray diffraction analysis of the nanocomposite showed that the cellulose peaks were not detectable due to overlap by the biopolymer itself. However, information regarding change of matrix crystallinity before and after processing was obtained. The used microscopes gave both nano- and microstructural information of cellulose whiskers in the biopolymer matrix. AFM was the most convenient method because the analysis could be performed under ambient conditions without any need for pretreatment of the samples, in contrast to electron microscopy. However, by comparing TEM and AFM it was evident that the geometry of the AFM tip affected the apparent size of the whiskers. In SEM the metal coating contributed to the size of the whiskers. Effort was made to obtain images without metal coating by lowering the accelerating voltage. However, the resolution appeared then to be insufficient. TEM analysis seemed to give the most genuine information on the cellulose whiskers in the matrix; however, lack of contrast is a challenge which needs to be solved.

## Introduction

Nanocomposites have attracted much attention due to their remarkable improvements in material properties when compared with the matrix alone or conventional composite materials (1-3). Layered silicates are the most widely used nanosized reinforcement for polymers, but the last decade has seen a great interest in the use of reinforcements from renewable resources, such as cellulose whiskers (3), starch crystals (4-6), and chitin whiskers (7-9).

The reinforcing ability of these nanoparticles lies in their high surface area and good mechanical properties (2,10,11); however, to obtain a significant increase in material properties the reinforcement should be well separated and evenly distributed in the matrix material. Different processing methods aided with a

**Kvien:**
PhD Student
**Tanem:**
Post Doctoral Fellow
**Oksman:**
Professor, Dept. of Engineering Design and Materials, Norwegian Univ. of Science and Technology, Trondheim, Norway

variety of chemicals (compatibilizers, surfactants, etc.) have been explored to fulfill these requirements (2,3). Detailed structural examination is essential to obtain knowledge on how these various processing routes affect the distribution of the nanoparticles in the matrix. This requires the use of techniques with sufficient nanometer scale resolution capabilities. However, bio-based nanocomposites are in general non-conductive and soft materials and will therefore put strong demands on both sample preparation and instrumentation. The use of electron microscopes will require special attention to electron dose, contrast, and methods to assess the bulk structure without significantly affecting the interesting morphology.

For structure determination of layered silicate-based nanocomposites, it is common to combine transmission electron microscopy (TEM) and wide angle x-ray diffraction (WAXD) (2). TEM has the sufficient resolution to obtain detailed information of defects in the bulk structure. The information obtained from TEM is from a very small cross-section of the sample, and it is challenging to obtain a total view of the sample. WAXD gives information on a larger area which gives the average degree of dispersion. WAXD, however, is not a convenient method for determining local structural defects in the nanocomposites (2). When only a small amount of the reinforcement is present in the composite, x-ray diffraction analysis may fail in detecting the crystalline structure of the reinforcement in the polymer. For layered-silicate based nanocomposites, false conclusions about no peaks appearing in the diffraction pattern because of exfoliation can then be drawn (12). Ray and Okamoto (2) emphasized that the structure of nanocomposites should not be solely based on WAXD patterns. Recently, several works reported structure determination of layered silicate-based nanocomposites using atomic force microscopy (AFM) (13-17).

Conventional scanning electron microscopy (SEM) is the most used method for structure determination of cellulose-, starch-, and chitin whisker based nanocomposites (4-6,8,18-20). SEM is reported to give information about the dispersion and orientation of the whiskers in the matrix and presence of aggregates and voids (3). However, the resolution in a conventional SEM is limited compared to TEM. In addition, the information from SEM is restricted due to the metal coating applied during sample preparation.

Matsumura and Glasser (21) pointed out that a disadvantage of electron microscopes are that they often are applicable only to biologically inactive, dehydrated samples and require extensive sample preparation, such as metal coating or staining. An advantage of AFM is that it can be applied in ambient air, liquid, or vacuum and that none or little pretreatment of the sample is required (21). Recently, AFM work has been reported for structure determination of cellulose-based nanocomposites using microfibrillated cellulose (MFC) as reinforcement (22). However, no work is reported on cellulose-, starch-, or chitin whisker-based nanocomposites.

In this work the structure of cellulose whiskers and their novel nanocomposites with biopolymers was investigated using TEM, SEM, AFM, and WAXD. The goal was to compare and explore these techniques.

## Experimental

### Materials

*Cellulose whiskers*

Cellulose whiskers were isolated from microcrystalline cellulose (MCC) by acid hydrolysis in our lab. The isolation procedure is described by Bondeson et al. (23).

*Nanocomposites*

Biopolymer nanocomposites containing 5 wt% cellulose whiskers were prepared in our lab by solution casting and extrusion. The specifications of the solution casting procedure are described in detail by Petersson et. al. (24). The extrusion process and the extrusion process is described by Oksman and Mathew (25).

### AFM

AFM measurements were performed with a NanoScope IIIa, Multimode SPM from Veeco. Calibration was performed by scanning a calibration grid with precisely known dimensions. All scans were performed in air with commercial Si Nanoprobes SPM Tips. Height and phase images were obtained simultaneously in Tapping mode at the fundamental resonance frequency of the cantilever with a scan rate of 0.5 line/second using j-type scanner. The free oscillating amplitude was 3.0V, while the setpoint amplitude was chosen individually for each sample.

For AFM analysis of cellulose whiskers, a droplet of the aqueous whisker suspension was allowed to dry on a freshly cleaved mica surface. For bulk analysis of the nanocomposites, samples were cut and polished to prepare rectangular sheets, embedded in epoxy, and allowed to cure overnight. The samples were then trimmed in a Reichert-Jung ultramicrotome with freshly cleaved glass knives to obtain a rectangular block surface, 50 by 500 $\mu m^2$ in cross section. For AFM analysis, the block surface should preferentially be as large as possible; however, in order to minimize smearing of the outermost surface during cutting, a small block surface is believed to be advantageous.

The final cutting was performed with a diamond knife using a cutting speed of 0.4 mm/second generating foils of 50 nm in thickness.

### Electron Microscopy

*Field emission scanning electron microscopy*

Samples for field emission scanning electron microscopy (FESEM) were examined in a Hitachi 4300S Field emission SEM (FESEM). The accelerating voltage applied was 20kV for the cellulose whiskers and 10 kV for the nanocomposites.

For preparation of the cellulose whiskers, a droplet of the diluted suspension was allowed to float on and eventually flow through a cupper grid covered with a holey carbon film. The samples were then stained by allowing the grids to float in a 2 wt% solution of uranyl acetate for 3 minutes. The grids with cellulose whiskers were mounted in a specialized holder, originally designed for scanning TEM to minimize the background signal.

To examine the bulk morphology of the nanocomposites, fractured surfaces were generated after cooling in liquid nitrogen. These surfaces were sputter-coated with gold/palladium before examination.

*TEM*

Samples for TEM were examined in a Philips CM 30 at 150kV. The cellulose whiskers were prepared in the same way as for FESEM analysis.

For analysis of the nanocomposites, the samples were cut and polished to prepare rectangular sheets, embedded in epoxy, and allowed to cure overnight. The samples were then trimmed in a Reichert-Jung ultramicrotome with freshly cleaved glass knives to obtain a rectangular block surface, 50 by 500 $\mu m^2$ in cross section. Thin foils approximately 50 nm in thickness were cut by a diamond knife and gathered onto cupper grids. The samples were then stained by allowing the grids to float in a 2 wt% solution of uranyl acetate for 3 minutes.

*WAXD*

The x-ray diffraction patterns of microcrystalline cellulose, cellulose whiskers, and nanocomposites were obtained using a Siemens Diffractometer D5005. Convenient samples of cellulose whiskers were prepared by crushing the freeze-dried aqueous whisker suspension with a mortar. Both the MCC powder and the cellulose whisker samples were pressed into a spherical sample holder 25 mm in diameter and 2 mm high. For analysis of the nanocomposites, spherical sheets with ~12-mm diameter were prepared. The samples were exposed for a period of 11 seconds for each angle of incidence (•) using a Cu Ka•$_{1,2}$ x-ray source with a wavelength (•) of 1.541Å. The angle of incidence was varied from ~5° to ~30° by steps of 0.06°. The periodical distances (d) of the main peaks were calculated according to Bragg's equation (• = 2dsin •). To eliminate preferential orientation, the specimens were rotated within the x-ray diffractometer as suggested by Eichhorn and Young (26).

## Results and Discussion

### Analysis of Cellulose Whiskers

SEM examination of the commercial MCC prior to acid hydrolysis has been reported elsewhere (27). It was shown that the MCC consisted of particles with a non-uniform size distribution. The average size was ~15 $\mu$m. The MCC particles consisted of agglomerated cellulose whiskers.

The diffractograms of MCC and the cellulose whiskers (i.e., after isolation treatment) are shown in **Figure 1**. To determine the crystallinity of the samples, the ratio of the crystalline area to the total area can be taken. However, to determine the crystalline area, the amorphous part has to be known. This can be obtained by x-ray diffraction of a completely amorphous cellulose sample. This was not done in this study and therefore no value of the crystallinity is given. However, by comparing the intensities of the diffraction peaks of both samples, it is possible to determine a change in crystallinity. The intensity of the peaks in the diffractogram of cellulose whiskers was significantly higher compared to the peak intensities in the diffractogram of MCC. Thus, crystallinity had increased after acid hydrolysis. This indicated that the microcrystalline cellulose contained both cellulose crystals and also amorphous cellulose regions, which were removed by the acid hydrolysis. Also, the increased crystallinity indicated that the acid hydrolysis was not too severe, i.e.,

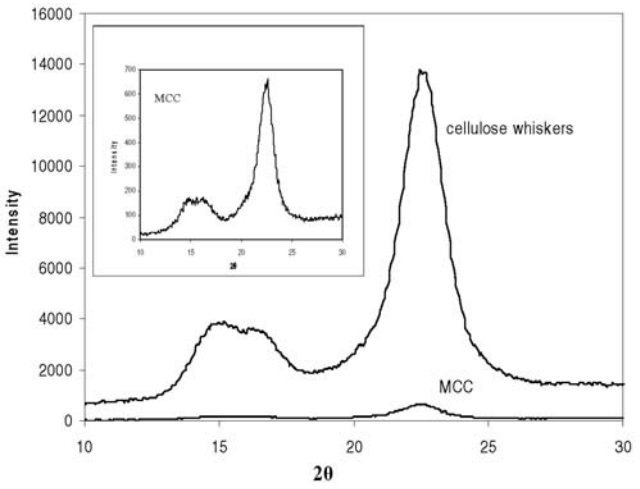


**Figure 1.** ~ *X-ray diffraction patterns of MCC and cellulose whiskers.*

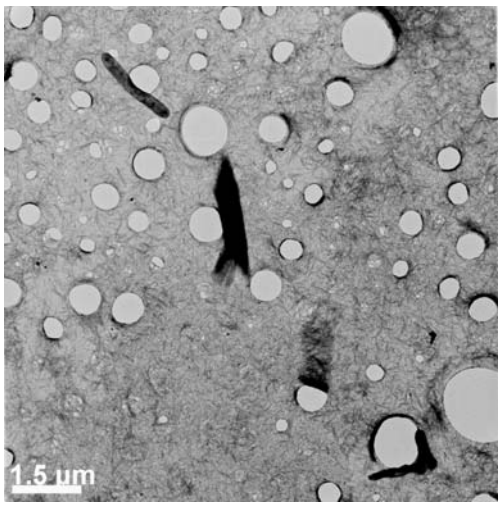


**Figure 2a.** ~ *TEM image revealing both cellulose whiskers and microstructured cellulose particles.*

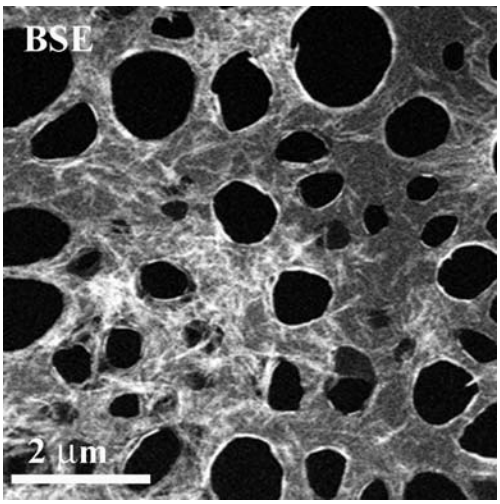


**Figure 3.** ~ *FESEM image showing an overview of the cellulose whisker sample.*

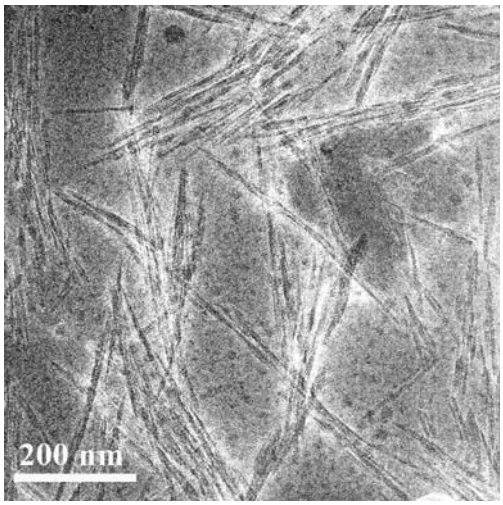


**Figure 2b.** ~ *TEM image showing the needle-like structure of cellulose whiskers.*

the crystal regions were not degraded. Both diffractograms, believed to represent typical cellulose I diffractograms, showed a peak at 2• = 22.6° and a shoulder in the region 2• =14° to 17° with two not well-defined peaks at ~15.5° and ~16.4°.

**Figures 2a and 2b** show an overview and a detailed image of the cellulose whisker sample from bright-field TEM analysis, respectively. In **Figure 2a** it can be seen that the holey carbon film was covered with cellulose whiskers. However, the image also revealed microstructured cellulose, i.e., the acid hydrolysis of the microcrystalline cellulose was not isolating all of the whiskers. At higher magnification, the cellulose whiskers appeared as needle-like structures (**Fig. 2b**). Uranyl acetate staining gave reasonable contrast between the whiskers and the carbon film. The whiskers themselves did not differ significantly in contrast from the carbon film. However, the presence of the heavy uranium in close vicinity of each whisker gave enough contrast for imaging. A tendency of agglomeration of the whiskers was observed. This was possibly due to the drying of the suspension on the carbon film covering the copper grids. Size determination was challenging due to agglomeration, but by comparing different images the length was roughly estimated to be between 400 nm and 800 nm and the width approximately 10 nm.

FESEM was found to be a quick and easy way to examine the cellulose whiskers. Back-scattered electrons, sensitive to the Z-contrast obtained by the staining, were used to identify the presence of large amounts of cellulose whiskers on the holey carbon film which can be seen in **Figure 3**. The whiskers were not evenly distributed but occurred densely in some areas and were almost completely missing in others. At higher magnification (**Fig. 4**), the presence of whiskers and agglomerates was more evident. However, low contrast and resolution made it difficult to discern the whiskers from the carbon foil. The presence and shapes of the whiskers were defined through the heavy elements surrounding the whiskers. Detailed measurements of the dimensions of the whiskers were difficult to perform. Secondary electron imaging was applied to achieve better resolution, however, it was still difficult to clearly discern individual whiskers from agglomerated structures (**Fig. 5**). An estimate of the width of the whiskers was therefore not obtained. However, most of the structures observed, believed to represent individual whiskers were 300 to 600 nm long, which is in good agreement to previous measurements.

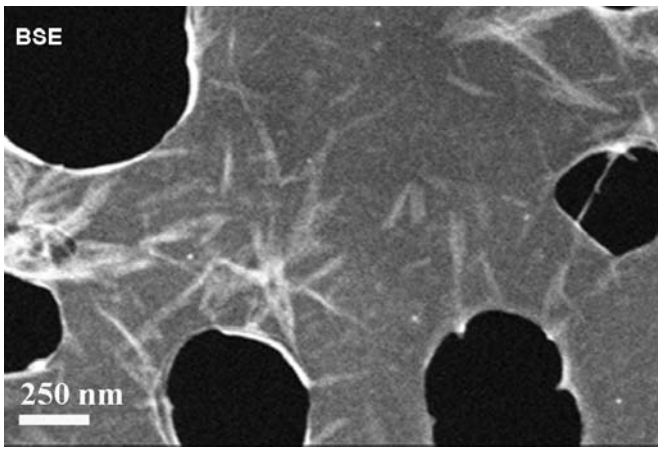


**Figure 4.** ~ *FESEM image of cellulose whiskers using backscattered electrons.*

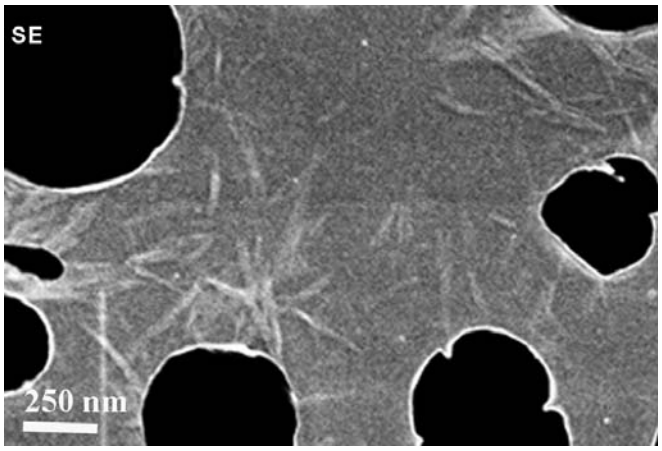


**Figure 5.** ~ *FESEM image of cellulose whiskers using secondary electrons.*

AFM analysis also revealed the presence of both nano- and microstructures (**Fig. 6**). From AFM images at higher magnification, it was obvious that the shape of the whiskers differed from the needle-like structure observed in TEM. The whiskers appeared lumped and significantly broader. This broadening effect can be explained by the tip used for imaging. In general, the AFM tips have a finite size and shape. As the tip passes over a sample with surface features of comparable size as the tip, the shape of the tip will contribute to the image that is formed (28). The AFM images from the cellulose whiskers will, therefore, in practice, be a convolution of the whiskers and the tip geometry. This will lead to a general broadening of the whiskers, and it is difficult to distinguish individual whiskers, from agglomerates. The broadening effect would probably be significantly reduced by applying high-resolution probes, which was not done here. To determine the actual diameter of the whiskers, the height difference

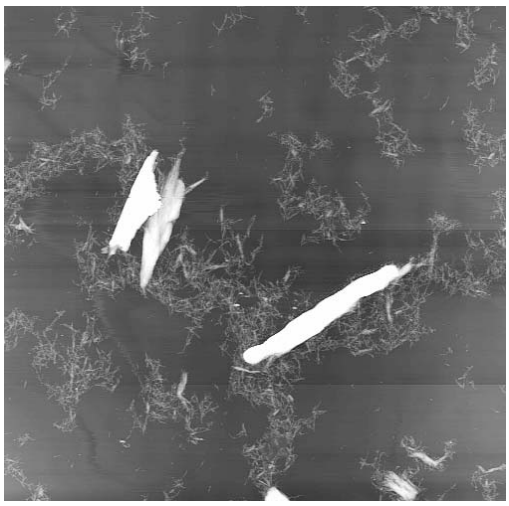

**Figure 6.** ~ *AFM phase image revealing both cellulose whiskers and microstructured cellulose particles.*

between the mica surface and the whiskers was used. This was obtained by line scans across several individual cellulose whiskers. The height difference between the mica substrate and the whiskers was ~10 to 15 nm (**Fig. 7**). This is consistent with TEM observations.

### Analysis of Cellulose Whiskers-Based Bionanocomposites

For cellulose-based nanocomposites, the WAXD method could not be interpreted as for layered silicate-based nanocomposites. Stacking of the pure silicate layers leads to a regular van-der-Waals gap between the layers called the interlayer or gallery (2). This regular stacking can be detected by a diffraction peak in the x-ray diffractogram of the pure silicate. When the polymer chains penetrate in this gallery, gallery height will increase which leads to a shift in the diffraction peak corresponding to the increased gallery height (d in Bragg's equation). For exfoliated nanocomposites the diffraction peak corresponding to the regular stacking of the silicate layers will disappear, because the layers are randomly distributed in the matrix. The diffractogram of cellulose as discussed above shows peaked corresponding to the three-dimensional arrangement of the cellulose chains in the crystallites. No peaks corresponding to the stacking of the crystallites were observed, which indicates that the cellulose whiskers were not regularly stacked together. It was expected the same diffraction pattern of the cellulose whiskers in the matrix would be observed, only with lower intensity due to the lower concentration or possibly degradation of the crystals. Thus, information regarding the cellulose whisker distribution in the matrix would not be obtained. However, x-ray diffraction of the cellulose nanocomposite

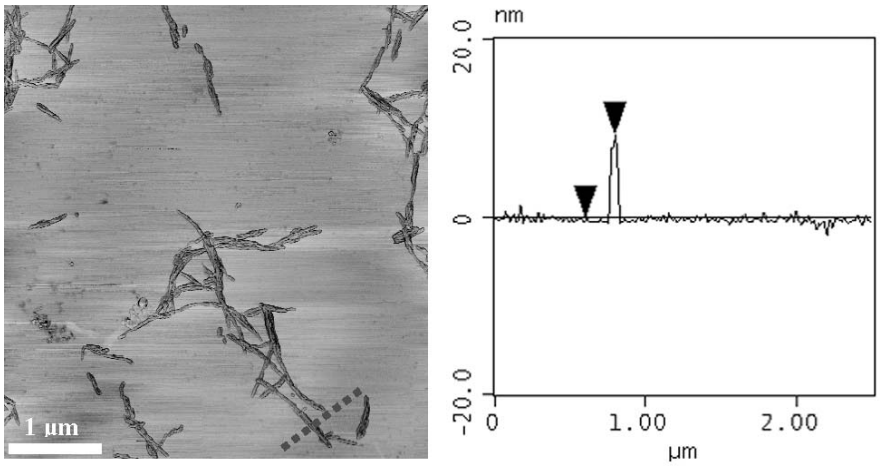


**Figure 7.** ~ *Line scan across cellulose whiskers showing the height difference between the mica surface and the whiskers.*

could give information of possible degradation of the cellulose whiskers and also change in crystallinity of the matrix.

X-ray diffractograms of the biopolymer polylactic acid (PLA) (**Fig. 8**) showed reflections at ~14.5°, ~16.5°, and ~19° which were due to diffraction from (010), (200) or (110), and (203)-planes, respectively (29). A secondary peak was observed at ~22.5°. In the diffractogram of the nanocomposite, the PLA reflections overlapped with the reflections of the cellulose crystal planes. This overlapping, together with the low cellulose concentration in the matrix, made it impossible to detect reflections from the cellulose. From the reflection intensities of the PLA crystal planes, it was evident that the PLA appeared more crystalline in the nanocomposite compared to pure PLA, which is a result of the preparation techniques.

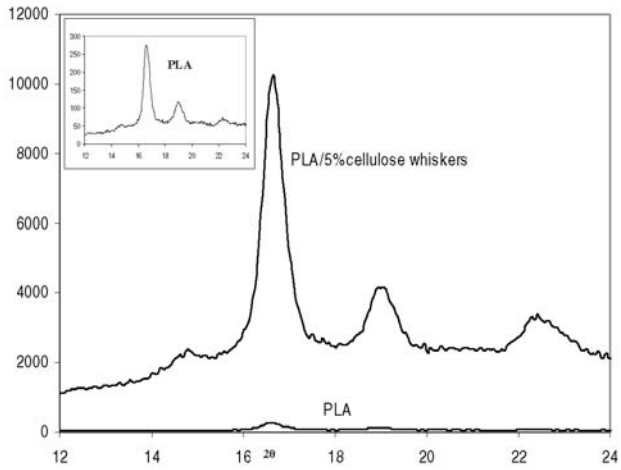


**Figure 8.** ~ *X-ray diffraction patterns of PLA and PLA/cellulose whiskers nanocomposite.*

For structure determination in TEM, high and low magnification were applied and several cross-sections of each sample were analysed to obtain data being representative for the sample (**Figs. 9a and 9b**). Areas with well dispersed cellulose whiskers were observed but also agglomerated whiskers were present. TEM analysis were challenging for several reasons. The major problem was lack of contrast between the whiskers and the biopolymer matrix. However, in some limited areas staining appeared to be more concentrated allowing some insight into the structure. Several routes to enhance the contrast between the matrix and the whiskers will be explored in a future study. Determination of the length of the whiskers in the matrix is in general uncertain due to sample preparation. A simple illustration describing the problem is presented in **Figure 10**. It was assumed that the whiskers were randomly distributed in the matrix. When preparing a sample for TEM-analysis, a sheet with ~50 nm thickness is cut. It is most likely that the whiskers are also cut to some extent in this procedure. In addition, the shapes and dimensions could be affected by the projection of the whisker from three-dimensional to two-dimensional.

FESEM examination of the fractured nanocomposite revealed cellulose whiskers in the biopolymer matrix (**Fig. 11**). The whiskers appeared to be randomly oriented in the matrix. However, the fractured surface also revealed agglomerated whiskers. If the adhesion between these agglomerates and the matrix is poor, the cracks will probably tend to propagate at the interphase. The agglomerates might, therefore, be overrepresented in the fractured surfaces. The size of the whiskers appeared broader than observed in TEM which is due to the coating of the fractured surface. It is uncertain whether the apparent single cellulose whiskers were individual whiskers or agglomerated whiskers. The use of FESEMs is known to enable

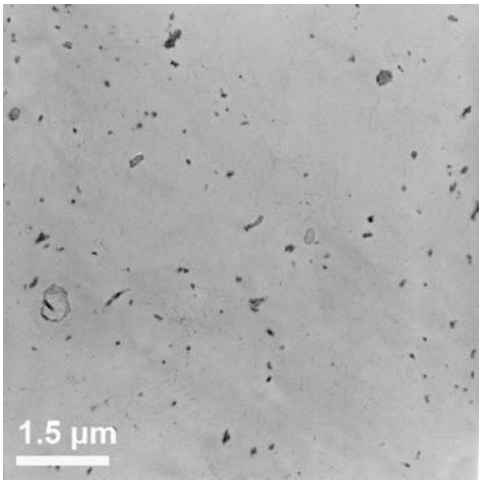


**Figure 9a.** ~ *TEM image showing an overview of the bionanocomposite.*

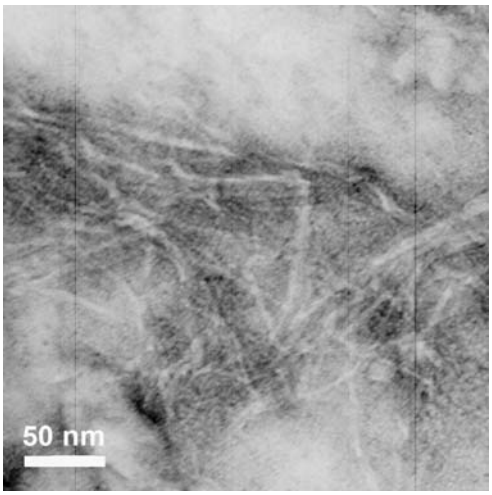


**Figure 9b.** ~ *TEM image showing detailed structure of the bionanocomposite.*

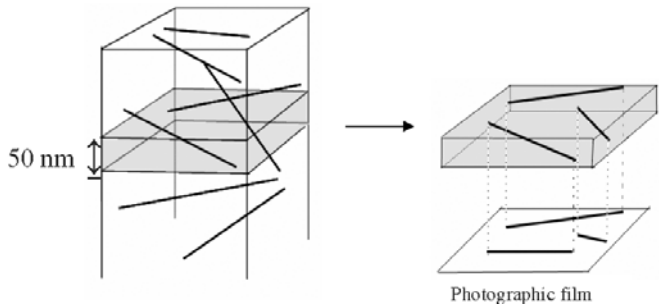


**Figure 10.** ~ *Illustration of composite sample preparation for analysis in TEM.*

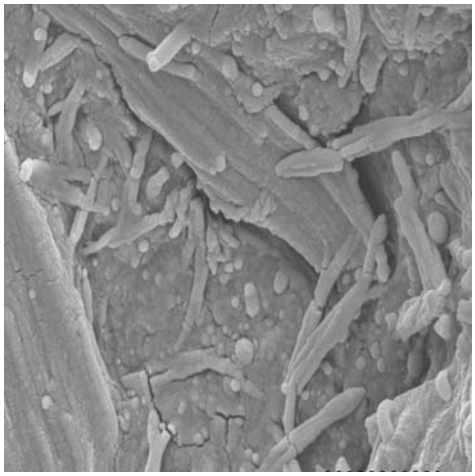

**Figure 11.** ~ *FESEM image of the cellulose whisker based nanocomposite.*

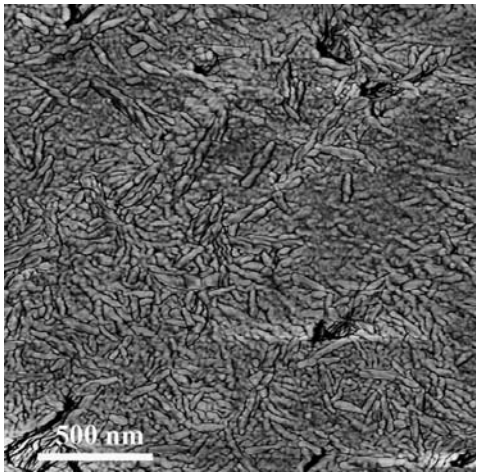


**Figure 12.** ~ *AFM phase image of cellulose whiskers in the biopolymer matrix.*

electron beams suitable for imaging, even at very low accelerating voltages. This could potentially eliminate the need for coating. However, the resolution is at the same time somewhat reduced. The examination of uncoated fractured surfaces at low accelerating voltages (1 kV) gave no further insight into the structures of the nanocomposites in this work.

AFM imaging of samples microtomed at room temperature gave no detailed information of the cellulose whiskers in the matrix. This was probably due to smearing effects during cutting, i.e., the polymer matrix was smeared out during cutting, partly covering the cellulose whiskers. On the other hand, samples cut at cryogenic temperatures enabled detailed information of the cellulose whiskers in the matrix, as shown in the phase contrast image in **Figure 12**. The whiskers partly protruded out of the biopolymer matrix. The reason for this was most probably due to difference in thermal expansion during heating from cryogenic temperatures. Theses images were recorded in air directly on the cryomicrotomed surface without any further treatment

of the sample. AFM has the necessary resolution capabilities without the need for staining and is therefore believed to be a good alternative to conventional TEM and SEM where the contrast between whiskers and matrix as well as stability of the sample under the electron beam are major challenges. However, the broadening effect in AFM has to be considered.

## Conclusions

In this work the structure of cellulose whiskers and their novel nanocomposites with biopolymers was investigated combining information from electron microscopy, AFM, and x-ray diffraction analysis. The aim was to compare and explore these techniques. The cellulose whiskers were isolated from MCC. The comparison of x-ray diffraction patterns of MCC with patterns from cellulose whiskers indicated that the isolation step of cellulose whiskers did not cause degradation but only removed residue amorphous regions in the MCC. From TEM it was possible to identify individual whiskers which enabled determination of their sizes and shape. In x-ray diffraction analysis of the nanocomposite, the cellulose patterns were not detectable due to overlap with the biopolymer itself. However, information regarding change of matrix crystallinity before and after processing was obtained. AFM, TEM, and SEM analysis enabled both nano- and microstructural information of cellulose whiskers in the biopolymer matrix. AFM was a convenient method because the analysis could be performed under ambient conditions without the need for pre-treatment of the sample, in contrast to electron microscopes. However, by comparing TEM and AFM, it was evident that the geometry of the AFM tip affected the apparent size of the whiskers. For analysis of the nanocomposite in FESEM, the metal coating attributed to the size of the whiskers. However, analysis without coating did not give sufficient resolution to obtain more detailed information. TEM analysis seemed to give the most genuine information of the cellulose whiskers in the matrix; however, lack of contrast is a challenge which need to be solved to use this method for bionanocomposites.

## Acknowledgments

Norwegian Research Council under the NANOMAT program is acknowledged for partial financial support of this work. Dr. Aji P. Mathew is acknowledged for interesting discussions.

## Literature Cited

1. Garces, J.M. et. al. 2000. Polymeric nanocomposites for automotive applications. Adv. Matr. 12(23).
2. Ray, S.S. and M. Okamoto. 2003. Polymer/layered silicate nanocomposites: A review from preparation to processing. Progress in Polymer Sci. 28(11):1539-1641.
3. Samir, M., F. Alloin, and A. Dufresne. 2005. Review of recent research into cellulosic whiskers, their properties and their application in nanocomposite Field. Biomacromolecules, 6(2):612.
4. Angellier, H., S. Molina-Boisseau, L. Lebrun, and A. Dufresne. 2005. Processing and structural properties of waxy maize starch nanocrystals reinforced natural rubber. Macromolecules. 38(9):3783.
5. Angellier, H., J-L. Putaux, S. Molina-Boisseau, D. Dupeyre, and A. Dufresne. 2005. Starch nanocrystal fillers in an acrylic polymer matrix. Macromol. Symp. 221(95).
6. Dubief, D., E. Samain, and A. Dufresne. 1999. Polysaccharide microcrystals reinforced amorphous poly(beta-hydroxyoctanoate) nanocomposite materials. Macromolecules. 32, 5765-5771.
7. Morin, A. and A. Dufresne. 2002. Nanocomposites of chitin whiskers from riftia tubes and poly(caprolactone). Macromolecules. 35:2190.
8. Nair, K.G. and A. Dufresne. 2003. Crab shell chitin whisker reinforced natural rubber nanocomposites 1. Processing and Swelling Behavior. Biomacromolecules. 4:657.
9. Paillet, M. and A. Dufresne. 2001. Chitin Whisker reinforced thermoplastic nanocomposites. Macromolecules. 34.
10. Grunert, M. and T.W. Winter. 2002. Nanocomposites of Cellulose acetate butyrate reinforced with cellulose nanocrystals. J. of Polymers and the Environment. 10(1/2).
11. Tashiro, K. and M. Kobayashi. 1991. Theoretical evaluation of three-dimensional elastic constants of native and regenerated celluloses: role of hydrogen bonds. Polymer. 32(8).
12. Kornmann, X., H. Lindberg, and L.A. Berglund. 2001. Synthesis of epoxy-clay nanocomposites: influence of the nature of the clay on structure. Polymer. 42:1303.
13. Jiang, T. et al. 2005. Study on solvent permeation resistance properties of nylon6/clay nanocomposite. European Polymer J. 41:459-466.
14. Kuan, H-C. et al. 2005. Hydrogen bonding, mechanical properties, and surface morphology of clay/waterborne polyurethane nanocomposites. J. of Polymer Sci., Part B: Polymer Physics. 43:1-12.
15. Park, H-M. et al. 2004. Effect of compatibilizer on nanostructure of the biodegradable cellulose acetate/organoclay nanocomposites. Macromolecules. 37:9076-9082.
16. Song, M. et al. 2005. A study on phase morphology and surface properties of polyurethane/organoclay nanocomposite. European Polymer J. 41:259-266.
17. Yalcin, B. and M. Cakmak. 2004. The role of plasticizer on the exfoliation and dispersion and fracture behaviour of clay particles in PVC matrix: A comprehensive morphological study. Polymer. 45:6623-6638.
18. Anglès, M.N. and A. Dufresne. 2000. Plasticized starch/tunicin whiskers nanocomposites. 1. Structural analysis. Macromolecules. 33(22):8344-8353.
19. Helbert, W., J.Y. Cavaillé, and A. Dufresne. 1996. Thermoplastic nanocomposites filled with wheat straw cellu-

lose whiskers. Part 1: Processing and mechanical behavior. Polymer Composites. 17(4):604.
20. Mathew, A. and A. Dufresne. 2002. Morphological investigation of nanocomposites from sorbitol plasticized starch and tunicin whiskers. Biomacromolecules. 3: 609.
21. Matsumura, H. and W.G. Glasser. 2000. Cellulosic nanocomposites. II. Studies by atomic force microscopy. J of Applied Polymer Sci. 78:2254-2261.
22. Yano, H. et. al. 2005. Optically transparent composites reinforced with networks of bacterial nanofibers. Adv. Mater. 17(2).
23. Bondeson, D., A.P. Mathew, and K. Oksman. Optimization of the Isolation of nanocrystals from microcrystalline cellulose by acid hydrolysis. Submitted to Biomacromolecules.
24. Petersson, L., K. Oksman, and A.P. Mathew. Poly(lactic acid) nanocomposite films using bentonite and hectorite layered silicates: Preparation, characterization and properties. Submitted to J. of Applied Polymer Sci.
25. Oksman, K. and A.P. Mathew. Poly(lactic acid)-cellulose whiskers nanocomposites processed by melt compounding. Submitted to Polymer.
26. Eichhorn, S.J. and R.J. Young. 2001. The Young's modulus of a microcrystalline cellulose. Cellulose. 8:197-207.
27. Mathew, A.P, K. Oksman, and M. Sain. Mechanical properties of biodegradable composites from poly lactic acid (PLA) and microcrystalline cellulose (MCC). J. of Applied Polymer Sci. (in press).
28. Markiewiez, P. and M.C. Goh. 1995. J. Vac. Sci. Technol. B13(3):1115.
29. Nam J.Y, S.S. Ray, and M. Okamoto 2003. Crystallization behaviour and morphology of biodegradable polylactide/layered silicate nanocomposite. Macromolecules 36:7126-7131.

Paper IV

# Structure and thermal properties of poly(lactic acid)/cellulose whiskers nanocomposite materials.

**L. Petersson[1], I. Kvien[1] and K. Oksman[1,2*]**

[1)] Department of Engineering Design and Materials,

Norwegian University of Science and Technology, Trondheim, Norway

[2)] Department of Wood and Bionanocomposites, Luleå University of Technology,

Skellefteå, Sweden

## Abstract

The goal of this work was to produce nanocomposites based on poly(lactic acid) (PLA) and cellulose nano whiskers (CNW). The CNW were treated with either tert-butanol or a surfactant in order to find a system that would show flow birefringence in chloroform. The nanocomposites were prepared by incorporating 5 wt % of the different CNW into a PLA matrix using solution casting. Field emission scanning electron microscopy showed that untreated whiskers formed flakes, while tert-butanol treated whiskers formed loose networks during freeze drying. The surfactant treated whiskers showed flow birefringence in chloroform and transmission electron microscopy showed that these whiskers produced a well dispersed nanocomposite. Thermogravimetric analysis indicated that both whiskers and composite materials were thermally stable in the region between 25 °C and 220 °C. The dynamic mechanical thermal analysis showed that both the untreated and the tert-butanol treated whiskers were able to improve the storage modulus of PLA at higher temperatures and a 20 °C shift in the tan δ peak was recorded for the tert-butanol treated whiskers.

*Keywords:* Solution Casting; Microscopy; Thermal Properties; Dynamic Mechanical Properties;
* Fax: +46-910-58-53-99, E-mail: kristiina.oksman@ltu.se

Correspondence to: Professor Kristiina Oksman,
Department of Wood and Bionanocomposites, Luleå University of Technology,
931 87 Skellefteå, Sweden
Phone +46-910-58-53-71, Fax: +46-910-58-53-99
E-mail address: kristiina.oksman@ltu.se

PhD Candidate Linnea Petersson,
Department of Engineering Design and Materials, Norwegian University of Science and Technology, R. Birkelands vei 2b, NO-7491, Trondheim, Norway

PhD Candidate Ingvild Kvien,
Department of Engineering Design and Materials, Norwegian University of Science and Technology, R. Birkelands vei 2b, NO-7491, Trondheim, Norway

## 1. Introduction

Lately, there has been an increased interest in the use of biopolymers due to more environmentally aware consumers, increased price of crude oil and the concern about global warming. Biopolymers are naturally occurring polymers that are found in all living organisms. The use of biopolymers will have a less harmful effect on our environment compared to the use of fossil fuel based commodity plastics [1]. Biopolymers are based on renewable resources and will degrade to form carbon dioxide, water and biomass. The amount of carbon dioxide released during degradation is the same amount as the renewable resource will harness during its cultivation. As a result carbon dioxide will not accumulate in the atmosphere due to the use of biopolymers. Biopolymers can today be retrieved from for example agricultural feedstock, marine fauna and microbial activities. Waste products from industries can also be utilized to produce biopolymers, for example waste from agriculture and marine food industries.

Poly(lactic acid) (PLA) is a commercially available biopolymer. It is a biodegradable thermoplastic polyester produced from L- and D-lactic acid, which is derived from the fermentation of corn starch [2]. The properties of PLA are determined by the weight ratio of the two lactic acid molecules. PLA can therefore vary from being an amorphous polymer to being a semi or highly crystalline material [2]. PLA is one of the few biopolymers available today which have similar properties as fossil fuel based commodity plastics. PLA produced by Cargill Dow has high mechanical strength and easy process- ability compared to other biopolymers and is often compared to polystyrene or PET [2]. However, PLA softens at lower temperatures compared to equivalent petroleum based polymers [3]. A low softening temperature results in a lower temperature of use of the material, which in turn will limit the number of application of the material. Preparation of nanocomposites has been considered a promising method to increase the softening temperature of biopolymers [4, 5].

In order to produce fully renewable and biodegradable nanocomposites both the polymer matrix and the nanoreinforcement have to be derived from renewable resources. Cellulose nano whiskers (CNW) have attracted significant attention during the last decade as potential nanoreinforcement in different polymers [6]. Cellulose is abundant in nature, and is found in plants, insects, shellfish and can also be produced by bacteria. Cellulose nano whiskers have good mechanical properties [6, 7]. It is thought that these whiskers have mechanical strength that corresponds to the binding forces of neighboring atoms [6]. As a result cellulose whiskers

have far better mechanical properties than a majority of the commonly used reinforcing materials. Biopolymer based nanocomposites have been produced by incorporating CNW into the following biopolymers matrices: cellulose acetate butyrate [8], poly(hydroxyalkanoates) [9], poly(lactic acid) [10], silk fibroin [11] and starch [12].

The use of cellulose nano whiskers as nanoreinforcement is a new field in nanotechnology and as a result there are still many obstacles remaining to their use. Firstly, cellulose nano whiskers are not commercially available. Secondly, their production is time consuming and is still associated with low yields. Thirdly, they are difficult to use in systems that are not water based due to their strong hydrogen bonding. This affects the production of PLA based nanocomposites when using PLA produced by Cargill Dow which is not water soluble. The whiskers have to be transferred from water to an appropriate solvent for this type of PLA. It has been reported that transferring whiskers from water to other solvents is possible [8, 13-16]. In order to determine if whiskers are well isolated in solutions flow birefringence is often used [13]. There are a few different treatments that have been used to achieve birefringence in other solvents than water as for example the use of a surfactant [13], poly(ethylene glycol) grafting [14] and partial silylation [15]. Heux et al. used a surfactant on whiskers from both cotton and tunicin in order to achieve birefringence in toluene [13]. Flow birefringence in chloroform has been achieved by poly(ethylene glycol) grafting [14] and partial silylation [16] of cellulose whiskers. Unfortunately, both these modifications are complicated processes to carry out. However, there is a negative side effect of using modified cellulose whiskers. It has been shown that modified whiskers have less reinforcing effect than unmodified whiskers. Grunert and Winter prepared nanocomposites with a hydrophobic thermoplastic matrix using trimethylsilylated cellulose whiskers [8]. They found that unmodified whiskers showed a better reinforcing performance than the trimethylsilylated whiskers. Similarly, the mechanical properties of nanocomposites containing chemically modified chitin whiskers from crab shell were found to be inferior to the unmodified nanocomposites [17].

The goal of this work was to produce poly(lactic acid) (PLA) based nanocomposites using cellulose nano whiskers (CNW). The nanocomposites were prepared by solution casting using chloroform as solvent. The CNW used in this study were treated in two different ways in order to find one system that would show flow birefringence in chloroform. The whiskers were either transferred to tert-butanol or modified with a surfactant prior to freeze drying. Untreated cellulose whiskers were used as reference. The structure of the materials was

studied using field emission scanning electron microscopy (FESEM) and transmission electron microscopy (TEM). Both thermogravimetric analysis (TGA) and dynamic mechanical thermal analysis (DMTA) were carried out in order to investigate the thermal properties of the produced nanocomposites.

## 2. Experimental

### 2.1 Materials

*Matrix:* Poly (lactic acid) (PLA), Nature Works ™ 4031 D, was supplied by Cargill Dow LLC, Minneapolis, USA. The material has a density of 1.25 g/cm3, glass transition temperature (Tg) of 58 °C and melting point of 160 °C. The molecular weight (Mw) of the PLA is between 195,000 - 205,000 g/mol.

*Reinforcement:* Microcrystalline Cellulose (MCC), Avicel PH 102, was supplied by FMC BioPolymer, Philadelphia, USA. Avicel PH 102 is commercially available and was used as a raw material for the production of cellulose nano whiskers (CNW).

*Chemicals:* Sulfuric Acid 95-97 % from Merck KGaA, Darmstadt, Germany was used during the CNW production. Sodium Hydroxide from SDS, France, was used during the neutralization of the CNW. Tert-Butanol was purchased from Merck KGaA, Darmstadt, Germany, and was used to replace water before freeze drying the whiskers. Beycostat A B09 from CECA S.A., France, was the surfactant used during this study. Chloroform was purchased from Merck KGaA, Darmstadt, Germany, and was used to redisperse the nanoreinforcements. Silicon 100 from Novatio Europe N.V., Belgium, was used to grease the Petri dishes prior to casting.

### 2.2 Processing of Cellulose Nano Whiskers

*CNW Production:* Microcrystalline Cellulose (MCC), 10 g/100 ml, was hydrolyzed in 9.1 mol/L sulphuric acid at 44 °C for 130 min. The excess of sulphuric acid was removed by repeated cycles of centrifugation, 10 min at 13 000 rpm (18 516 g, Jouan MR 23 I, USA). The supernatant was removed from the sediment and was replaced by deionized water. The centrifugation continued until the supernatant became turbid. After the centrifugation the suspension containing cellulose nano whiskers was dialysed against deionized water. The final suspension had a pH of 3.5.

*CNW Treatments:* CNW were prepared by neutralizing the suspension containing the cellulose nano whiskers and acted as a reference in this experiment. The neutralization was

carried out by adding drops of a 1 wt % (0.25 N) NaOH solution to the whiskers. B-CNW (butanol cellulose nano whiskers) were prepared by transferring cellulose whiskers from the neutralized suspension to tert-butanol by using centrifugation. The supernatant was replaced by a solution of tert-butanol and deionized water. The tert-butanol content of the solution was increased in a stepwise manner until pure tert-butanol was used. S-CNW (surfactant cellulose nano whiskers) were prepared by following the guidelines given by Heux et al. [13]. After dialysis the surfactant, Beycostat A B09, was added to the suspension containing whiskers in proportion of 4:1 (w/w) using an estimated weight of the cellulose nano whiskers. The pH of the suspension was then adjusted to 8.5 using the same 1 wt % NaOH solution as above.

### 2.3 Processing of Nanocomposites

*CNW Dispersion:* The three suspensions containing whiskers were freeze dried in a Flexi-Dry MP, Kinetics Thermal Systems, USA. After freeze drying, chloroform was directly added to the whiskers forming 1 wt % suspensions. In order to improve the dispersion of the whiskers in chloroform the suspensions were exposed to 3 intervals of sonification (UP200S, Hielscher Ultrasonics GmbH, Germany) each lasting for 2 min. In between the cycles the suspensions were placed in an ice bath.

*PLA Preparation:* A 10 wt % solution of PLA in chloroform was prepared by stirring the solution on a hot plate at 60 °C until the pellets were fully dissolved (4 h).

*Film Preparation:* The nanocomposites were prepared by solution casting. The formulations, see Table I, were mixed and run in a Waring Blender for 3 min. The blender was used to thoroughly stir the two solutions together. The formulations were then casted in Petri dishes greased with silicon and left to evaporate in room temperature for one day. The films were then placed in a vacuum oven at 40 °C for two weeks in order to remove all remaining chloroform. The prepared films had a thickness of 0.25 mm and a total dry weight of 5 g.

### 2.4 Characterization

#### 2.4.1 Electron Microscopy

Microcrystalline cellulose, freeze dried whiskers and fracture surfaces of the nanocomposite films were examined in a field emission scanning electron microscope (FESEM), Hitachi 4300S, Japan. The accelerating voltage applied was 5.0 kV. The fracture surfaces were generated after cooling in liquid nitrogen. All samples were sputter-coated with platinum before examination. The cellulose whiskers and the nano structure of the composites were examined in a transmission electron microscope (TEM), Philips CM30, the Netherlands, at an

acceleration voltage of 100 kV. To examine the cellulose whiskers a droplet of the diluted suspension was allowed to float on and eventually flow through a copper grid covered with a porous carbon film. To examine the nanocomposites, the samples were cut and polished to rectangular sheets, embedded in epoxy and allowed to cure overnight. The final ultra microtoming was performed with a diamond knife at room temperature generating foils being 50 x 500 $\mu m^2$ in cross-section and approximately 50 nm in thickness. These foils were gathered onto Cu grids. All samples were stained by allowing the grids to float in a 2 wt % solution of uranyl acetate for 2 min.

### 2.4.2 Thermogravimetric Analysis (TGA)

The thermal stability of both freeze dried whiskers and nanocomposites was investigated using a TA Instruments TGA Q500, USA. The samples were heated from room temperature up to 500 °C with a heating rate of 10 °C/min and a nitrogen flow of 100 ml/min. Three samples were used to characterize each material.

### 2.4.3 Dynamic Mechanical Thermal Analysis (DMTA)

Dynamic mechanical properties of the nanocomposites were measured using a Rheometric Scientific DMTA V, USA, in tensile mode. The measurements were carried out at a constant frequency of 1 Hz, a strain amplitude of 0.05 %, a temperature range of 15 °C – 100 °C, a heating rate of 3 °C/min and gap distance of 20 mm. The samples were prepared by cutting strips from the films with a width of 5 mm. Four samples were used to characterize each material.

## 3. Results and discussion

### 3.1. Processing and Structure

The microcrystalline cellulose prior to acid hydrolysis is shown in Figure 1. These particles were ~10-50 μm and consisted of aggregated cellulose whiskers [18]. After hydrolysis the suspension showed flow birefringence as presented in Figure 2. This indicated the presence of isolated cellulose whiskers, which was confirmed by transmission electron microscope (TEM) analysis, see Figure 3. The whiskers were ~5 nm in width and ~200 nm in length as found in other studies on cellulose whiskers from wood [19-21]. These unmodified whiskers will be referred to as CNW (cellulose nano whiskers).

The goal of the processing was to obtain flow birefringence in chloroform. During the freeze drying process the whiskers tend to aggregate. As a consequence redistribution in chloroform is difficult. Two strategies to avoid aggregation during freeze drying were explored in this study. First, one set of cellulose whiskers were transferred from the reference solvent to tert-butanol, B-CNW (butanol cellulose nano whiskers). Tert-butanol has a melting point of 23-25 °C, which allows the suspension to freeze faster and thereby avoiding aggregation of the cellulose whiskers during the freezing process. The second strategy was to use a surfactant, S-CNW (surfactant cellulose nano whiskers). The surfactant chosen had been used earlier by Heux et al. to create birefringence in toluene using whiskers from cotton and tunicin [13]. It was expected that the surfactant would hinder hydrogen bonding between the cellulose whiskers during freeze drying and further aid the distribution of the cellulose whiskers in chloroform. Field emission scanning electron microscopy (FESEM) images of the freeze dried whiskers are presented in Figure 4. As can be seen the whiskers formed flakes during the freeze drying process. In the detailed images of the CNW and B-CNW flakes it is possible to trace the cellulose whiskers that made up these flakes. The whiskers in the B-CNW flakes appeared more loosely bonded compared to the whiskers forming the CNW flakes. It thus seemed that the use of tert-butanol limited the aggregation of the cellulose whiskers during freeze drying. The S-CNW flakes appeared thicker compared to the fine CNW and B-CNW flakes. The freeze dried CNW and B-CNW flakes were both fluffy in texture, while the S-CNW whiskers were sticky. The surfactant was apparently still present in the system, covering the cellulose whiskers.

After freeze drying, the whiskers were dispersed in chloroform aided by sonification. The S-CNW suspension showed flow birefringence in chloroform, as seen in Figure 5. It was evident that the S-CNW suspension contained a large number of single cellulose whiskers. The CNW and B-CNW suspensions precipitated at rest and did not show birefringence in chloroform. The whisker flakes in the CNW and B-CNW suspensions were apparently difficult to separate into single whiskers and instead remained as aggregates in the chloroform. The precipitation was slightly larger in the CNW suspension compared to the B-CNW suspension. Hence it seemed that a compatibilizer or chemical treatment of the cellulose whiskers was required in order to produce a stable suspension of cellulose whiskers in chloroform. The initial idea for this experiment was to process the chloroform suspensions in a homogenizer in order to improve the dispersion and avoid the use of chemical modification. A homogenizer has the ability to decrease the size of agglomerates and has been

used to produce cellulose microfibrils [22]. This proved to be difficult due to the low boiling point of chloroform, 61 °C. The solutions that were run through the homogenizer showed degradation through a color change at very low pressures and short cycle times.

Fracture surfaces of the produced composite materials were analyzed in a FESEM. In the PLA/CNW composite the cellulose whiskers seemed poorly distributed. The whiskers were present in flakes as identified earlier, see Figure 6a. At higher magnifications it could be seen that these flakes had a compact structure and a poor interfacial adhesion to the PLA. The PLA/CNW material can not be classified as a nanocomposite material. The cellulose whiskers appeared to be better distributed in the PLA/B-CNW nanocomposite as seen in Figure 6b. The material contained smaller agglomerates which were more evenly distributed in the material compared to PLA/CNW. The agglomerates seemed less compact and with good interfacial adhesion to the PLA. It thus seemed that the freeze dried B-CNW flakes had been penetrated by PLA chains. In the PLA/S-CNW nanocomposite no agglomerates of cellulose whiskers were observed. This indicated a well distribution of single cellulose whiskers in the PLA. The PLA/S-CNW nanocomposite did however appear to be very porous as seen in Figure 6c. This was probably caused by the presence of surfactant in the material. Foam was generated during processing of the materials containing surfactant and it was therefore believed that air was trapped in the materials.

The materials containing surfactant were white, while the other materials were transparent, see Figure 7. This was probably due to the porous structure of the materials as seen in FESEM. The samples containing surfactant were pressed on a laboratory press (LPC 300, Fontijne Grotnes B.V., The Netherlands) at 162 °C and 18 MPa in order to see if these materials would turn transparent when the porosity was removed. Figure 8 shows that both these materials did in fact turn transparent after they were melted and pressed.

The nanostructure of the materials was analyzed in a transmission electron microscope (TEM). For the PLA/CNW composite it was found that the majority of the whiskers were present in flakes. Figure 9a shows a cross-section of a whisker flake in the PLA matrix. It consisted of tightly packed cellulose whiskers. In the PLA/B-CNW nanocomposite it was possible to detect looser agglomerates of whiskers than in the PLA/CNW material, as can be seen in Figure 9b. This indicates that the loosely bonded network created using tert-butanol during the freeze drying process allowed the PLA chains to penetrate in between the cellulose

whiskers. In the PLA/S-CNW nanocomposite it was found that the cellulose whiskers were more evenly distributed in the PLA matrix. Small clusters of loosely aggregated whiskers were found throughout the samples studied of this material, see Figure 9c. The darker area surrounding the whiskers is due to negative staining by uranyl acetate. The cluster formation may indicate that the surfactant did not have access to single whiskers but rather encapsulated several whiskers that were held together by hydrogen bonding. This can possibly be improved by better mixing of the whiskers and surfactant in the water suspension prior to freeze drying. The structural study concluded that in order to achieve a well distribution of the cellulose whiskers in PLA a chemical modifier is required.

### 3.2. Thermal Properties

One of the goals when incorporating whiskers into PLA was to increase the temperature region where PLA can be used. In this study both thermogravimetric analysis (TGA) and dynamic mechanical thermal analysis (DMTA) were carried out in order to investigate the thermal properties of the produced materials. The results from the TGA are presented in Figure 10, which shows residual weight vs. temperature for both whiskers and composite materials. Figure 10 concludes that all materials were thermally stable in the region below 220 °C. The recommended processing temperature of PLA is 200 °C and both whiskers and composites were able to maintain more than 91% of their original weight at this temperature. In Figure 10a one could detect a slight decrease in weight for all materials below 150 °C which was due to the moisture content of these materials. This graph also shows that the CNW and B-CNW started to degrade earlier than MCC and S-CNW. This is most likely due to the acid hydrolysis used to produce the whiskers. The weight reduction of the S-CNW whiskers seemed to occur more stepwise than for the other materials and the S-CNW whiskers also had higher residual weight at 400 °C. This can be explained by the high content of surfactant used to modify these whiskers. In Figure 10b it was possible to distinguish a slightly improved thermal stability of the materials containing surfactant. On the whole, TGA showed that there was no degradation taking place in either whiskers or composites resulting in large weight reductions in the temperature region where PLA is either processed or used, 25 - 220 °C.

DMTA provides information on mechanical behavior, molecular relaxations as well as interactions taking place in the produced materials as the temperature is varied. The storage

modulus as a function of temperature and the tan δ peak for the produced materials are shown in Figure 11. These results showed that all whiskers were able to improve the storage modulus of pure PLA at higher temperatures. Figure 11a presents the DMTA results for PLA, PLA/CNW and PLA/B-CNW. As can be seen the CNW and B-CNW whiskers were unable to improve the storage modulus of PLA in the elastic region. At higher temperatures where the PLA matrix softened the reinforcing effect of the two whiskers increased due to their ability to restrict the motions of the PLA chains. At 60 °C the B-CNW whiskers showed a larger improvement in storage modulus than the CNW whiskers, a 64 % improvement vs. a 23 % improvement. This can be explained by the structure of the B-CNW nanocomposite. The B-CNW whiskers were better dispersed in the PLA matrix and formed looser networks with increased surface area compared to the tight CNW flakes. The TEM analysis (Figure 9b) also showed that PLA chains had been able to penetrate the B-CNW whiskers which would have a large affect on the segmental motion of the PLA chains. The tan δ peaks presented in Figure 11a supported this. The CNW whiskers showed a slight shift in the tan δ peak, 5°C, indicating only minor hindering of the segmental motions of the PLA matrix. The B-CNW whiskers on the other hand showed a much larger shift in tan δ peak, 20 °C, which indicated significant change in the segmental motions of the PLA matrix. Similar behavior has been reported before when polymer chains have penetrated CNW bundles, but not to the same extent [23]. These results showed that the surface area of the incorporated CNW governed the improvement of the storage modulus of PLA in the plastic region.

Figure 11b presents the DMTA results for PLA and the two materials containing surfactant. As can be seen the materials containing 20 wt % of surfactant showed reduced storage modulus in the elastic region compared to pure PLA. This can be explained by the large amount of surfactant added to these materials, decreased crystallinity and the porous structure seen in the FESEM study (Figure 6c). At higher temperatures where the PLA matrix softened a different behavior was seen, for example at 67 °C the PLA/S material was able to improve the storage modulus of pure PLA with 38 %. This together with the tan δ delta peaks shown in Figure 11b indicated a high level of interaction between the PLA matrix and the surfactant. The tan δ peak of PLA/S showed a 22 °C shift and increased intensity compared to the peak for pure PLA. The increased intensity indicates that the surfactant was able to hinder the crystallization process in PLA and the large shift demonstrated to which large extent the surfactant was able to hinder the segmental movements of the PLA matrix. Figure 11b also presented the results for the PLA/S-CNW nanocomposite. The PLA/S-CNW material was

able to increase the storage modulus of PLA/S in the elastic region, for example with 83 % at 20 °C. This can be explained by the well dispersed whiskers inside the PLA/S matrix and a softer matrix than pure PLA. The PLA/S and PLA/S-CNW materials had similar tan δ peak temperatures and also showed similar storage modulus values in this region. After the tan δ peak temperature when the PLA/S material softened the well dispersed whiskers were able to carry load and increase the storage modulus of the PLA/S material. Above 55 °C the PLA/S-CNW nanocomposite was also able to improve the storage modulus of the pure PLA, even though the material contains 20 wt % less PLA. The DMTA analysis also indicated that the interaction between the surfactant and PLA seemed to be larger than the interaction between PLA and the whiskers. It is possible that the surfactant was coating the whiskers and preventing a direct interaction between the PLA and the cellulose whiskers. It also seemed that there was no or little interaction between the whiskers and the surfactant modified PLA. An interaction would have lead to a shift in the tan δ peak to higher temperatures for the PLA/S-CNW material.

The DTMA study showed that the incorporated whiskers were able to hinder the motions of the PLA chains in the matrix and thereby increasing the temperature of use of the PLA. The dispersion of the whiskers inside the matrix was of great importance since it governed the available surface area of the whiskers. When a surfactant is used to improve the dispersion of the whiskers it is important to investigate the relationship between the surfactant and the matrix. The interaction between the surfactant and the matrix should be less pronounced and the amount of surfactant should be optimized in order for the whiskers to reinforce the matrix both in the elastic and plastic zone.

## 4. Conclusions

The goal of this work was to produce nanocomposites based on poly(lactic acid) (PLA) and cellulose nano whiskers (CNW). The nanocomposites were prepared by solution casting using chloroform as solvent. The CNW used in this study received different treatments after their production in order to find a system where the whiskers would show flow birefringence between cross polarized light. The whiskers were either transferred to tert-butanol or modified with a surfactant prior to freeze drying. Untreated cellulose whiskers were used in this experiment as a reference.

The whiskers showed different flake like structures after the freeze drying process. The CNW flakes were thin and tightly packed with whiskers. Tert-butanol was able to limit the aggregation of the cellulose whiskers during the freeze drying process and as a result the B-CNW whiskers were more loosely bonded compared to the CNW whiskers. The S-CNW flakes appeared thicker compared to the other two types of flakes. It was apparent that the surfactant was still present in the system covering the cellulose whiskers. The S-CNW whiskers were the only whiskers that were able to show flow birefringence in chloroform. The sonification was unable to break down the CNW and B-CNW flakes to form single isolated whiskers which could show flow birefringence in chloroform. From this experiment it seems that a compatibilizer or chemical treatment of the cellulose whiskers is required in order to produce a stable suspension of cellulose whiskers in chloroform. FESEM and TEM revealed that the whiskers were best dispersed in the PLA/S-CNW material and that the other two materials contained agglomerated cellulose whiskers. The structure of the PLA/B-CNW material was better than the PLA/CNW material due to the loose network of the B-CNW whiskers. When studying the PLA/S-CNW material it is believed that the surfactant did not have access to single whiskers but rather encapsulated several whiskers that were held together by hydrogen bonding. In order to make sure that single whiskers are modified either a more efficient modifier has to be used or the whiskers have to be more vigorously stirred after the surfactant has been added to the water solution. It is important when creating biodegradable nanocomposites that high demands are placed on the environmental impact of the surfactant.

The TGA performed to investigate the thermal stability of the produced materials showed that both whiskers and composites were thermally stable in the region between 25 °C and 220 °C. 220 °C is the maximum processing temperature of this PLA. The DMTA performed to investigate the thermal properties of the produced materials showed that all whiskers were able to improve the storage modulus of PLA in the plastic zone. The DMTA analysis also showed that the surfactant treated whiskers were able to improve the storage modulus of the PLA/S material in the elastic zone. The results from the DMTA analysis also indicated that the surfactant used in this study had a higher level of interaction with the PLA matrix than with the modified whiskers. The surfactant caused a large decrease in the storage modulus of the PLA. This can be explained by the large amount of surfactant used (20 wt %), decreased crystallinity and increased porosity in the material. As a result the amount and type of surfactant used to modify cellulose whiskers have to be tailored for the biopolymer matrix

used. The DMTA analysis also indicated that well dispersed cellulose whiskers have a large potential in improving the mechanical properties of biopolymers.

## Acknowledgements

The authors would like to thank Cargill Dow LLC, Minneapolis, USA for the supplied Nature Works™ PLA polymer. We would also like to thank David Granger and Tone Borge at the Department of Chemical Engineering at NTNU for helping us to get started with the TGA work.

## References

1. Krochta JM, De Mulder-Johnston C. Edible and Biodegradable Polymer Films: Challenges and Opportunities. Food Technology 1997;51:61-74.

2. Lunt J. Large-scale production, properties and commercial applications of polylactic acid polymers. Polym Degrad Stab 1998;59:145-151.

3. Sinclair RG. The case for polylactic acid as a commodity plastics. Polym Mater Sci Eng. 1995;72:133-135.

4. de Vlieger JJ. Green plastics for food packaging. In: Ahvenainen R, editor. Novel food packaging techniques, England: Woodhead Publishing Limited, 2003, p 519-534.

5. Alexandre M, Dubois P. Polymer-layered silicate nanocomposites: preparation, properties and uses of a new class of materials. Mater Sci Eng, R 2000;28:1-63.

6. Azizi Samir MAS, Alloin F, Dufresne A. Review of Recent Research into Cellulosic Whiskers, Their Properties and Their Application in Nanocomposite Field. Biomacromolecules 2005;6:612-626.

7. Hamad W. Cellulosic Materials: Fibers, Networks and Composites. The Netherlands: Kluwer Academic Publishers, 2002, p 47.

8. Grunert M, Winter WT. Nanocomposites of Cellulose Acetate Butyrate Reinforced with Cellulose Nanocrystals. J Polym Environ 2002;10:27-30.

9. Dufresne A, Kellerhals MB, Witholt B. Transcrystallization in Mcl-PHAs/Cellulose Whiskers Composites. Macromolecules 1999;32:7396-7401.

10. Oksman K, Mathew AP, Bondeson D, Kvien I. Manufacturing process of cellulose whiskers/Polylactic acid nanocomposite. Compos Sci Technol 2006;66:2776-2784.

11. Noishiki Y, Nishiyama Y, Wada M, Kuga S, Magoshi J. Mechanical Properties of Silk Fibroin-Microcrystalline Cellulose Composite Films. J Appl Polym Sci 2002;86:3425-3429.

12. Anglès MN, Dufresne A. Plasticized Starch/Tunicin Whiskers Nanocomposite Materials. 2. Mechanical Behavior. Macromolecules 2001;34:2921-2931.

13. Heux L, Chauve G, Bonini C. Nonflocculating and Chiral-Nematic Self-ordering of Cellulose Microcrystals Suspensions in Nonpolar Solvents. Langmuir 2000;16:8210-8212.

14. Araki J, Wada M, Kuga S. Steric stabilization of a cellulose microcrystal suspension by poly(ethylene glycol) grafting. Langmuir 2001;17:21-27.

15. Goussé C, Chanzy H, Excoffier G, Soubeyrand L, Fleury E. Stable suspensions of partially silylated cellulose whiskers dispersed in organic solvents. Polymer 2002;43:2645-2651.

16. Goussé C, Chanzy H, Cerrada ML, Fleury E. Surface silylation of cellulose microfibrils: preparation and rheological properties. Polymer 2004;45:1569-1575.

17. Dong XM, Revol J-F, Gray DG. Effect of microcrystallite preparation conditions on the formation of colloid crystals of cellulose. Cellulose 1998;5:19-32.

18. Orts WJ, Godbout L, Marchessault RH, Revol J-F. Enhanced ordering of liquid crystalline suspensions of cellulose microfibrils: A small angle neutron scattering study. Macromolecules 1998;31:5717-5725.

19. Gopalan Nair K, Dufresne A, Gandini A, Belgacem MN. Crab Shell Chitin Whiskers Reinforced Natural Rubber Nanocomposites. 3. Effect of Chemical Modification of Chitin Whiskers. Biomacromolecules 2003;4:1835-1842.

20. Mathew AP, Oksman K, Sain M. Mechanical properties of biodegradable composites from poly lactic acid (PLA) and microcrystalline cellulose (MCC). J Appl Polym Sci 2005;97:2014-2025.

21. Araki J, Wada M, Kuga S, Okano T. Flow properties of microcrystalline cellulose suspension prepared by acid treatment of native cellulose. Colloids Surf A 1998;142:75-82.

22. Revol J-F, Bradford H, Giasson J, Marchessault RH. Helicoidal self-ordering of cellulose microfibrils in aqueous suspension. Int J Biol Macromol 1992;14:170-172.

23. Kvien I, Tanem BS, Oksman K. Characterization of Cellulose Whiskers and Their Nanocomposites by Atomic Force and Electron Microscopy. Biomacromolecules 2005;6:3160-3165.

24. Malainine ME, Mahrouz M, Dufresne A. Thermoplastic nanocomposites based on cellulose microfibrils from opuntiaficus-indica parenchyma cell. Compos Sci Technol 2005;65:1520-1526.

25. Petersson L, Oksman K. Biopolymer based Nanocomposites: Comparing Layered Silicates and Microcrystalline Cellulose as Nanoreinforcement. Compos Sci Technol 2006;66:2187-2196

**Caption to Table**

Table I Prepared formulations [wt %]

**Table I**

| *Materials* | *PLA* | *CNW* | *Surfactant* |
|---|---|---|---|
| PLA | 100 | - | - |
| PLA/S | 80 | - | 20 |
| PLA/CNW | 95 | 5 | - |
| PLA/B-CNW | 95 | 5 | - |
| PLA/S-CNW | 75 | 5 | 20 |

**Caption to Figures**

Figure 1. The structure of Avicel Ph 102 particles.

Figure 2. Flow birefringence of the produced whiskers (1.5 wt %) in deionized water.

Figure 3. The structure of the produced whiskers analyzed with TEM.

Figure 4. The structure of the freeze dried whiskers prior to dispersion analyzed with FESEM. a) CNW, b) B-CNW and c) S-CNW

Figure 5. Flow birefringence of 1.5 wt % S-CNW in chloroform.

Figure 6. Fracture surfaces of the nanocomposite films analyzed with FESEM.
a) PLA/CNW, b) PLA/B-CNW and c) PLA/S-CNW

Figure 7. Image showing the appearance of the different materials.
a) PLA, b) PLA/CNW, c) PLA/B-CNW, d) PLA/S-CNW and e) PLA/S

Figure 8. Image showing the appearance of PLA/S-CNW and PLA/S (a) before and (b) after pressing.

Figure 9. TEM analysis of the nanocomposite films.
a) PLA/CNW, b) PLA/B-CNW and c) PLA/S-CNW

Figure 10. TGA analysis of (a) whiskers and (b) nanocomposites.

Figure 11. Storage modulus curves and tan δ peaks from DMTA analysis.
a) PLA, PLA/CNW and PLA/B-CNW
b) PLA, PLA/S and PLA/S-CNW

Figure 1

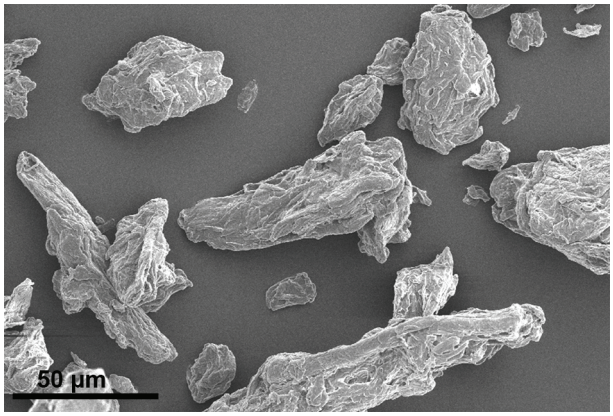

Figure 2

Figure 3

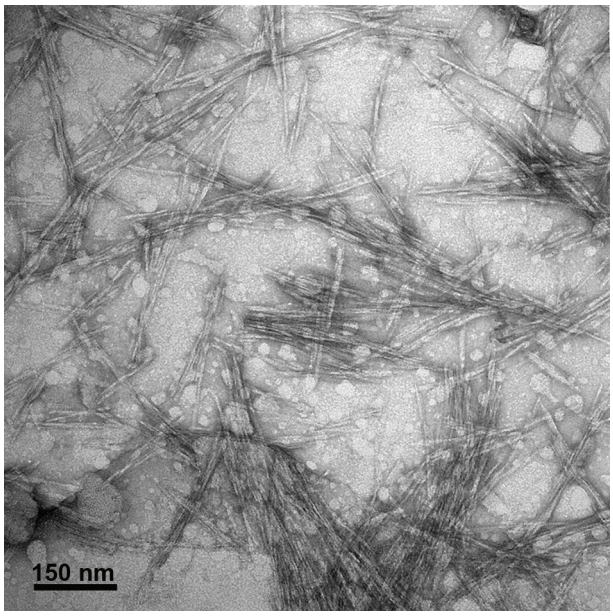

Figure 4

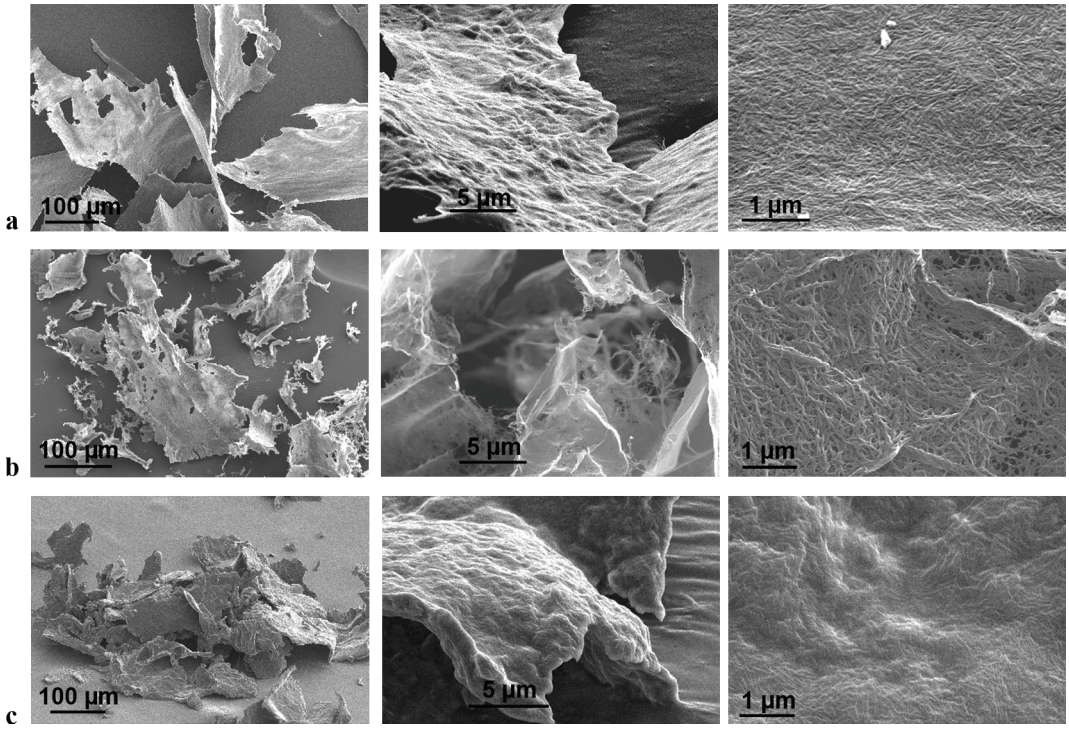

Figure 5

Figure 6

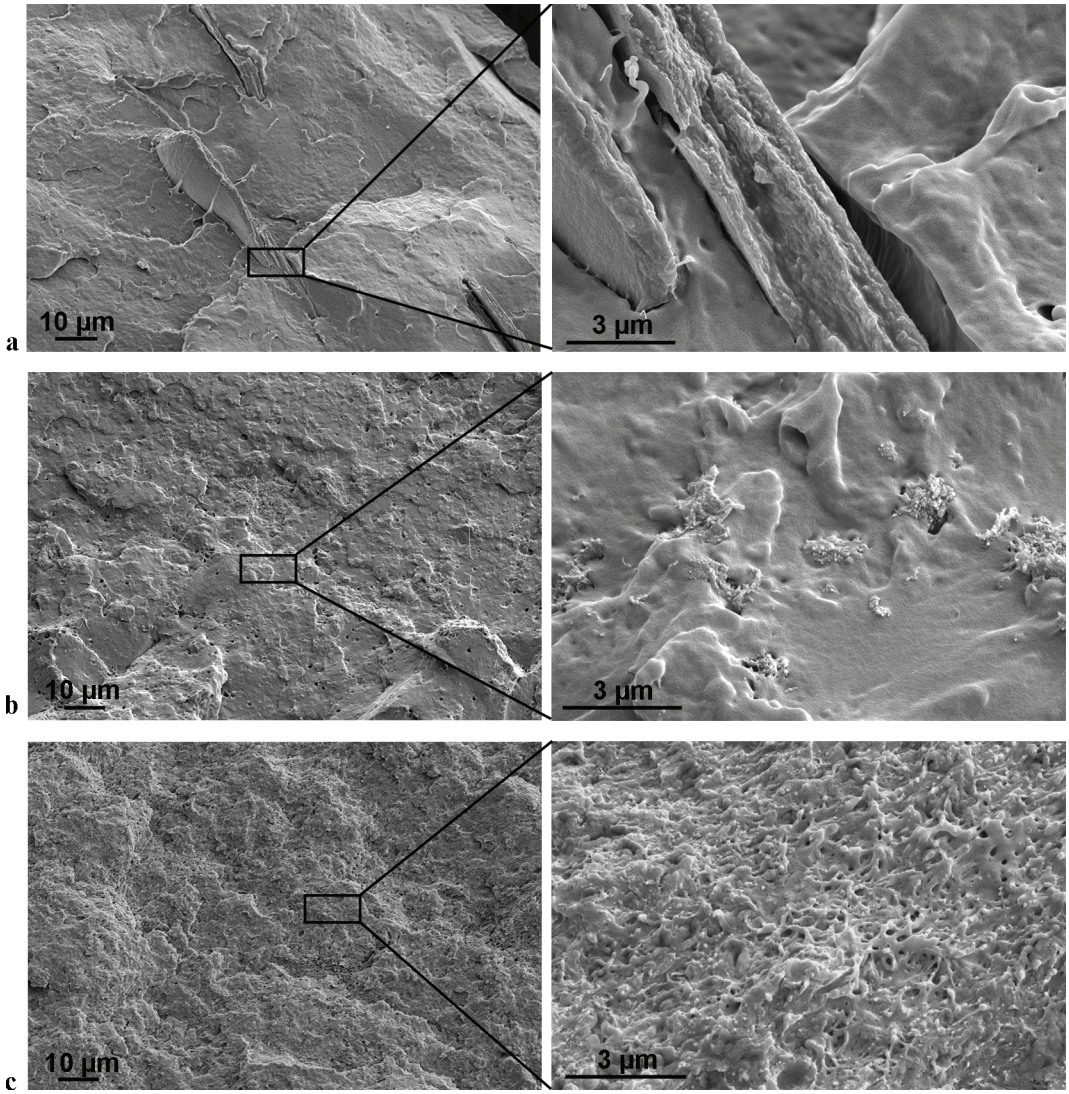

Figure 7

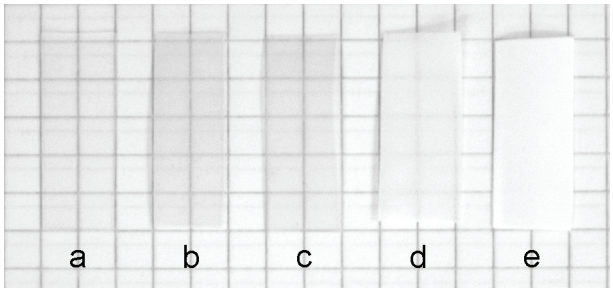

Figure 8

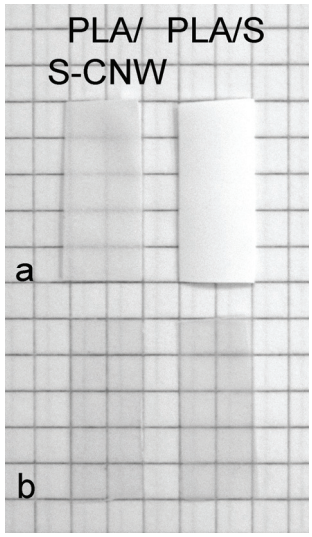

Figure 9

a

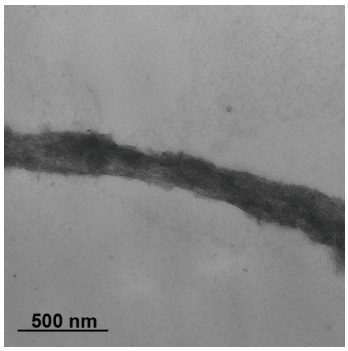


b

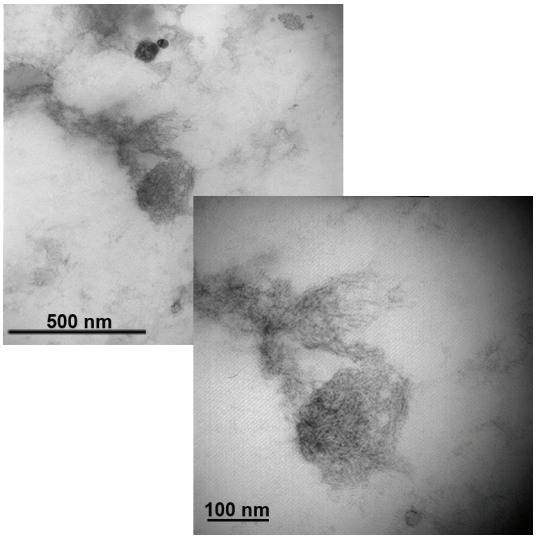


c

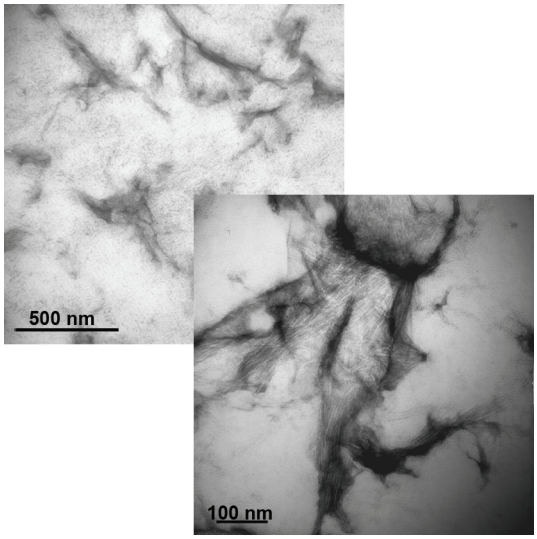

Figure 10

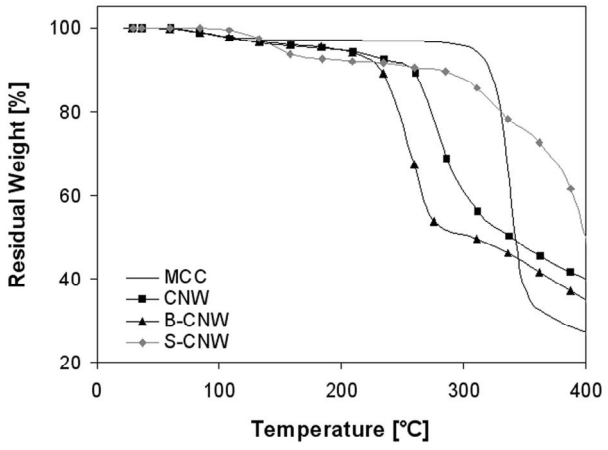
Residual Weight [%]
100
80
60
40
20
0
100
200
300
400
Temperature [°C]
MCC
CNW
B-CNW
S-CNW

a

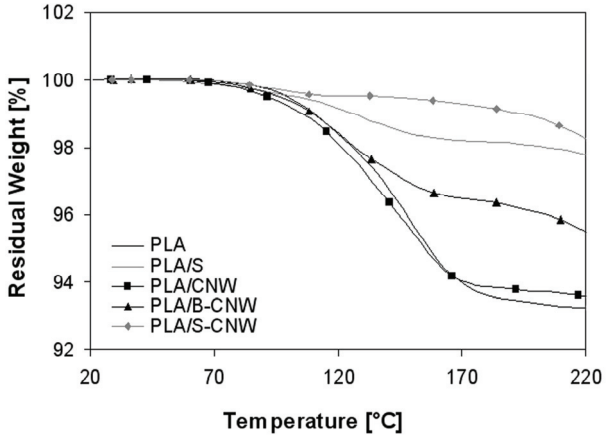
Residual Weight [%]
102
100
98
96
94
92
20
70
120
170
220
Temperature [°C]
PLA
PLA/S
PLA/CNW
PLA/B-CNW
PLA/S-CNW

b

Figure 11

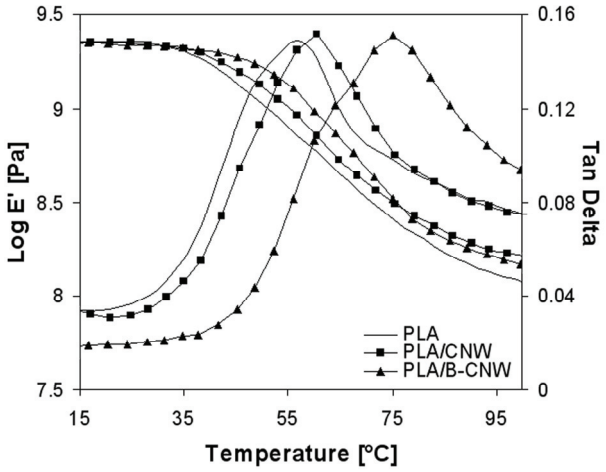
9.5
9
8.5
8
7.5
Log E' [Pa]
0.16
0.12
0.08
0.04
0
Tan Delta
15
35
55
75
95
Temperature [°C]
PLA
PLA/CNW
PLA/B-CNW

a

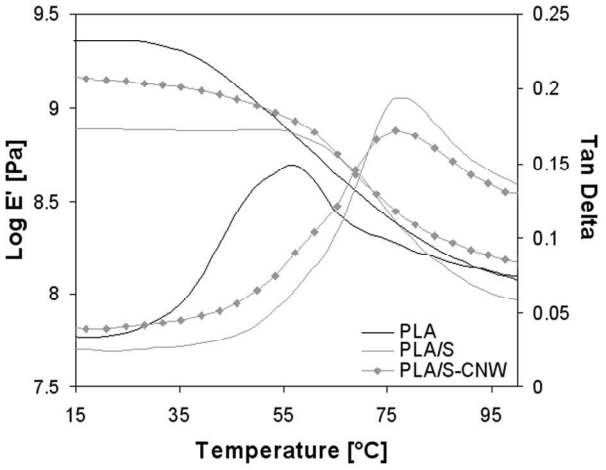
9.5
9
8.5
8
7.5
Log E' [Pa]
0.25
0.2
0.15
0.1
0.05
0
Tan Delta
15
35
55
75
95
Temperature [°C]
PLA
PLA/S
PLA/S-CNW

b

Paper V

Paper V: Kvien, I ; Tanem, BS ; Oksman, K: Characterization of Cellulose Whiskers and Their Nanocomposites by Atomic Force and Electron Microscopy. Biomacromolecules, 6(2005), 3160-3165 is not included in the pdf due to copyright.

Paper VI

# Characterization of starch based nanocomposites

*I. Kvien,[1)] J. Sugiyama,[2)] M. Vortrubec,[1)] K. Oksman[1,3)*]*

1) Department of Engineering Design and Materials, Norwegian University of Science and Technology, Rich. Birkelandsvei 2b, 7491 Trondheim, Norway

2) Research Institute for Sustainable Humanosphere (RISH), Kyoto University, Uji, Kyoto 611-0011, Japan

3) Division of Manufacturing and Design of Wood and Bionanocomposites, Luleå University of Technology, SE-931 87 Skellefteå, Sweden

* Author for correspondence (e-mail: kristiina.oksman@ltu.se; phone +46 910585371; fax: +46 910585399)

## Abstract

The goal of this study was to characterize the nanostructure and the properties of starch based nanocomposites with either cellulose nano whiskers or layered silicates (synthetic hectorite) as reinforcements. Modified potato starch was used as matrix with water and sorbitol as plasticizers and with 5 wt% of either of the reinforcements. Two methods were explored to prepare samples for transmission electron microscopy examination; chemical fixation and freeze etching. It was possible to characterize the nanostructure both parallel and perpendicular to the nanocomposite surface by the freeze etching technique. Both nanocomposites showed well distributed reinforcements in the starch matrix. Dynamic mechanical thermal analysis showed that the storage modulus was significantly improved at elevated temperatures, especially for the layered silicate nanocomposite. Both nanocomposites showed a significant improvement in tensile properties compared to the pure matrix.

Keywords: Cellulose whiskers/crystals, layered silicates, nanocomposites, biopolymer, electron microscopy, sample preparation, mechanical properties

## 1. Introduction

Biopolymers are attracting considerable attention as a potential replacement for petroleum based plastics due to an increased consciousness for sustainable development. Biopolymers maintain the carbon dioxide balance after their degradation and are readily biodegradable which will save energy on waste disposal. The limited performance and high cost of these materials are today restricting the competitiveness to traditional thermoplastics. One way to enhance the material properties and to broaden the possible applications for biopolymers is to produce nanocomposites [1].

Starch is a biopolymer which is abundant in nature, is inexpensive and increasingly used as packaging material. It has however poor mechanical properties and a high water affinity. Some studies reported on the preparation of starch based nanocomposites using cellulose nano whiskers (CNW) [2-6] and layered silicates (LS) [7-12]. Starch is hydrophilic and nanocomposites prepared by solution casting and melt blending of unmodified CNW [2-6] and unmodified LS [8,11] are reported to contain well dispersed reinforcements in contradiction to the use of for example modified LS. There is however only limited insight into the nanostructure of the starch based nanocomposites. For starch containing cellulose nano whiskers as reinforcement, no transmission electron microscopy (TEM) work is reported in literature. For these materials scanning electron microscopy (SEM) has exclusively been utilized for structure determination which only gives limited insight into the nanostructure. The resolution of a conventional SEM is limited compared to TEM and there is a need for a more thorough investigation of the structure of CNW/starch nanocomposites. The nanostructure of the layered silicate based nanocomposites is traditionally characterized by a combination of TEM and wide angle X-ray diffraction (WAXD) [13]. However, for starch based nanocomposites with LS as reinforcement only two studies report on nanostructure characterization using TEM [8,11]. This is probably because thermoplastic starch

has a strong water affinity and thus conventional sample preparation techniques can not be used to prepare samples for TEM. Preparation of biological samples for TEM examination involves fixation of the specimens, dehydration and infiltration of a resin. Different methods are widely described in literature [14]. Fixation, by cross-linking the starch, will render the starch less hydrophilic [15]. In a previous study on amylose, amylopectin and starch films the samples were fixed in 2 % glutaraldehyde [16]. It was however found that the fixation was only effective for the amylose film and both amylopectin and starch films partly dissolved in the preparation step. One way to exclude water from the fixation step for water soluble specimens is to use vapour fixation [17]. However, different specimens require different fixations and preparative procedures. A major drawback of this method is that the morphology of the sample can be changed upon fixation. Another method for preparation of samples for TEM which also excludes water from the system is the freeze-etching method. By this method the chemical fixation is replaced by freeze fixation and a replica of the freeze-etched surface is prepared. Replication is an old and well-known method for the preparation of specimens for TEM examination [18]. The method is applicable for beam sensitive materials or materials which can not be prepared by conventional preparation methods, such as water soluble samples. The method is however time consuming and the interpretation of the images is difficult.

The goal of this study was to characterize the nanostructure and the properties of starch based nanocomposites with either cellulose nano whiskers or layered silicates as reinforcements. Modified potato starch was used as matrix with water and sorbitol as plasticizers and with 5 wt% of either of the reinforcements. Two methods were explored to prepare samples for TEM examination; chemical fixation and freeze etching. In addition, the structure of the materials was studied by field emission scanning electron microscope, WAXD and differential scanning

calorimetry. The thermal and mechanical performance was analyzed by dynamic mechanical thermal analysis and tensile testing.

## 2. Experimental Section

### *2.1 Materials*

Matrix: Modified normal potato starch, Perlcoat 155, was kindly supplied by Lyckeby Industrial AB (Kristianstad, Sweden). The starch is a hydroxypropylated and oxidized starch, which has good film-forming properties [19]. The degree of substitution with respect to hydroxypropyl groups is 0.11 and with respect to carboxylic acid groups is 0.04 [19]. Normal potato starch contains about 21 % amylose and 79 % amylopectin. The water content of the starch was 18 wt% and was used without predrying. D-Sorbitol was used as plasticizer and was supplied by Fluka Chemie GmbH (Buchs, Schweiz).

Reinforcement: The microcrystalline cellulose (MCC) was kindly supplied by Borregaard Chemcell (Sarpsborg, Norway). It is a powder with particle size of 5-50 μm containing >93 % MCC. The layered silicates (synthetic smectite clay/synthetic hectorite) were supplied by Rockwood Additives Limited (Cheshire, U.K.). The tradename is Laponite B and is not organically modified. The bulk density is 0.7-1.3 kg/dm$^3$. The thickness of the disc-shaped sheets is 1 nm and they are 25-40 nm in diameter.

### *2.2 Processing of nanocomposites*

Separation of nanoreinforcement

The cellulose whiskers were isolated from microcrystalline cellulose (MCC) by acid hydrolysis as described by Bondeson et. al [20]. The layered silicates (LS) were dispersed in water at 25 ˚C for 24 hours with stirring. During this time the suspension was sonificated (Hielscher UP 200S,

Germany) three times for 5 minutes. The concentration of both nanoreinforcement suspensions was 0.5 wt%.

Film preparation

Starch, sorbitol and CNW or LS (67/28/5) were mixed by first dispersing starch in 100 g of the suspension containing the reinforcement. The gelatinization of starch was performed by stirring this mixture for 30 min at 95 ˚C. The sorbitol was dissolved in approximately 5 ml water and added to the suspension. The suspension was then poured onto polystyrene petri dishes and the water was evaporated at 70 ˚C overnight. The obtained films were conditioned for at least three weeks in a desiccator with a saturated solution of magnesium nitrate at 25 ˚C, which gives a relative humidity of 53 % according to ASTM E 104. Films with a thickness of 0.2 mm were obtained. The final composition and sample codes of the materials are given in Table 1.

### *2.3 Characterization*

*2.3.1. Microscopy*

Optical light microscope (OM) observations were performed using a Leica DMLB. OM was used in order to follow the gelatinization process of starch granules. The magnification used was x 20.

The starch film and nanocomposites were examined in a Hitachi 4300S Field emission scanning electron microscope (FESEM). The accelerating voltage applied was 5 kV. To examine the bulk morphology of the nanocomposites, both fracture surfaces and ultra microtomed surfaces were examined. The surfaces were sputter-coated with platinum before examination.

Transmission electron microscope (TEM) was used to investigate the nanostructure of the materials. The cellulose nano whiskers were examined in a Philips CM 30 at 150 kV and the

layered silicates and nanocomposites were examined in a Jeol JEM-2000 EX II at 100 kV. To examine the cellulose whiskers and clay particles a droplet of the diluted suspensions was allowed to float on and eventually flow through a copper grid covered with a porous carbon film. The whiskers were stained by floating the grids in a 2 wt% solution of uranyl acetate for 2 min.

The sample preparation of the nanocomposites for TEM was made using chemical fixation and freeze-etching. For chemical fixation small pieces (30 x 30 mm) of the nanocomposite films were put on a metal net in a glass vessel. 0.8 g *p*-formaldehyde was put in the bottom of the glass vessel. The glass vessel was evacuated and then heated in an oven at 100 ºC for 24 h. The samples were then post fixed and stained in OsO4-vapor, rinsed in water and dehydrated in ethanol series. The ethanol was then solvent replaced by propylene oxide followed by resin infiltration and curing with Epon 812.

For the freeze-etching technique the nanocomposite films were cut to rectangular sheets, mounted on holders and then rapidly frozen in liquid propane at -183 ºC. The films were freeze-fractured and etched before replicas of the freshly cleaved surface were prepared by carbon coating and shadowing with platinum at 25º. The replicas were gathered onto formvare coated copper grids. Replicas both parallel and perpendicular to the film surface were prepared.

*2.3.2 Wide angle X-ray diffraction (WAXD)*

The X-ray diffraction patterns of the LS, starch film and the nanocomposites were obtained using a Siemens Diffractometer D5005 (Erlangen, Germany). The samples were exposed for a period of 11s for each angle of incidence ($\theta$) using a Cu $K\alpha_{1,2}$ X-ray source with a wavelength ($\lambda$) of 1.541 Å. The angle of incidence was varied from ~4º to ~28º by steps of 0.06º. The periodical distances (d) of the main peaks were calculated according to Bragg's equation ($n\lambda = 2d\sin\theta$).

*2.3.3 Tensile Testing*

Tensile testing was carried out using a miniature material tester, Rheometric Scientific MiniMat 2000 (New Jersey, USA), with a 1000 N load cell at a crosshead speed of 2 mm/min. The samples were prepared by cutting strips from the films with a width of 5 mm. The length between the grips was 15 mm and seven samples were used to characterize each material. The results obtained from the MiniMat 2000 can only be used for comparison, because the strain values are based on the rotational movement of the drive shaft.

*2.3.4 Dynamic Mechanical Thermal Analysis (DMTA)*

Dynamic mechanical properties of the nanocomposites were measured using a Rheometric Scientific DMTA V (New Jersey, USA) in tensile mode. The measurements were carried out at a constant frequency of 1 Hz, a strain amplitude of 0.05 %, a temperature range of -60°C – 180°C, a heating rate of 3 °C/min and gap distance of 20 mm. The samples were prepared by cutting strips from the films with a width of 5 mm. Four samples were used to characterize each material.

*2.3.5 Differential Scanning Calorimetry (DSC)*

Differential scanning calorimetry (DSC) was performed with Q100 (TA Instruments, New Castle, DE, USA) with a Refrigerated Cooling System (RSC). The samples were placed in a sealed DSC-cell and at least two parallels of each material were tested. Each sample was heated from -60 ºC to +250 ºC at a heating rate of 10 ºC/min. The glass transition temperature ($T_g$) was taken as the midpoint of the transitions.

## 3. Results and Discussion

### *3.1 Processing and structure*

The microcrystalline cellulose prior to acid hydrolysis and the layered silicate (synthetic hectorite) before swelling in water are shown in Fig. 1. The particles were ~5-50 μm. ***(Fig.1)*** TEM analysis of the suspension after acid hydrolysis of MCC revealed cellulose nano whiskers which had a needle-like structure (Fig. 2a). The whiskers were ~5 nm in width and ~200 nm in length as determined in a previous study [21]. The layered silicates had a disc-like structure with diameter 25-40 nm as seen from TEM observation in Fig. 2b. The clay suspension consisted of well separated clay sheets. ***(Fig. 2)***

The gelatinization process of starch was followed by light microscopy. Upon gelatinization the starch granules undergoes structural changes. The granules swell and are disrupted as shown in Fig. 3. The amylose leaches out of the swollen granules and the texture becomes gel-like [22]. ***(Fig. 3)***

For processing of the nanocomposites the starch granules were first dispersed in the suspension containing the reinforcement and then gelatinized before the sorbitol was added. This strategy was reported to result in a well dispersed nanocomposite with layered silicates as reinforcement [10]. The starch matrix was thereby allowed to interact with the reinforcement prior to addition of plasticizer. This procedure was reported to hinder the accumulation of plasticizer in the clay-starch interface [10]. This will be discussed in the section about mechanical properties.

In order to determine if whiskers are well distributed in solutions flow birefringence is often used [23]. Fig. 4 shows a picture of the suspension of starch, sorbitol and CNW prior to casting. As can be seen the suspension showed flow birefringence, which indicated a well distribution of the CNW in the starch/sorbitol/water suspension. ***(Fig. 4)***

After casting, the films were transparent and no visible agglomerates in the nanocomposites could be seen. The appearance of the films is shown in Fig. 5. This indicated well distributed nanoreinforcement in the starch matrix. ***(Fig. 5)***

In Fig. 6 fracture surfaces of the films are seen. The surfaces of the starch film and S-LS nanocomposite were very smooth while the S-CNW nanocomposite was rougher. Small white particles were detectable in the S-CNW nanocomposite and it is uncertain whether this was due to small clusters of agglomerated cellulose whiskers emerging from the matrix, the matrix itself evolving due to the influence by the electron beam or contamination during sample preparation. There were no big agglomerates of cellulose whiskers detectable which indicates a homogenous distribution of the cellulose whiskers in the matrix. In the S-LS nanocomposite the surface seemed smooth and there were no layered silicate sheets detectable. This can be due to lack of resolution, the coating of the platinum particles or because of well distributed clay sheets. No agglomerates of layered silicates were detectable. Ultramicrotomed surfaces of the samples were also investigated. The appearance of these surfaces resembled those of the fractured surfaces as seen from the pictures in Fig. 7. ***(Fig. 6) (Fig. 7)***

For transmission electron microscopy analysis of the nanocomposites it was found that the sample preparation was challenging. After chemical fixation by *p*-formaldehyde vapor, the films appeared less brittle and more rubber-like than before treatment. It thus seemed that the treatment was effective in cross-linking the starch. However, after the dehydration steps and embedding in resin, it was still not possible to obtain ultra thin sections of the nanocomposites. The sections instantly disappeared from the water surface after sectioning and it was therefore not possible to analyze the samples in TEM by this method. It was however found that it was possible to prepare starch based nanocomposite for TEM analysis by using the freeze-fracture technique. This technique allowed examination of the bulk structure both parallel and perpendicular to the film surface. In Fig. 8 and 9 replicas of the S-CNW and S-LS nanocomposites, respectively, are shown. Both reinforcements were well distributed in the starch matrix, although they appeared denser in some areas. In Fig. 8a the presence of cellulose nanowhiskers was observed as a fibrillated texture

in the starch matrix. This texture was not observed in the S-LS nanocomposite. These observations indicate that the CNW were removed by the knife during cutting and therefore small holes were formed from the whisker pullouts. The texture may also be due to underlying structure of cellulose whiskers. In other areas the cellulose nano whiskers seemed to protrude from the surface, as observed for the cross section replica in Fig. 8b. There was a tendency for the CNWs to arrange parallel to the film surface. Similar trend was seen for the S-LS nanocomposite. The silicate sheets were observed as disc-like structures with the same size as observed in the TEM image of the dried layered silicate suspension in Fig. 2b. In the cross section replica (Fig. 9b) only a part of the sheets was observed, which suggest a tendency for the layered silicates to arrange parallel to the film surface. From the cross section replica it seemed that the S-LS nanocomposite had an exfoliated structure. In areas where the presence of the layered silicates was denser the distance between the sheets was difficult to determine, and the nanocomposite might locally have an intercalated structure. ***(Fig. 8) (Fig. 9)***

Wide angle X-ray diffractograms of the samples are shown in Fig. 10. Both the starch film and the nanocomposites showed an amorphous behavior. No diffraction peak was observed, but rather a broad hump located at around $2\theta = 20^{\circ}$. The diffractogram of the pure LS powder did not show a well-defined 001 peak. The Laponite B particles are relatively small and therefore have a random orientation when prepared as pressed powder which can prevent the 001 peak from showing up very well. However, in the diffractogram of the freeze dried LS suspension the 001 peak appeared at around $2\theta = 7^{\circ}$. The layers were now more oriented in the 001 plane. This corresponds to a distance between the layers of 1.24 nm according to Braggs law. In the diffractogram of the S-LS nanocomposite, no signal from the 001 peak was observed which indicates that the distance between the silicate sheets was larger than detectable by the low angle limit. The starch molecules

or sorbitol and water were thus probably able to penetrate between the silicate sheets and thereby creating an exfoliated structure. It is worth noting that there was only 5 wt% LS in the nanocomposite and therefore the X-ray diffraction analysis may fail in detecting the crystalline structure of the reinforcement in the polymer. However, the TEM observations showed that the silicate sheets were arranged parallel to the film surface and was therefore expected to give a detectable signal if the distance between the sheets had been in the range detectable by the analysis. ***(Fig. 10)***

### *3.2 Mechanical and thermal properties*

Tensile testing

The mechanical properties of the starch film and the nanocomposites are given in Table 2. Both nanocomposites showed an improvement in tensile modulus, yield strength and elongation at break compared to the pure matrix. The CNW and LS nanocomposites showed an improved tensile modulus compared to the neat material by 90 MPa (24 %) and 100 MPa (27 %), respectively. This is a significant improvement compared to other studies on starch nanocomposites with 5 wt% reinforcement [2,3,6,10,11]. The tensile strength was only slightly improved, a result which is also reported in earlier studies. In this study the starch matrix as received contained hydroxypropyl groups which might contribute to restricted interaction with the highly hydrophilic reinforcements.

Unexpectedly, the elongation at break was increased for both nanocomposites compared to the pure matrix. This behavior has not earlier been reported for CNW based starch nanocomposites, but has been reported for LS based nanocomposites [10,11]. Pandey [10] explained that the increased elongation at break was due to the processing of their materials in which the plasticizer was mixed after starch diffusion inside the gallery and would therefore migrate throughout the

system and retaining the plasticizer efficiency. The gelatinization of starch together with cellulose whiskers prior to addition of plasticizer has not been reported earlier and might explain the increased elongation at break in this study. This indicates that the sorbitol was not present on the surface of the reinforcement as reported earlier when glycerol was used as plastizicer [6], but was distributed throughout the material. In addition, the moisture content was slightly higher in the nanocomposites, and this may also be the reason for the increased elongation at break. Typical stress-strain curves for the materials are given in Fig. 11. ***(Fig. 11)***

Dynamic mechanical thermal analysis

The storage modulus of the starch film and nanocomposites as a function of temperature is given in logarithmic scale in Fig. 12a. The CNW nanocomposite showed an improved storage modulus above room temperature compared to the starch film. The S-LS nanocomposite showed an improved storage modulus over the entire temperature span. The improvement in storage modulus was more pronounced at elevated temperatures for both nanocomposites where the molecular relaxation for the starch matrix occurs. The starch film showed a rather large standard deviation in the storage modulus up to room temperature. This might be due to difficulties in accurate measurement of the soft starch matrix prior to testing and thickness variations throughout the sample. At room temperature (25 ºC) the CNW and the LS nanocomposites showed an improvement of 74 MPa (17 %) and 705 MPa (162 %), respectively, compared to the pure starch film. At 60 ºC the improvement was even more; a 102.7 MPa (160 %) and 250 MPa (388 %) increase of the storage modulus for the CNW and the LS nanocomposite, respectively, compared to the pure starch film. This is a significant improvement compared to earlier dynamic mechanical data with similar reinforcement content [2,6,11]. It was calculated that the theoretical available surface area of the layered silicate sheets was 4 times higher than the available surface area of the

cellulose nano whiskers. This might explain the more efficient reinforcing effect of the clay sheets. The tensile modulus of the LS nanocomposite did not seem to correlate with the storage modulus measured from dynamic mechanical data. This might be due to the fact that dynamic mechanical measurements involve weak stresses. Higher stresses are utilized in tensile testing and thus, the interaction between the reinforcement and matrix may be destroyed in this case [6]. ***(Fig. 12)***

In Fig. 12b the tan delta is shown for the same temperature range, showing three different relaxation peaks. The first peak was seen at –10º and it is suggested to be caused by the relaxation of sorbitol [24]. The peaks were slightly lower for the nanocomposites, but these materials also contained less sorbitol. The position of the peaks was not altered for the three materials. However, the next transition which occurred at 50 ºC for the starch material and is attributed to the relaxation of the starch [6,24,25] was shifted to higher temperatures for the nanocomposites. The peaks were not well-defined and therefore the shift in the tan delta peak was difficult to estimate, but the peaks were lower and broader than for the pure matrix. Thus, the starch chains were altered by the introduction of nanoreinforcement and therefore the relaxation of starch was done in a higher and broader temperature range. This indicates interaction between the starch and reinforcement and that the nanoreinforcement was well dispersed in the starch matrix. This also strengthens the conclusion from the tensile testing that the plasticizer was not present in the starch/reinforcements interfacial zone. It was not possible to complete the measurement of the starch film during the third transition due to extensive drop in mechanical properties. The third transition was probably due to melting of crystals in the starch matrix. This was unexpected since the X-ray analysis concluded all materials to be amorphous. However, the DMTA measurements were done several weeks after the X-ray analysis and therefore the crystal formation may be due to aging of starch through crystallization. This is known as retrogradation and is caused by reassociation during storage of amorphous gelatinized starch into a more ordered state [26].

Differential scanning calorimetry (DSC)

DSC was performed to confirm the thermal transitions and to investigate further the third transition observed in DMTA analysis. The results from DSC are given in Table 3. The results are only approximately values since the transitions were taking place over a broad temperature range and were therefore difficult to estimate accurately. The results correlated quite well with DMTA analysis. A melting point was found for all three materials. Interestingly, the melting point of the two nanocomposites was significantly shifted to higher temperatures. It thus seemed that the presence of the nanoreinforcement in the starch matrix influenced the size and amount of crystals formed in the starch matrix.

## 4. Conclusions

The goal of this study was to characterize the nanostructure and the properties of starch based nanocomposites with two different nano reinforcements, cellulose nano whiskers (CNW) or layered silicates (LS). Modified potato starch was used as matrix with water and sorbitol as plasticizers and with 5 wt% nano reinforcement content.

Two methods were explored to prepare the samples for transmission electron microscopy examination; chemical fixation and freeze etching. It was found that the chemical fixation with *p*-formaldehyde vapour treatment of starch was not sufficient to enable ultrathin sectioning of the nanocomposite films. It was however shown that it was possible to characterize the nanostructure both parallel and perpendicular to the nanocomposite surface by preparation of replicas prior to

TEM examination. Both reinforcements were well distributed in the starch matrix, although some agglomerations were found in some areas.

From X-ray diffraction analysis it was found that all the prepared materials were amorphous. X-ray analysis showed well distributed silicate sheets in the starch matrix, as seen by TEM observations.

Both nanocomposites showed an improvement in tensile modulus, yield strength and elongation at break compared to the pure matrix. The CNW and LS nanocomposites showed an improved tensile modulus compared to the neat material by 90 MPa (24%) and 100 MPa (27%), respectively. The order of the addition of plasticizer was concluded to influence the elongation at break for both nanocomposites. It was found that the plasticizer was not present in the starch/reinforcements interfacial zone. The dynamic mechanical thermal analysis showed that at room temperature the storage modulus of CNW and LS nanocomposites were improved by 74 MPa (17 %) and 705 MPa (162 %), respectively, compared to the pure starch film. At 60 ºC the improvement was 102.7 MPa (160 %) and 250 MPa (388 %) for the CNW and the LS nanocomposite compared to the pure starch film.

## Acknowledgements

Borregaard AS (Sarpsborg, Norway) is acknowledged for the microcrystalline cellulose and Lyckeby Industrial AB (Kristianstad, Sweden) is acknowledged for the starch. The Norwegian Research Council under the NANOMAT program is acknowledged for financial support of this work. The Laboratory of Active Biobased Materials at RISH, Kyoto University, Japan, and in particular Professor Hiroyuki Yano and Shin-ichirou Iwamoto are acknowledged for providing equipment and help with the formaldehyde treatment of starch. A special thanks to Chiori Itoh and Dr. Thi Thi Nge at The Laboratory of Biomass Morphogenesis and Information at the Research Institute for Sustainable Humanosphere (RISH), Kyoto University, Japan, for all the help with sample preparation and TEM observations.

## References


[1] A.K. MOHANTY, L.T. DRZAL and M. MISRA, Polym. Mater. Sci. Eng. 88 (2003) 60

[2] Y. LU, L. WENG and X. CAO, Carbohydr. Polym. 63 (2006) 198

[3] Y. LU, L. WENG and X. CAO, Macromolecular Bioscience 5 (2005) 1101

[4] A.P. MATHEW and A. DUFRESNE, Biomacromolecules 3 (2002) 609

[5] M.N. ANGLÈS and A. DUFRESNE, Macromolecules 33 (2000) 8344

[6] M.N. ANGLÈS and A. DUFRESNE, Macromolecules 34 (2001) 2921.

[7] H-T. LIAO and C-S. WU, J. Appl. Polym. Sci. 97 (2005) 397

[8] B. CHEN and J.R.G. EVANS, Carbohydr. Polym. 61 (2005) 455

[9] M. CHEN, B. CHEN and J.R.G. EVANS, Nanotechnology 16 (2005) 2334

[10] J.K. PANDEY and R.P. SINGH, Starch/Stärke 57 (2005) 8

[11] H-M. PARK, W-K. LEE, C-Y. PARK, W-J. CHO and C-S. J. HA, Mater. Sci. 38 (2003) 909

[12] H-M. WILHELM, M-R. SIERAKOWSKI, G.P. SOUZA and F. WYPYCH, Carbohydr. Polym. 52 (2003) 101

[13] S.S. RAY and M. OKAMOTO, Progr. Polym. Sci. 28 (2003) 1539

[14] A.M. GLUERT, in “Practical Methods in Electron Microscopy” (North Holland Publishing Company. 1975)

[15] Z. ZHU and S. CAO, Textile Research Journal 74(3) (2004) 253

[16] Å. RINDLAV-WESTLING, M. STADING and P. GATENHOLM, Biomacromolecules 3 (2002) 84

[17] M. GROTE, Microsc. Res. Tech. 21 (1992) 242

[18] L.C. SAWYER and D.T. GRUBB, in "Polymer Microscopy" (Chapman and Hall, London, 1994)

[19] A. JANSSON and L. JÄRNSTRÖM, Cellulose 12 (2005) 423

[20] D. BONDESON, A. MATHEW and K. OKSMAN, Cellulose 13(2) (2006) 171

[21] I. KVIEN, B.S. TANEM and K. OKSMAN, Biomacromolecules 6(6) (2005) 3160

[22] A.M. HERMANSSON and K. SVEGMARK, Trends Food Sci. Technol. 7 (1996) 345

[23] L. HEUX, G. CHAUVE and C. BONINI, Langmuir 16 (2000) 8210

[24] S. GAUDIN, D. LOURDIN, P.M. FORSSELL and P. COLONNA, Carbohydr. Polym. 43 (2000) 33

[25] M.F. BUTLER and R.E. CAMERON, Polymer 41 (2000) 2249

[26] A.P. MATHEW and A. DUFRESNE, Biomacromolecules 3 (2002) 1101

## Tables

Table 1 Composition of the starch film and the nanocomposites

Table 2 Tensile properties of the starch film and the nanocomposites

Table 3 DSC results of the starch film and the nanocomposites

**Table 1**

| Sample code | Dry starch [%] | Sorbitol [%] | Water [%] | Layered silicate [%] | Cellulose whiskers [%] |
|---|---|---|---|---|---|
| S | 62.3 | 31.8 | 5.9 | - | - |
| S-CNW | 58.2 | 29.6 | 6.9 | - | 5.3 |
| S-LS | 57.7 | 29.4 | 7.7 | 5.2 | - |

**Table 2**

| Materials | Tensile modulus [MPa] | Yield strength [MPa] | Elongation at break [%] |
|---|---|---|---|
| Starch | 370 ± 35 | 11.3 ± 1.0 | 25 ± 11 |
| S-CNW | 460 ± 10 | 13.7 ± 1.3 | 32 ± 10 |
| S-LS | 470 ± 45 | 12.5 ± 1.3 | 31 ± 12 |

**Table 3**

| Sample | $T_g$ sorbitol [ºC] | $T_g$ starch [ºC] | $T_m$ [ºC] |
|---|---|---|---|
| Starch | -17 | 55 | 134 |
| S-CNW | -12 | 70 | 154 |
| S-LS | -11 | 79 | 160 |

## Caption to Figures

Fig. 1 The structure of a) MCC and b) layered silicate particles prior to separation.

Fig. 2 a) Bright field TEM image of stained cellulose whiskers and b) layered silicate sheets after mixing in water for 24 hours.

Fig. 3 Starch granules seen in polarized light at a) room temperature and b) at 95ºC after 30 minutes.

Fig. 4 A suspension of starch, sorbitol and cellulose nanowhiskers in water showing flow birefringence when observed through crossed polarizers.

Fig. 5 Transparent films of starch, S-LS and S-CNW nanocomposites.

Fig. 6 FESEM pictures of fracture surfaces of a) starch b) S-CNW and c) S-LS nanocomposites.

Fig. 7 FESEM pictures of ultramicrotomed surfaces of a) starch b) S-CNW and c) S-LS nanocomposites.

Fig. 8 TEM images of replica of S-CNW nanocomposite a) parallel and b) perpendicular to the film surface.

Fig. 9 TEM images of replica of S-LS nanocomposite a) parallel and b) perpendicular to the film surface.

Fig 10 Wide angle X-ray diffraction of the starch, layered silicate and nanocomposites.

Fig. 11 Stress-strain curves of starch film, S-CNW and S-LS nanocomposites.

Fig. 12 a) Storage modulus and b) tan delta curves of the starch and nanocomposites.

Fig. 1

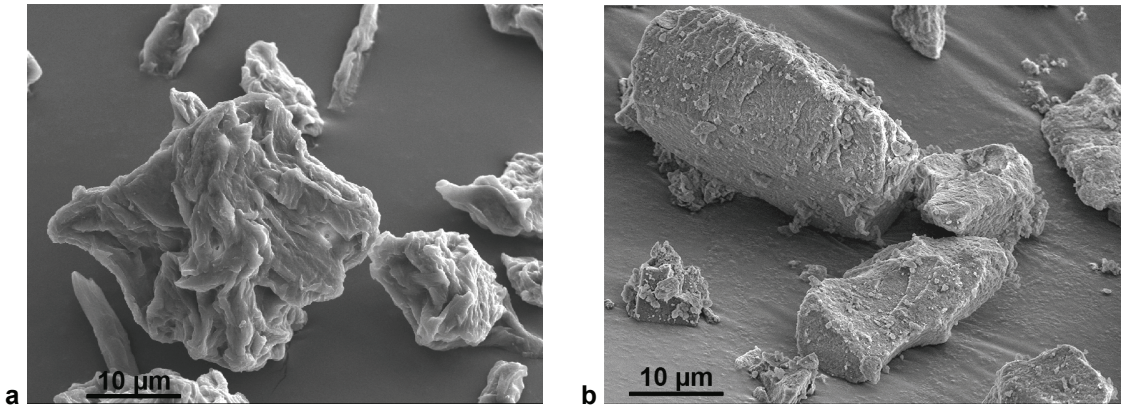

Fig. 2

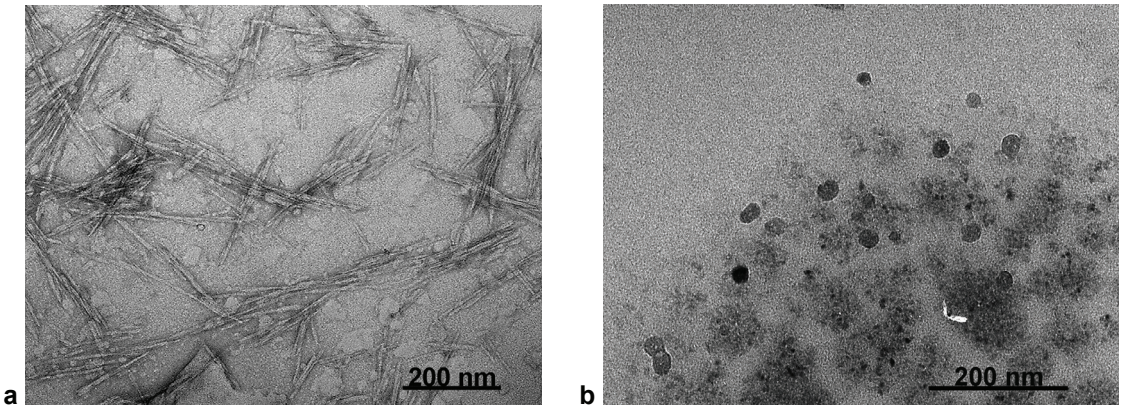

Fig. 3

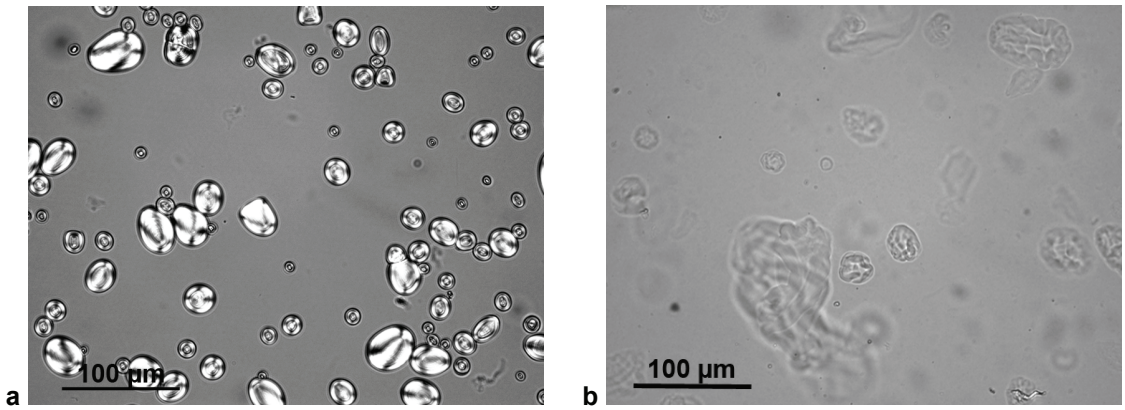

Fig. 4

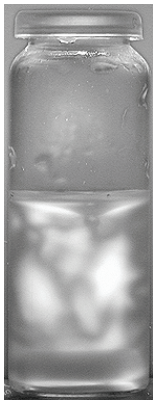

Fig. 5

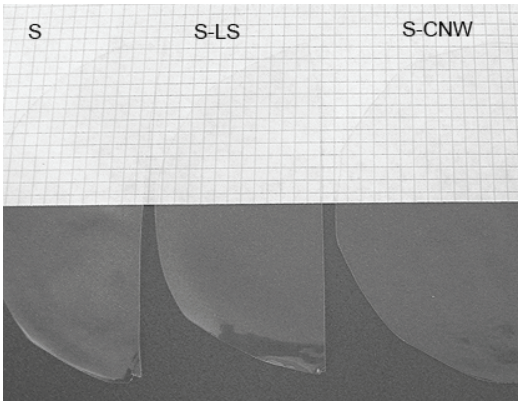

Fig. 6

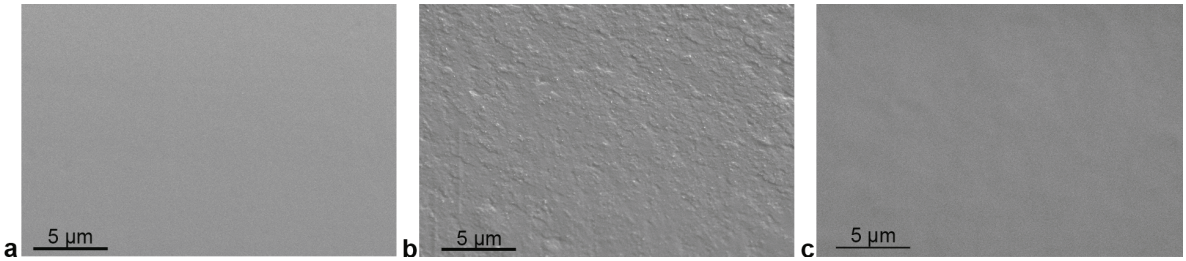

Fig. 7

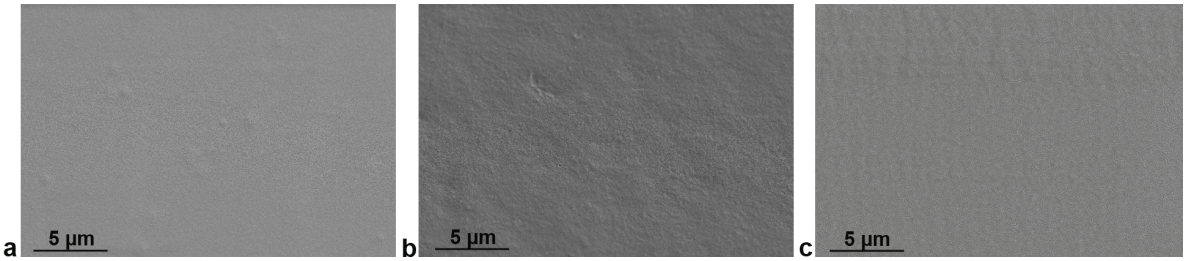

Fig. 8

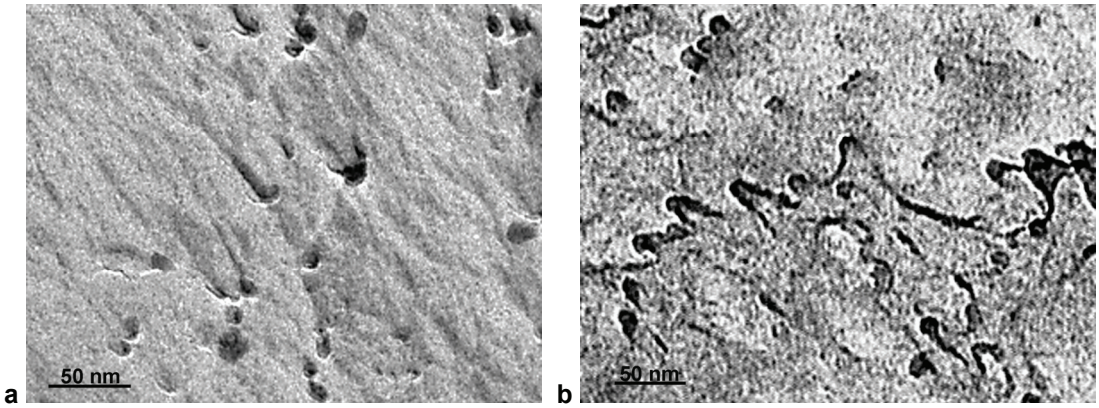

Fig. 9

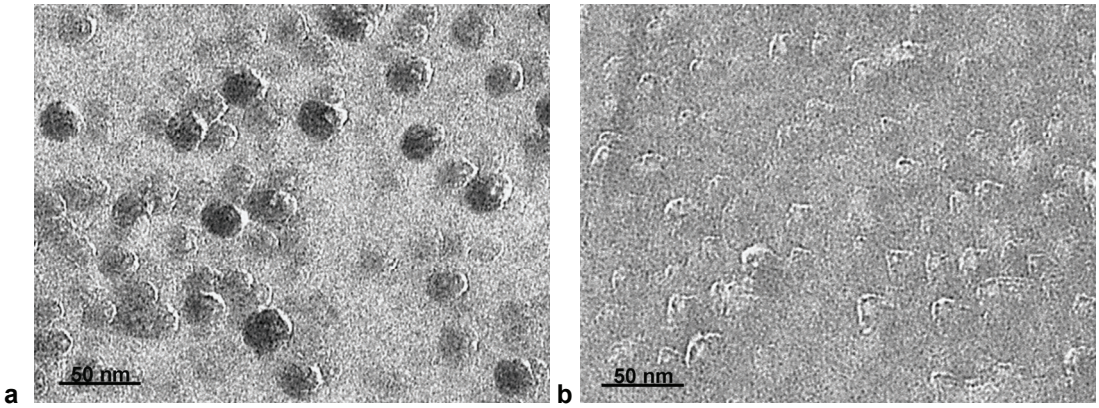

Fig. 10

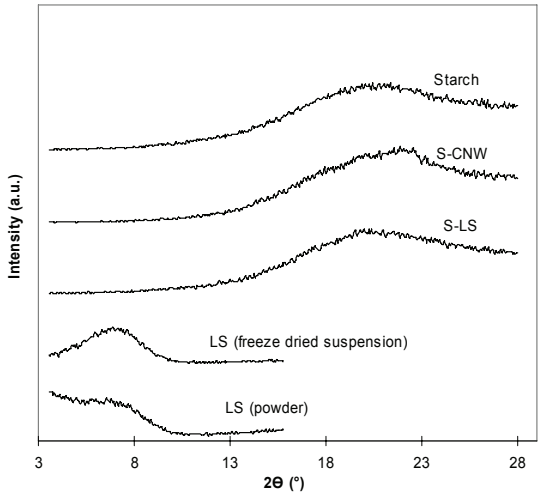
Starch
S-CNW
S-LS
LS (freeze dried suspension)
LS (powder)
Intensity (a.u.)
3
8
13
18
23
28
2Θ (°)

Fig. 11

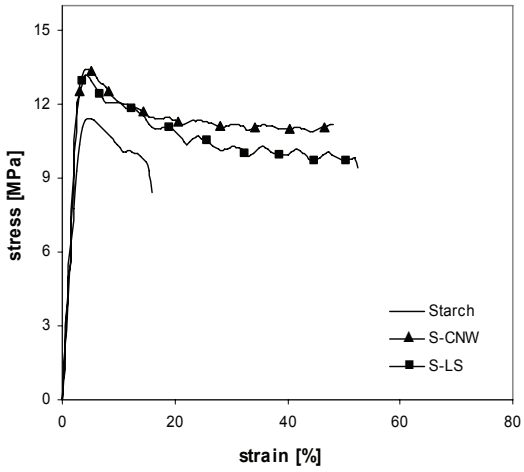

Fig. 12

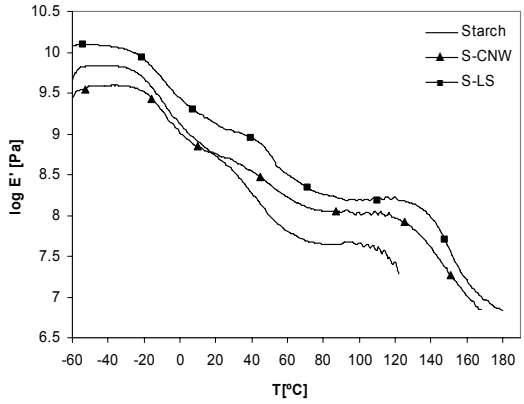
Starch
S-CNW
S-LS
log E' [Pa]
T[ºC]
10.5
10
9.5
9
8.5
8
7.5
7
6.5
-60 -40 -20 0 20 40 60 80 100 120 140 160 180

**a**

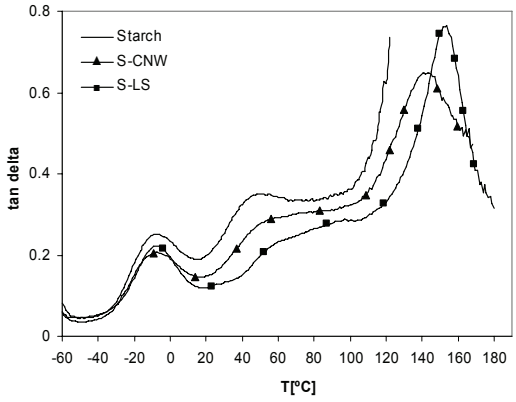
Starch
S-CNW
S-LS
tan delta
T[ºC]
0.8
0.6
0.4
0.2
0
-60 -40 -20 0 20 40 60 80 100 120 140 160 180

**b**

Paper VII

# Orientation of Cellulose Nanowhiskers in Polyvinyl Alcohol (PVA)

**I. Kvien[1] and K. Oksman[1,2*]**

[1)] Department of Engineering Design and Materials, Norwegian University of Science and Technology, Trondheim, Norway.

[2)] Division of Manufacturing and Design of Wood and Bionanocomposites, Luleå University of Technology, SE-931 87 Skellefteå, Sweden

* E-mail: kristiina.oksman@ltu.se; phone +46 910585371; fax: +46 910585399

## Abstract

The goal of this study was to align cellulose nanowhiskers in a polymer using a strong magnetic field and thereby obtain a unidirectional reinforced nanocomposite. Cellulose whiskers (2 wt%) were incorporated in a polyvinyl alcohol matrix using solution casting with water as the solvent. The suspension was cast and the water was evaporated while a homogenous magnetic field of 7 T was applied. Different microscopy investigations of prepared nanocomposites indicated that the cellulose whiskers were oriented perpendicular to the direction of the magnetic field. The dynamic mechanical thermal analysis further strengthened the idea of alignment because the results showed that the dynamic modulus of the nanocomposite was around 2 GPa higher at room temperature in the aligned direction compared to the transverse direction.

**PACS** 81.05.Lg; 81.05.Qk; 82.35.Np

## 1. Introduction

The utilization of cellulose nanowhiskers (CNW) as reinforcement in nanocomposites has attracted significant attention during the last decade [1, 2]. The interest is due to their renewable nature, abundance, good mechanical properties and large specific surface area. The theoretic elastic modulus has been calculated to 167.5 GPa [3]. The size of the CNW depends on the source, and is for example around 5 nm in width and 200 nm in length for whiskers from wood [4-6]. It has been reported that cellulose whiskers in suspension can be oriented by superconducting magnets [7], shearing forces [8] and by an electric field [9]. The magnetic orientation of a whisker with its long axis perpendicular to the field is owing to the negative diamagnetic anisotropy of cellulose [7, 9]. The aim of this study was to utilize the capability of cellulose whiskers to align in a magnetic field in order to prepare a unidirectional reinforced nanocomposite. In this novel study we align cellulose whiskers in a polymeric matrix and present dynamic mechanical behavior of the nanocomposite in the aligned and transverse directions. Cellulose nanowhiskers (2 wt%) were incorporated in a polyvinyl alcohol matrix using solution casting with water as the solvent. The suspension was cast and the water evaporated while a homogenous magnetic field with a magnetic flux density of ~7 T was applied. The structure of the material was studied by optical light microscope, field emission scanning electron microscope and atomic force microscope. The dynamic mechanical thermal properties of the nanocomposite were analyzed both in the transverse and parallel direction to the magnetic field.

## 2. Experimental

### *2.1 Materials and processing*

The matrix used in this study was water soluble polyvinyl alcohol (PVA, 107, Celanese Chemicals, Germany). The reinforcement was cellulose nanowhiskers (CNW) separated from

microcrystalline cellulose (MCC), which was kindly supplied by Borregaard Chemcell (Sarpsborg, Norway). It is a powder with particle size of 5-50 μm containing > 93 % MCC.

The cellulose nanowhiskers were isolated from MCC by acid hydrolysis. The isolation procedure is described by Bondeson et al. [10]. PVA was dissolved in water (10 wt%) at 80 ºC for 4 hours and the cellulose whiskers were added to the solution, producing a 0.2 wt% suspension of CNW in water and PVA. The suspension was sonificated for 2 minutes (Hielscher UP 200S, Germany) and then cast on glass slides and placed in the isocenter of a horizontal bore MR magnet (Bruker BioSpec 70/20). The water was evaporated in a magnetic field of 7.05 T overnight and a transparent film of 2 wt% CNW in PVA with thickness 0.09 mm was obtained.

*2.2 Characterization*

Optical light microscope (Leica DMLB, Wetzlar, Germany) observations were performed using polarized light at x 20 magnifications. The nanocomposite was examined in a field emission scanning electron microscope (FESEM, Hitachi 4300S, Hitachi Science System Ltd, Japan). The accelerating voltage applied was 5 kV. The surfaces were sputter-coated with platinum before examination. One sample was etched with ionized argon gas to remove the soft polymer from the surface. The etching time was 90 minutes (3 kV, 1 mA) without rotation of the sample. This sample was also characterized by atomic force microscope (AFM) (NanoScope IIIa, multimode SPM, Veeco, California, USA). The scans were performed in air with commercial Si Nanoprobes SPM tips. Height and phase images were obtained simultaneously in tapping mode at the fundamental resonance frequency of the cantilever with a scan rate of 0.5 lines/s using a j-type scanner. For analysis of the CNW, a droplet of the aqueous whisker suspension was dried on a freshly cleaved mica surface prior to AFM examination.

Dynamic mechanical thermal analysis (DMTA) of the prepared nanocomposites was carried out in tensile mode (Rheometric Scientific DMTA V, New Jersey, USA). The measurements were carried out at a constant frequency of 1 Hz, a strain amplitude of 0.05 %, a temperature range of 10 °C – 120 °C, a heating rate of 3 °C/min and gap distance of 10 mm. The samples were prepared by cutting strips from the films with a width of 4 mm. Two samples were used to characterize each material.

## 3. Results and Discussion

An AFM image of the cellulose nanowhiskers (CNW) is shown in Figure 1. The dimensions of the whiskers were ~5 nm in width and ~200 nm in length as determined in an earlier study [6].

In Figure 2 the dissolved PVA is observed through crossed polarized films before and after the addition of cellulose whiskers. The suspension containing cellulose whiskers showed flow birefringence which is due to the liquid crystalline behavior of CNW and is an indication of a stable distribution of the cellulose whiskers in the PVA solution.

After casting, the films were transparent. In polarized optical micrographs the nanocomposite was bright at ~45° and dark at 0° and 90° between the magnetic field direction and polarization plane (Figure 3). This indicated that the cellulose nanowhiskers were aligned in the PVA matrix, either parallel or transverse to the field direction.

The FESEM image of a fracture surface of the nanocomposite indicated aligned cellulose whiskers perpendicular to the field direction as seen from the underlying structure in Figure 4a. This has been reported earlier for orientation of a suspension of CNW in a magnetic field [7]. In the fracture surface the PVA matrix covered the cellulose whiskers. In order to remove the softer PVA matrix and reveal the cellulose crystals the polymer was etched by ionized argon gas. After etching a highly oriented structure was observed, as seen in Figure 4b which was

expected to be caused by alignment of cellulose whiskers. It must however be noted that sample preparation can introduce artifacts. It has been reported that ion etching on polymer samples can introduce some directionality in the structure [11], thus the sample may appear more oriented than it actually is. The surface of the etched nanocomposite was also investigated in AFM as seen in Figure 5. Again, the surface showed a highly oriented structure, also at nanoscale.

The dynamic mechanical properties of the nanocomposite were measured in the parallel and transverse direction to the magnetic field as a function of temperature, shown in Figure 6. The storage modulus is in logarithmic scale and the tan delta peak in linear scale. The peak of the tan delta curve was located around 59 °C. As can be seen the storage modulus in the transverse direction to the magnetic field was remarkably higher than in the parallel direction up to around 50 °C where the PVA molecules relaxed. At room temperature (25 °C) the storage modulus in the transverse direction was 6.19 ± 0.2 GPa and 4.21 ± 0.06 GPa in the parallel direction. This is a significant difference compared to earlier studies of the reinforcing effect of cellulose nanowhiskers [2] and it strongly suggests alignment of cellulose whiskers.

## 4. Conclusions

The goal of this work was to study if it was possible to align cellulose whiskers in a polymer using a strong magnetic field and thereby obtain a unidirectional reinforced nanocomposite. Polyvinyl alcohol (PVA) with 2 wt% cellulose nanowhiskers was prepared by solution casting with water as the solvent. The structure analysis indicated that the cellulose nanowhiskers oriented perpendicular to the direction of the magnetic field. The dynamic mechanical thermal analysis showed that the dynamic modulus of the nanocomposite transverse to the field direction was around 2 GPa higher than along the field direction at room temperature which further indicated aligned cellulose nanowhiskers.

## Acknowledgements

Borregaard AS, Norway, is acknowledged for the microcrystalline cellulose and Norwegian Research Council under the NANOMAT program is acknowledged for financial support of this work. The Department of Neuroscience at NTNU, Norway, and in particular Oddbjørn Sæther is acknowledged for the use and help with the MR-instrument.

## References

1. M.A.S. Azizi Samir, F. Alloin, A. Dufresne, Biomacromolecules **6**, 612 (2005)
2. A. Dufresne, J. Nanosci. Nanotechnol. **6**, 322 (2006)
3. K. Tashiro, M. Kobayashi, Polymer **32**, 1516 (1991)
4. J. Araki, M. Wada, S. Kuga, T. Okano, Colloids Surf., A **142**, 75 (1998)
5. J-F. Revol, H. Bradford, J. Giasson, R.H. Marchessault, D.G. Gray, Int. J. Biol. Macromol. **14**, 170 (1992)
6. I. Kvien, B.S. Tanem, K. Oksman, Biomacromolecules **6**, 3160-5 (2005)
7. J. Sugiyama, H. Chanzy, G. Maret, Macromolecules. **25**, 4232 (1992)
8. N. Yoshiharu, K. Shigenori, W. Masahisa, O. Takeshi, Macromolecules **30**, 6395 (1997)
9. D. Bordel, J-L. Outaux, L. Heux, Langmuir **22,** 4899 (2006)
10. D. Bondeson, A. Mathew, K. Oksman, Cellulose **13,** 171 (2006)
11. L.C. Sawyer, D.T. Grubb, *Polymer Microscopy* (Chapman and Hall London 1994)

## List of figure captions

**Figure 1.** AFM topography image of cellulose nanowhiskers from a dried water suspension.

**Figure 2.** Observation through crossed polarized films of **a)** a water solution of PVA and **b)** a suspension of cellulose whiskers in PVA solution showing flow birefringence.

**Figure 3.** Optical microscope picture of the nanocomposite showing reflected light at ~45º in polarized light indicating alignment of cellulose whiskers.

**Figure 4.** FESEM pictures of **a)** a fracture surface and **b)** an etched surface of the CNW nanocomposite showing a highly oriented structure.

**Figure 5.** AFM phase image of an etched surface of the CNW nanocomposite showing a highly oriented structure.

**Figure 6.** Storage modulus and tan delta peak of the PVA nanocomposite in the transverse and parallel direction to the magnetic field

**Fig 1.**

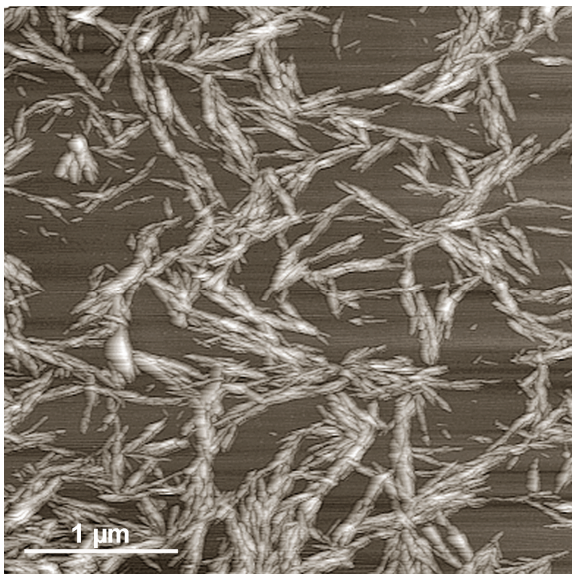

**Fig 2**

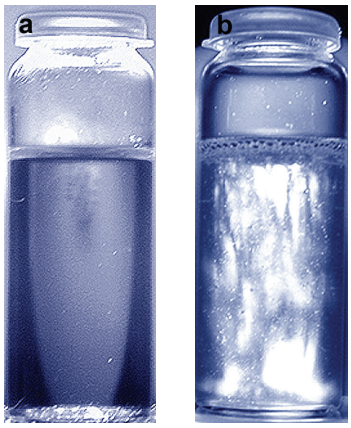

**Fig 3**

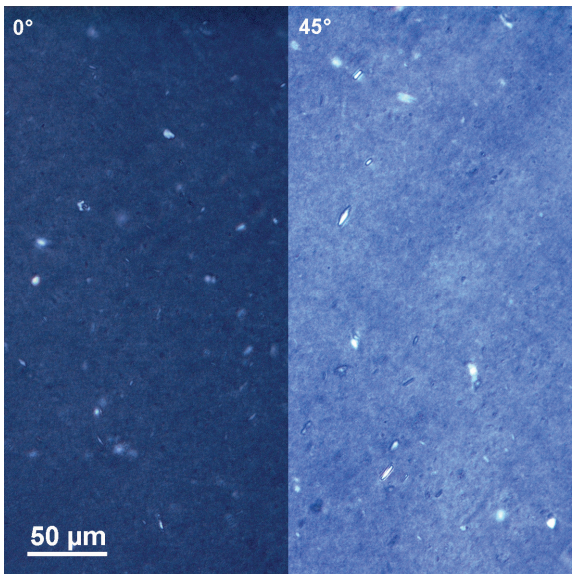

**Fig 4**

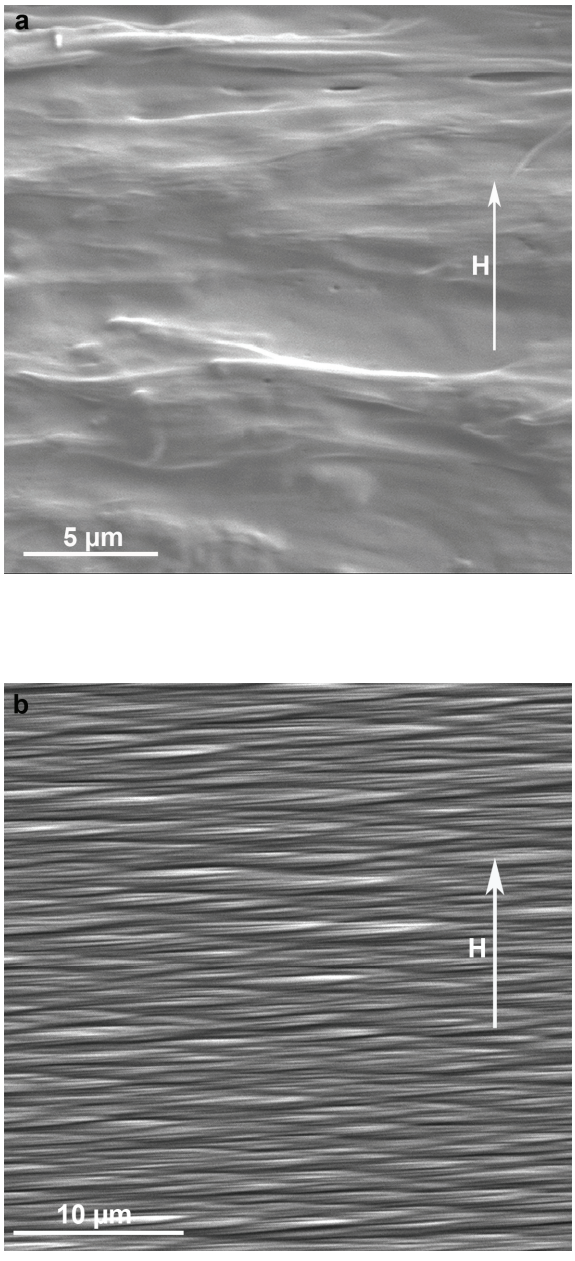

**Fig 5**

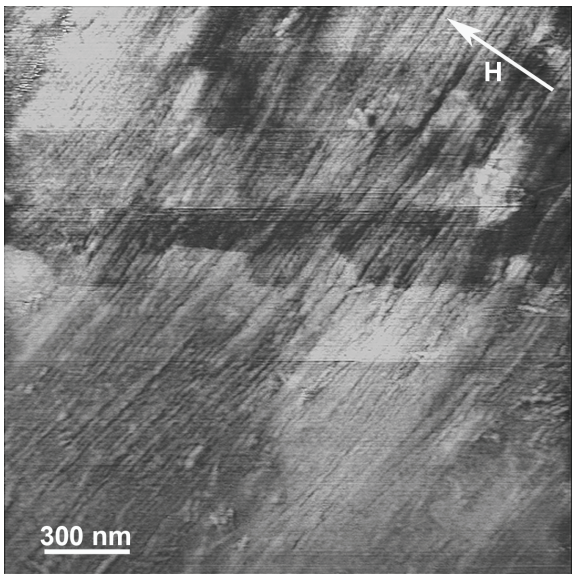

**Fig 6**

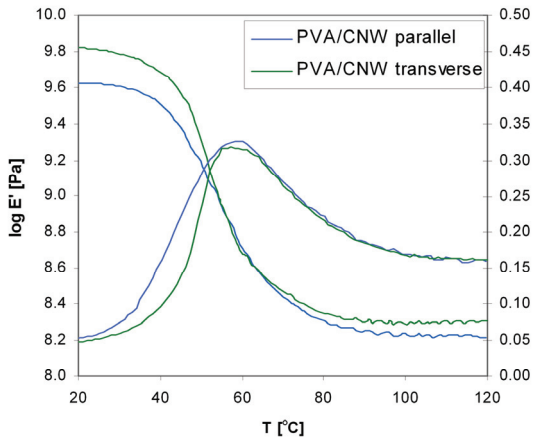
PVA/CNW parallel
PVA/CNW transverse
log E' [Pa]
T [°C]
10.0
9.8
9.6
9.4
9.2
9.0
8.8
8.6
8.4
8.2
8.0
0.50
0.45
0.40
0.35
0.30
0.25
0.20
0.15
0.10
0.05
0.00
20
40
60
80
100
120